ACTIVE CONTROL OF THE SOUND RADIATION FROM A FINITE LINE SOURCE USING NOVEL DIRECTIONAL SECONDARY SOURCES

HU QI

PhD

The Hong Kong Polytechnic University

2019

The Hong Kong Polytechnic University

Department of Building Services Engineering

Active control of the sound radiation from a finite line source using novel directional secondary sources

HU QI

A thesis submitted in partial fulfillment of the requirements for the degree of Doctor of Philosophy

August 2019

Certificate of Originality

I hereby declare that this thesis is my own work and that, to the best of my knowledge and belief, it reproduces no material previously published or written, nor material that has been accepted for the award of any other degree or diploma, except where due acknowledgement has been made in the text.

(Signed)

HU QI (Name of Student)

Abstract

Abstract of thesis entitled: Active Control of the Sound Radiation from a Finite Line Source Using Novel Directional Secondary Sources

Submitted by: HU QI

For the degree of: Doctor of Philosophy

at The Hong Kong Polytechnic University in August 2019.

This thesis is concerned with the active control of the sound radiated from a finite line source, which is a frequently encountered theoretical acoustic source in traffic noise control problems, in free field. To achieve an active noise control in three-dimensional free space is mostly challenging, and the primary noise considered in this study of extended spatial range, that produces a complex sound field, add extra difficulties. Some previous researches on active noise control are focused on the noise reduction capability to create required and acceptable quiet zones in restricted areas. This study is focused on a much wider region of noise reduction from the sound wave radiated from the finite line source, in order to reduce the possibility of sound pressure amplification.

An active control system, consists of multiple secondary sources and error microphones with a typical arrangement where the controllers and sensors are equally spaced and positioned in two parallel rows, is proposed to achieve the research objective. The strengths of secondary sources are determined by the least square algorithm. Further optimization of the locations of control sources and error microphones is investigated by a performance descriptor evaluated on a rectangular strip positioned in the far field where noise attenuation is mostly required.

The main contribution of this thesis is the introduction of a novel type of secondary sources specifically for a directional primary sound field. Conventional secondary sources of compact size radiate sound wave omnidirectionally, resulting in spillover effect in off-axis areas. The new secondary source proposed here, being of a multi-part construction, possess a reasonably directional radiation pattern even with very small physical size at low frequencies.

Through a comprehensive numerical study, the newly devised directive secondary sources prove to be properly effective for global noise reduction. Though the global control performance becomes weaker as frequency increases, the noise reduction within the central region of the receiver plane remains significant in all the cases included in the present study.

Publications arising from the thesis

Hu, Q., & Tang, S. K. (2019). Active cancellation of sound generated by finite length coherent line sources using piston-like secondary source arrays. *The Journal of the Acoustical Society of America*, *145*(6), 3647-3655.

Hu, Q., & Tang, S. K. (2017). The usage of directional secondary sources to actively control a finite line source. In *INTER-NOISE and NOISE-CON Congress and Conference Proceedings*, 255(2), 5332-5339.

Acknowledgements

I would like to thank my chief supervisor Prof. Tang Shiu-Keung for his supervision and guidelines. His intelligent suggestions always enlighten me a lot and I treasured every discussion with him. I would also like to express my sincerest gratitude to every person who have provided his or her help during my PhD study.

Specially thanks to my wife, Wang Meng, I will not finish this work without her tremendous support and consistent understanding.

Additionally, I also want to express my thanks to Dr. Choy Yat Sze for her generous recommendation.

In the last, many thanks to my parents and my sister for their selfless love and care.

Table of Contents

List of Figures

List of Tables

1 Introduction and literature review

1.1 Research background

Noise control is always an important issue nowadays in compact and densely populated cities as excessive exposure to noise is hazardous to human health [Kryter, 1985]. It is now also understood that prolonged exposure to noise even at level well below statutory control level is problematic too [Kang et al., 2013]. There is a recent report from WHO [WHO, 2013] warning that noise has become the second environmental pollution leading to human death in western Europe. Though there is no similar study in other parts of the world, it is believed that the problem is not just European.

There have been many passive and active mitigation methods proposed in the past few decades to help alleviate this worldwide problem. There are many daily life examples of passive methods. The massive roadside noise barrier [Kurze, 1974] is a typical example applied in the outdoors. In the indoors, dissipative silencers and sound absorption panels are commonly used [Fry, 2013]. The plenum window design of Tong et al. [Tong et al., 2015] is also a passive noise reduction device, but it can allow for a reasonable level of natural ventilation inside the associated residential flats.

Active control, where a secondary sound system is used to cancel an unwanted sound [Nelson and Elliott, 1991], is less popular though it has been proven workable in the confined air conditioning and ventilation ductwork [Canevet, 1978]. In the indoors, complete global reduction of noise by active mean is basically not possible and thus, the creation of quiet zones is the focus

[Joseph et al., 1994; Lau and Tang, 2001]. When the primary source is confined such that the propagation of noise from the source to the receivers is basically understood, active control using multiple secondary sources and error sensors is effective [Tao et al., 2016]. Active control can also be combined with passive methods for improved performance. Examples of these works include the active noise barrier edges of Omoto and Fujiwara [Omoto and Fujiwara, 1993] and Hart and Lau [Hart and Lau, 2012], the active window edges of Kwon and Park [Kwon and Park, 2013] and the investigation of active control effectiveness inside plenum windows of Huang et al. [Huang et al., 2011] and Tang et al. [Tang et al., 2016].

Standalone active environmental noise control system, which is not attached to a passive device, for cancelling noise in the free field is not commonly found in existing literature. Wright and Vuksanovic [Wright and Vuksanovic, 1996; 1997] have developed a theory to investigate the active control of non-compact primary noise source using monopole secondary source array. They observed excellent noise cancellation at specific locations, but sound amplification could be serious at some other locations. Guo et al. [Guo et al., 1997] studied the creation of quiet zone in the free field by a control source array. Duhamel and Sergent [Duhamel and Sergent, 1998] described a formulation for attenuating actively an incoherent line source. There are also efforts studying the use of multipoles to cancel the sound from a compact primary source (for instance, Bolton et al. [Bolton et al., 1995] and Chen et al. [Chen et al., 2010]).

Noise barriers in the countryside or sub-urban areas are not so welcomed by the residents as they tend to block the sight of views. In the indoors, there are noises from linear air grilles or similar non-compact structures in the building occupied zones which cannot be screened because of air distribution and air flow performance issues [Miller, 1977]. The virtual barrier idea of Tao et al. [Tao et al., 2016] is therefore an interesting option for noise control. In this thesis, an attempt is made to attenuate noise from a finite length coherent line source in free field using an array of directional secondary sources of reasonably small size to create a virtual noise barrier. The effective control zones will be examined in detail.

1.2 Literature review

The traditional passive methodology of noise control becomes invalid and impractical as the acoustic wavelengths are considerably long, while the active approach works well. The patent published by Paul Lueg [1936] is considered as the starting point of the active noise control, which is an idea to use an acoustic source to modify the existing sound field by introducing a secondary destructive sound wave. Twenty years after this profound patent, Olson [1953; 1956] studied a feedback active control system for noise reduction, in which the high frequency performance is limited by the analog feedback control structure and the low frequency performance is restricted by the loudspeaker response. At the contemporaneous time, Simshauser and Hawley [1955] proposed active noise canceling headsets, which provide a successful practice of active sound attenuation in small regions. With the advances of control theory and fast and reliable electronic hardware, the practical implementation of active noise control then became possible.

Although the first attempt of active noise control is about the sound propagation in a duct, studies on the active control of acoustic radiation into free space are as early as of 1950s [Conover, 1956; Ross, 1978; Hesselman, 1978; Angevine, 1981; Berge et al., 1987]. These early researches were of one practical purpose to reduce the noise generated by electrical transformers, in which loudspeakers, as the secondary control sources, were usually placed near the transformer to provide quiet zones at required locations in the residential area. Conover [1956] first published the experiment result out of the laboratory, which applied the active noise control on a much larger scale in the free field. Expect the work of Conover, other researchers [Kido, 1975; Jessel and Angevine, 1980] were continuously devoted themselves into the active reduction of the transformer noise.

The studies of the active noise control can be generally divided into two disciplines: one is on the physical principles and mechanisms and the other is of electronic control system design. This thesis is focused on the former. As the characteristics of primary source and the acoustic environment are usually nonstationary with varying frequency content, amplitude and phase of the radiating noise or the effects of changing atmospheric conditions, the electronic control system for active noise control is required to be adaptive [Alexander, 2012; Clarkson, 1993; Burgess, 1981; Warnaka et al., 1981]. In addition, the controller designed for active noise control system is desirable to be digital [Ross, 1981].

From the electronic control perspective, there are two different model of the control strategy for the active noise control: the feedforward control and the feedback control. Besides, a combination of the feedforward and feedback control structures, which is referred as a hybrid active noise control system [Swanson, 1989], was an improved proposal of active control system design. In the cases of using active noise control methods in the acoustic field of large dimension and extensive space, it is necessary to use a multi-channel electronic control system, which consists of several secondary sources, error microphones and/or some reference sensors. Possible industrial application scenarios include the interior of cars [Elliott et al., 1988; McDonald et al., 1991; Kurata, 1991; Ross, 1991], the flight cabin of helicopters [Simpson et al., 1989; Dorling et al., 1989; Elliot et al., 1990], etc.

The application of active control to the noise radiation problems in free field or open space has been of great interest lasting for a long time both from the perspective of active noise control [Conover, 1956; Ross, 1978; Craig, 1993; Gee and Sommerfeldt, 2004; Lin et al., 2004] and of active structural acoustic control [Clark and Fuller, 1992; Snyder et al., 2004; Duke et al. 2009; Sun et al., 2017]. There are two strategies in active control of sound radiation in free space: one is to achieve global attenuation; the other is to control the noise locally, such as the case that as all-around sound reduction is not necessary, the free-field active noise control then aims at significant sound cancellation into particular spatial section to provide enough quiet areas. Nelson et al. [Nelson et al., 1987a; Elliott et al., 1991] developed a set of matrix equations through an impedance-based approach for an unambiguous quantification of the minimum power output of a distribution of a number of monopole sources, which enabled the discussion on the global performance of the active noise control as only simple sources are involved. Guo et al. published a series of papers on the investigation of local attenuation of sound pressure in free space using multiple control sources and error microphones arranged in two parallel lines [Guo et al., 1997] and in two parallel planes [Guo and Pan, 1997], in which they indicated a range of optimal spatial configurations of the active control system for less increase in total power output and larger size of quiet zones. The authors also considered the effects of ground reflections [Guo and Pan, 1998] and the possibility of broadband noise control [Guo and Pan, 1999]. Wright and Vuksanovic [1996; 1997] proposed an Electronically Controlled Acoustic Shadow model for active environmental noise control in unrestricted space. They studied the sound cancellation of a flat, in-phase primary source by an active wall consisting of monopole cancellers, then extended this model to more practical scenarios, involving more complicated primary sources, and considering the use of directional secondary sources, wind effect, etc. [Wright and Vuksanovic, 1999]. Other work on the active noise reduction into particular directions included the studies of Santiago and Bernhard [1993] who examined the active noise control in a section of free field from monopole, dipole and quadrapole primary sources.

Apart from the number and locations of the secondary sources, the active attenuation of primary source radiation also depends on the type of secondary sources used in the control system. Other than the most common secondary sources of simple monopoles, Bolton et al. discussed the use of secondary multipoles thoroughly [Bolton, 1995]. This research has drawn a conclusion that using secondary sources of multipoles is more efficient in some instances than an array of monopoles for global cancellation and acceptable global far-field reduction can be achieved by using secondary multipoles even placed at a relatively large distance from the primary source. Except this straightforward extended idea of using secondary sources of higher than monopole order, a compound secondary source was proposed by Chen et al. [2010], which consisted of two closely located loudspeakers with different strength ratio and opposite phase, for global active noise reduction in free field. Chen and Koopmann [2002] theoretically studied the potential of using planar sound sources to actively control the low-frequency sound radiation from vibrating panel, in which both the secondary sources and primary sources are modeled as simply supported rectangular panels. Given different acoustic environments, a radially vibrating spherical baffled piston was used to create quiet zones analytically by Azarpeyvand [2005] in a diffuse sound field. More recently, the spherical loudspeaker array [Tanaka and Tanaka, 2010] and the parametric array loudspeaker (PAL) [Rafaely, 2009] are utilized as the control sources in an active noise control system. By using a spherical loudspeaker array for local active noise reduction, the quiet zones created are much larger than the limited ones by monopole sources; the latter innovatively introduced secondary source focused on the capability of sound suppression at the designated control positions without causing spillover in other areas. Besides, a method to design a planar first-order loudspeaker array is introduced and theoretically explored by Bu et al. [2018] for global active noise control. This radical structure of loudspeaker array benefits the source locations and the authors also proposed an alternative planar array of monopole pairs for more practical implementation. Except the previously mentioned secondary sources, Giouvanakis et al. [2019] use a compound acoustic source of quadrupole type to create an adaptive sound source, being able to change its radiation pattern for active control of sound in a closed space.

As the development of active noise control, especially during the last three decades, the research field of the active noise control becomes extremely large and vigorous, where the number of publications and patents are enormous including a mass of high-quality review papers [Warnaka and Glenn, 1982; Ffowcs, 1984; Leitch and Tokhi, 1987; Jessel, 1988; Ahuja and Stevens, 1991; Tichy, 1991; Guicking, 1992 & 2007; Elliott and Nelson, 1993; Fuller and Flotow, 1995; Kleiner and Svensson, 1995; Hansen, 1997 & 2004; Kuo and Morgan, 1999; Peake and Crighton, 2000; Hansen et al., 2007; Guo et al., 2007; PAWEŁCZYK, 2008; Kajikawa et al., 2012 & 2013; Qiu et al., 2014]. Plentiful reviews focused on specific issues of active noise control, e.g. the active control of combustion instabilities [McManus et al., 1993], the active techniques for aerospace and vibro-acoustic control [Gardonio, 2002], the active noise and vibration control in road vehicles [Elliott, 2008], the algorithms of virtual sensing [Moreau et al., 2008], the applications in vehicles and inner ear [Elliott, 2009], the effects of reflective surfaces [Boodoo, 2015], the active noise control on sound quality enhancement [Jiang and Li, 2018], etc. Additionally, some reviews paid attention on the critical aspect of control system design in active noise control [Kuo and Morgan, 2000; George and Panda, 2013].

In many existing literatures, the primary sources tackled are mostly modeled as simple point sources, an array of point sources, or extended radiator of certain simple geometry and usually are of compact physical size. We cope with a finite simple line source in this thesis. Such a theoretical model is frequently encountered in the context of traffic noise control. A theoretical investigation by similar motivation has been conducted by Duhamel and Sergent [1998], who explored the possibility of the use of active control methods to solve the outdoor environmental noise problems by modeling the primary source as an incoherent line source. Their work suggested that the active approach is effective in a limited space domain depending on the frequency and the length of the source. To achieve a noise attenuation in all directions in free field by active methods is always very challenging. Most researches of free-field active noise control have paid attention on sound reductions in the required spaces, while it might result in potential sound increase elsewhere. As indicated by Nelson [Nelson et al., 1987a], reductions of the total power output can be achieved only if the secondary sources are close to the primary noise source within a distance less than one-half wavelength. Even though the total free-field acoustic power radiated by the combination of both primary sources and secondary sources is reduced, it does not guarantee a global sound mitigation everywhere [Cunefare and Koopmann, 1991]. Hence, the first primary purpose of this study is to achieve an overall reduction of the radiation from the primary line source or to alleviate the spillover effect and enlarge the extent of quiet zone as possible.

The obvious incentive of introducing the secondary sources different from the conventional and readily implemented point sources is to improve its active control performance globally or locally. Furthermore, a large number of secondary sources are required for appropriate active attenuation of the sound radiation from a large and complex acoustic source with the correspondingly added control channels causing extra system intricacies and signal processing burden [Chen et al., 2010; Chen and Koopmann, 2002], and yet the use of secondary sources other than simple point sources can reduce the number of controllers used in some cases.

For low frequency noise to which the active method is advantageous, conventional compact secondary sources act as monopoles, while the studied primary source in this thesis attains a multi-lobe radiation pattern with strong directionality. From the point of view that the active acoustic control works by utilizing the destructive interference of sound waves, normal compact secondary sources, radiating the sound wave omnidirectionally, will not make an efficient active control in the open space. The first motivation of this study is thus to introduce a novel type of secondary sources that possess high directivity with very compact size and within low-frequency range and can achieve exceptionally improved performance than the simple point sources or piston sources.

This thesis is organized as follows. After the introduction and literature review of Chapter 1, Chapter 2 provide a theoretical formulation of the proposed active control system for actively controlled sound field calculation. Then the active control results by conventional secondary sources, like simple point sources and baffled circular piston sources, are illustrated in Chapter 3, followed with a short discussion on the active control performance and properties of the ANC system by secondary source arrays. Chapter 4 and Chapter 5 are the main contributions of this study. Chapter 4 starts with the motivations and justifications of the novel idea on piston-like directional secondary sources and follows on a detailed analysis of its acoustical characteristics, especially focusing on the directionality. Additionally, a geometric optimization of the established ANC system regarding the separating distances of the controllers and sensor is conducted with specified cost function using least squares method. The active control results by new secondary sources are achieved by the given formulation in the previous chapter. With the knowledge of the active noise reduction performance at discrete frequencies, the possibility of broadband noise control using the same scheme is thoroughly explored. Moreover, the system scalability with respect to the length of primary line source is also analyzed based on a mass of numerical results. The last chapter concludes the whole thesis and recommends some future works.

2 Active Control Formulation

2.1 The control system setup

The active control system setup for the following discussion is illustrated in figure 2.1, which is similar to that of Wright and Vuksanovic [1996]. Multiple equally distanced secondary sources and error microphones are arranged in two parallel lines being of the orientation of the primary line source, which is modeled as a coherent line source of length l. The Cartesian coordinates then are deployed for numerical computation, where the geometrical center of the primary line source coincides with the original. The number of secondary sources and error microphones are assumed equal in this discussion for simplicity. The former is separated at a distance of d_s and the separation distance of the latter is d_e as shown in figure 2.1. All the acoustic control actuators are positioned relatively close to the primary source at a distance of d_{ss}, while the error sensors are located in the far field, at a distance of d_{mp}, where noise reductions are required. There is a narrow planar rectangular strip, perpendicular to the xy-plane and containing all error sensors, referred to as the monitoring plane S_{mp} in the subsequent discussion, which is used to examine the acoustic far-field as the active control system is in action. In the later analysis, the performance of the proposed active control system is described by the sound pressure level reduction on the monitoring plane, measured by the length of l_{mp} and the height of h_{mp}. The whole control system is geometrically configured axial-symmetrically with the x-axis, and all the sound sources are fixed on the horizontal xy-plane.

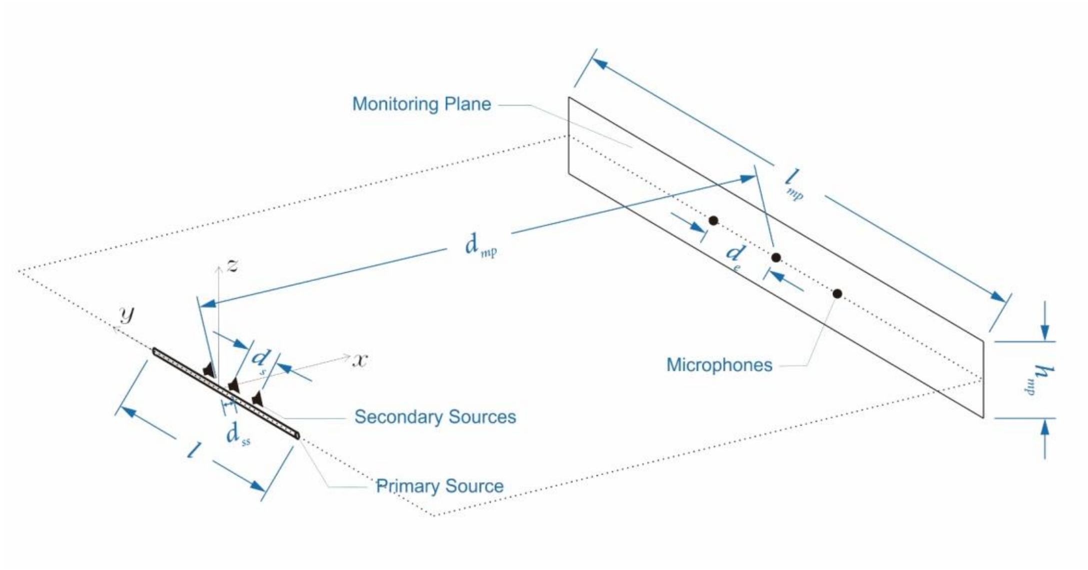

Figure 2. 1 The geometric arrangement of the active control system with multiple secondary sources and error microphones

2.2 The theoretical formulation

As subsequent analysis is examined in frequency domain on a pure-tone acoustic field, the time-dependent variation term, $e^{-j\omega t}$, is eliminated. For a far-field observer point, the sound pressure radiated by the primary coherent line source only at any far-field point $\mathbf{x} = (x, y, z)$ is [Kinsler et al., 1999]

$$p(\mathbf{x}) = j\frac{\rho c k}{4\pi}\frac{\sin\left(\frac{kl}{2}\sin\theta\right)}{\frac{kl}{2}\sin\theta}\frac{Q_l}{r}e^{-jkr} \qquad (2.1)$$

where $j = \sqrt{-1}$, r is the radial distance from the acoustic center of the primary source to the position of the far field point, $r = \sqrt{x^2 + y^2 + z^2}$, ω is the angular frequency of the harmonic radiation, $k = \omega/c$ is the wavenumber, c is the sound propagating speed, and ρ is the density of air. Q_l and l are the source strength and the length of the primary source respectively. θ is the deviation angle from the xz-plane, $\sin\theta = y/r$. When $y/r \to 0$, the factor $\sin\left(\frac{kl}{2}\sin\theta\right)/\frac{kl}{2}\sin\theta \to 1$. The sound pressure created by an axisymmetric compact secondary source located at $\mathbf{x}_s = (x_s, y_s, 0)$ at far-field position $\boldsymbol{x}$ is, for $|\mathbf{x} - \mathbf{x}_s| \gg source\ radius$

$$p_s(\mathbf{x}) = j\frac{\rho ck}{4\pi} D_s(|\mathbf{x} - \mathbf{x}_s|, \varphi)\frac{Q_s}{|\mathbf{x} - \mathbf{x}_s|}\mathrm{e}^{-jk|\mathbf{x}-\mathbf{x}_s|} \tag{2.2}$$

where Q_s is the complex source strength and D_s the directivity factor which is in general a function of the distance $|\mathbf{x} - \mathbf{x}_s|$ and the angle between the vector $\mathbf{x} - \mathbf{x}_s$ and the surface normal of the sound source, φ. For a simple point source, which radiates omnidirectionally, $D_s = 1$. Suppose there are N number of secondary sources and thus N number of error microphones, the net sound pressure at the i th error microphone at $\mathbf{x}_{ei} = (x_{ei}, y_{ei}, z_{ei})$ by the superposition of the acoustic radiation from the primary source and the secondary sources in action is

$$p_{ei} = p(\mathbf{x}_{ei}) + \sum_{n=1}^{N} p_{sn}(\mathbf{x}_{ei}) \tag{2.3}$$

where $p(\mathbf{x}_{ei})$ is the sound pressure from the primary source and $p_{sn}(\mathbf{x}_{ei})$ is the sound pressure from the nth secondary source. The optimization of the secondary source strengths is performed by the least square method, in which the total potential energy [Nelson et al., 1987b] at the error microphones is chosen as the cost function and minimized. The cost function is calculated by

$\mathbf{p}_e^{\boldsymbol{H}}\mathbf{p}_e$, where $\mathbf{p}_e = [p_{e1}, p_{e2}, p_{e3}, \dots, p_{eN}]$ and $\mathbf{p}_e^{\boldsymbol{H}}$ represents the Hermitian transpose of $\mathbf{p}_e$, in which $\mathbf{p}_e$ can be expressed by the matrix equation that

$$\mathbf{p}_e = \boldsymbol{Z}_{pe} Q_l + \boldsymbol{Z}_{se} \mathbf{Q}_s \tag{2.4}$$

where $\boldsymbol{Z}_{pe}$ is a $N \times 1$ matrix with its ith element represented by

$$\boldsymbol{Z}_{pe}(i) = j\frac{\rho ck}{4\pi} \frac{\sin\left(\frac{kl}{2}\sin\theta_i\right)}{\frac{kl}{2}\sin\theta_i} \frac{e^{-jk|\mathbf{x}_{ei}|}}{|\mathbf{x}_{ei}|} \tag{2.5}$$

and $\boldsymbol{Z}_{se}$ is a $N \times N$ matrix with ith row and nth column element being of

$$\boldsymbol{Z}_{se}(i,n) = j\frac{\rho ck}{4\pi} D_s(|\mathbf{x}_{ei} - \mathbf{x}_{sn}|, \varphi_{in}) \frac{e^{-jk|\mathbf{x}_{ei} - \mathbf{x}_{sn}|}}{|\mathbf{x}_{ei} - \mathbf{x}_{sn}|} \tag{2.6}$$

and the secondary source strength vector $\mathbf{Q}_s$, the secondary source strength vector, is a column vector of $N \times 1$ elements, $\mathbf{Q}_s = [Q_{s1};\ Q_{s2}, Q_{s3}, \dots, Q_{sN}]$.

The cost function is essentially a quadratic function of the unknown complex secondary source strengths, for a given geometric arrangement of the primary noise source, secondary sources and error microphones, existing a unique minimum [Nelson et al., 1987a; Cunefare and Koopmann, 1991]. And the associated secondary sources for its minimum is referred as the optimal secondary sources, $\mathbf{Q}_{s,opt}$, which is

$$\mathbf{Q}_{s,opt} = -\alpha^{-1}\beta = -\left(\boldsymbol{Z}_{se}{}^{H}\boldsymbol{Z}_{se} + \gamma\boldsymbol{I}\right)^{-1}\boldsymbol{Z}_{se}{}^{H}\mathbf{P}_{pe} \tag{2.7}$$

Since the number of controllers is equal to the sensors, then

$$\mathbf{Q}_{s,opt} = -\boldsymbol{Z}_{se}{}^{-1}\boldsymbol{Z}_{pe}Q_l. \tag{2.8}$$

Details of the optimization process can be found in Appendix and the references by Tang et al. [Tang et al., 2016] and Duhamel [Duhamel and Sergent, 1998]. With all the above equations, the sound pressure at any point on the vertical monitoring plane can be calculated. The resultant sound pressure after active control, at the receiving point $\mathbf{x}$ is

$$p_{controlled}(\mathbf{x}) = p(\mathbf{x}) - \boldsymbol{Z}_s\boldsymbol{Z}_{se}{}^{-1}\boldsymbol{Z}_{pe}Q_l \tag{2.9}$$

where $\boldsymbol{Z}_s$ is a $N \times 1$ row vector with its ith element of $\boldsymbol{Z}_s(i) = j\frac{\rho ck}{4\pi}D_s(|\mathbf{x} - \mathbf{x}_{si}|, \varphi)\frac{\mathrm{e}^{-jk|\mathbf{x}-\mathbf{x}_{si}|}}{|\mathbf{x}-\mathbf{x}_{si}|}$.

It is obvious that the active control results are highly dependent on the type of secondary sources and their locations. Apart from the distribution of sound pressure on this monitoring plane, the reduction of the average sound pressure level on this plane will also be used as a descriptor of the active control performance. The following contents first focuses on the active control performance at low frequencies, and the effects of the directional secondary sources used for controlling the coherent primary line source is of particular interest in this thesis.

3 Active Control with Simple Secondary sources

3.1 The use of simple secondary sources

For illustration purpose, the following geometric parameters are settled: the error microphones are separated from the primary source at 100m, $d_{mp} = 100m$; the secondary sources are positioned at a distance of 1m, $d_{ss} = 1m$; the length of the finite primary line source is 10m, $l = 10m$. The span of the monitoring plane is fixed with $l_{mp} = 500m$ and $h_{mp} = 50m$ in the foregoing analysis unless otherwise specified. A long horizontal span length is chosen here in order to understand the effective spatial range of the active control. The simplest secondary sources are the simple point sources and circular pistons.

For simple point sources, $D_s = 1$ and for baffled axially oscillating circular pistons of radius r_o [Kinsler et al., 1999],

$$D_s = \frac{4J_1(kr_o \sin\varphi)}{kr_o \sin\varphi} \tag{3.1}$$

where J_1 is the Bessel function of the first kind and $\sin\varphi = |\mathrm{y} - \mathrm{y}_s|/|\mathbf{x} - \mathbf{x}_s|$.

To examine the effectiveness of the control system, the sound pressure levels evaluated on the monitoring plane in the far field will be averaged along the z coordinate, as the variation of the sound field mainly occurs along the y coordinate rather than along the z axis. Then the averaged sound pressure levels are plotted against y axis to indicate the overall sound distribution before and after control. The primary line source strength is set at a constant value, $Q_l = 1\, m^3/s$.

3.2 Active control performance at discrete low-frequencies

We started the analysis of active control performance on different type of secondary sources by using the most common secondary sources of simple point sources and a typical directional source of the baffled piston sources.

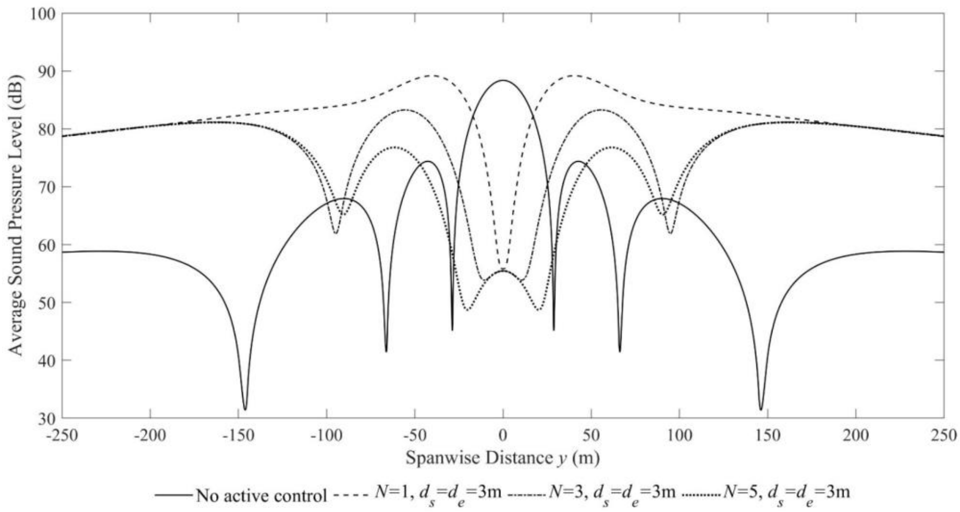

Figure 3. 1 Spanwise variation of averaged sound pressure level on the monitoring plane at the low frequency of 125 Hz with piston control sources of $r_o = 0.5m$.

Figure 3.1 shows the spanwise sound pressure variation, logarithmically averaged along the height of z-direction, on the monitoring plane at the frequency of 125 Hz with different number of secondary sources with $\mathrm{r_o} = 0.5\mathrm{m}$. All the secondary sources are symmetrically located about y axis. From a feasible point of view, it is impractical to install a circular piston source of radius 0.5m. It is used here for illustration purpose to display its effect only. It can be observed that the effectiveness of the active control is very good at locations near to the central plane of the system. However, there is considerable sound amplification at the region $|y| > 2l$ on the monitoring plane. Similar observations have been made by Wright and Vuksanovic [Wright and Vuksanovic, 1996]. For the case of a single secondary source with a single error microphone located on the centerline of the system, the resultant sound has a magnitude even higher than the maximum sound level in the "no control" case due to the constructive interface between the secondary source and the primary noise source. The attenuation zone becomes larger and the amplitude of the resultant sound field is lowered as N increases, but such effect is not obvious at the far-away monitoring points. It is found that the circular piston gives only slightly better performance than the monopoles at this frequency. The comparison of the control results by the monopole source and piston source are illustrated in figure 3.2.

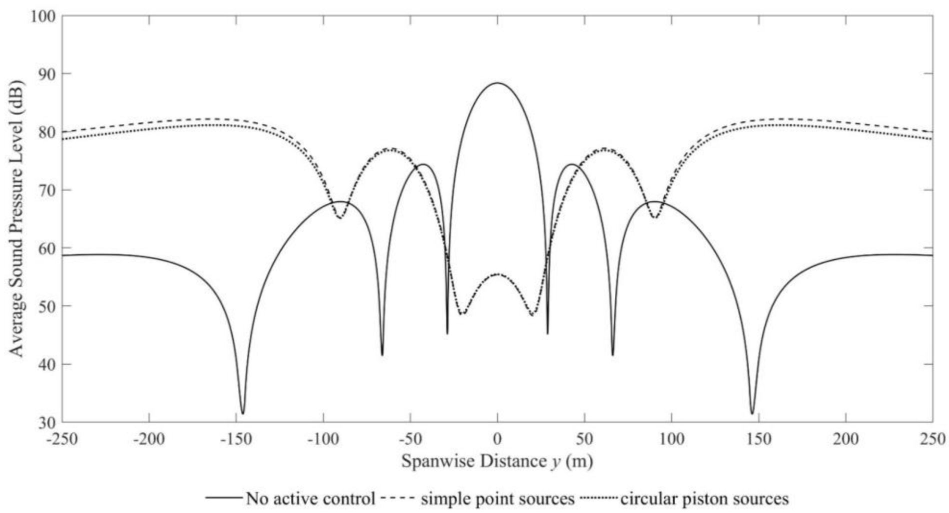

Figure 3. 2 Comparison of spanwise variations of averaged sound pressure level on the monitoring plane at the frequency of 125 Hz with monopole sources and piston sources of $r_o = 0.5m$ respectively ($N = 5, d_s = d_e = 3m$).

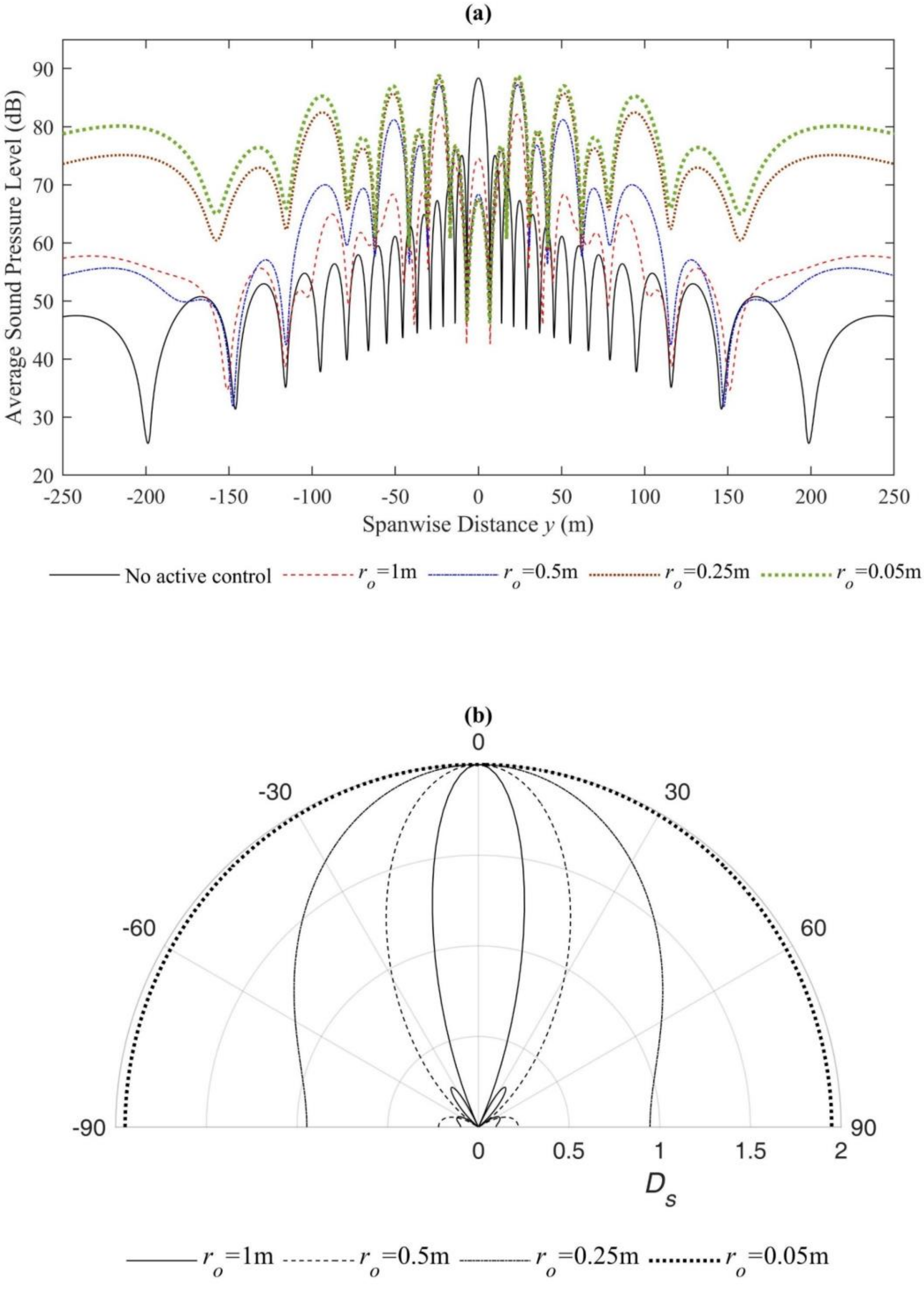

Figure 3. 3 (a) Spanwise variation of averaged sound pressure level on the monitoring plane at the frequency of 500 Hz with piston control sources of different radii ($N = 5, d_s = d_e = 3m$); (b) Effect of r_o on the directivity factor, D_s, pattern of piston radiation at the frequency of 500Hz.

Figure 3.3(a) shows the performance of the active control when the sound frequency is increased to 500Hz with N fixed at 5. One can observe that the control is always effective on the very central area of the monitoring plane. However, the performance of the active control becomes worse as r_o decreases. Figure 3.3(b) displays the directivity factor pattern of a piston source with different radii at 500 Hz with respect to φ in its radiation semispherical. A smaller piston diameter results in less directional sound radiation as shown in figure 3.3(b). Though the effectiveness of the active control depends also on the characteristics of the primary sound source [Qiu and Hansen, 2000], the results shown in figure 3.3(a) and 3.3(b) tend to suggest that a less directional secondary source could lower the overall performance of the present active control system. Nevertheless, a smaller secondary source can allow more such sources to be used within a fixed spatial span for the enhancement of active control performance. The main objective of this study is to derive a reasonably compact secondary control source system which can achieve broadband active reduction of sound generated by a finite length coherent line source.

4 The New Secondary source and Its Performance

4.1 The introduction of new secondary sources

As already discussed earlier, the directional secondary sources of traditional type, i.e. the baffled piston sources, do not efficiently reduce the sound radiation from a coherent finite line source of comparatively large extent at the low frequencies, except using impractical large circular piston sources, since the small piston source radiates the sound field omnidirectionally like a simple point source. A novel construction of the secondary source will be devised and introduced in this study to attain a directional radiation pattern within a practical small physical size.

As schematically presented in figure 4.1, a new secondary source consists of an outer annulus of outer radius r_o and an inner circular piston core of radius r_i, being able to independently oscillate with specified amplitude and relative phase. Both the inner-part and outer-part are vibrating axially, and an infinite baffle is assumed to the new source. This construction is inspired by the simple acoustic source model of baffled circular piston that possesses a readily closed-form solution, computed by Bessel function of first kind, for its sound radiation in far field. Its directivity can be controlled by adjusting the phase difference between as well as the magnitudes of the two vibrating components. Apart from its directivity, its size is also a major concern and the effect of source radius on the effectiveness of the active control will be examined.

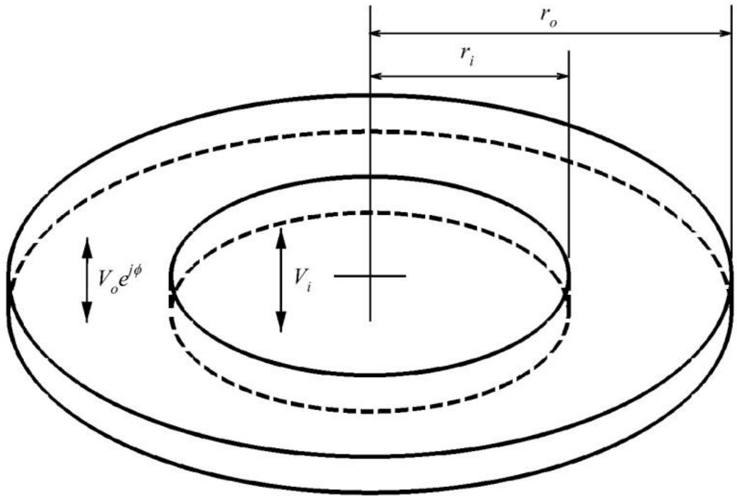

Figure 4. 1 Construction of the newly proposed secondary source

There are several parameters concerning this novel construction of piston-like secondary source as shown in figure 4.1: the radius of the whole control source is denoted by r_o, while the radius of the piston core is r_i; the axially oscillating velocity of the inner part is represented by V_i, and the outer part is $V_o e^{j\phi}$ where ϕ represents the phase difference in radians. The complex sound pressure at a point $\mathbf{x}$ due to this source, positioned at $\mathbf{x}_s$ is

$$p = j\frac{\rho c k Q}{\pi}\frac{e^{-jk|\mathbf{x}-\mathbf{x_s}|}}{|\mathbf{x}-\mathbf{x}_s|}\left[\frac{J_1(kr_i\sin\varphi)}{kr_i\sin\varphi} + e^{j\phi}R_v\left(R_r^2\frac{J_1(kr_o\sin\varphi)}{kr_o\sin\varphi} - \frac{J_1(kr_i\sin\varphi)}{kr_i\sin\varphi}\right)\right] \tag{4.1}$$

where ϕ is the phase difference between the two vibrating surfaces, $Q = \pi r_i^2 V_i$ (assigned as a nominal source strength of the new secondary source), $R_v = V_o/V_i$, $R_r = r_o/r_i$ and the suffices o and i represent quantity associated with the outer annulus and inner core respectively. It can be inferred from equation 4.1 that the sound field generated by this concentric piston source can be set more directional than that of a single piston of the same r_o at the same frequency.

The directivity D of an axisymmetric source can be defined using the formula [Kinsler et al., 1999]:

$$D = 2\left(\int_0^{\pi/2} Q^2(\varphi)\sin\varphi\, d\varphi\right)^{-1} \tag{4.2}$$

where Q is referred to as the directional factor and calculated by $Q = p(|\mathbf{x}-\mathbf{x}_s|,\varphi)/p(|\mathbf{x}-\mathbf{x}_s|,0)$. If Q is explicitly known, then the directivity of the sound source is numerically obtained. As for our new source, the directional factor is,

$$Q(\varphi) = \frac{\frac{2J_1(kr_i\sin\varphi)}{kr_i\sin\varphi} + e^{j\phi}R_v({R_r}^2\frac{2J_1(kr_o\sin\varphi)}{kr_o\sin\varphi} - \frac{2J_1(kr_i\sin\varphi)}{kr_i\sin\varphi})}{1 + e^{j\phi}R_v({R_r}^2 - 1)} \tag{4.3}$$

By substituting equation (4.3) into equation (4.2), the corresponding directivity of the new secondary source then can be calculated by

$$D = \frac{2\left[1 + e^{j\phi}R_v({R_r}^2 - 1)\right]^2}{\int_0^{\pi/2}\left(\frac{2J_1(kr_i\sin\varphi)}{kr_i\sin\varphi} + e^{j\phi}R_v({R_r}^2\frac{2J_1(kr_o\sin\varphi)}{kr_o\sin\varphi} - \frac{2J_1(kr_i\sin\varphi)}{kr_i\sin\varphi})\right)^2\sin\varphi\, d\varphi} \tag{4.4}$$

It is straightforward to show that the magnitude of D is the largest when $\phi = \pi$ for a fixed pair of R_v and R_r. In the rest of the discussions, ϕ is set equal to π. The two components of the newly proposed secondary source are vibrating out-of-phase. Therefore, the directivity of the proposed new source is only determined by R_v, R_r and r_o, $D = D(R_v, R_r, r_o)$.

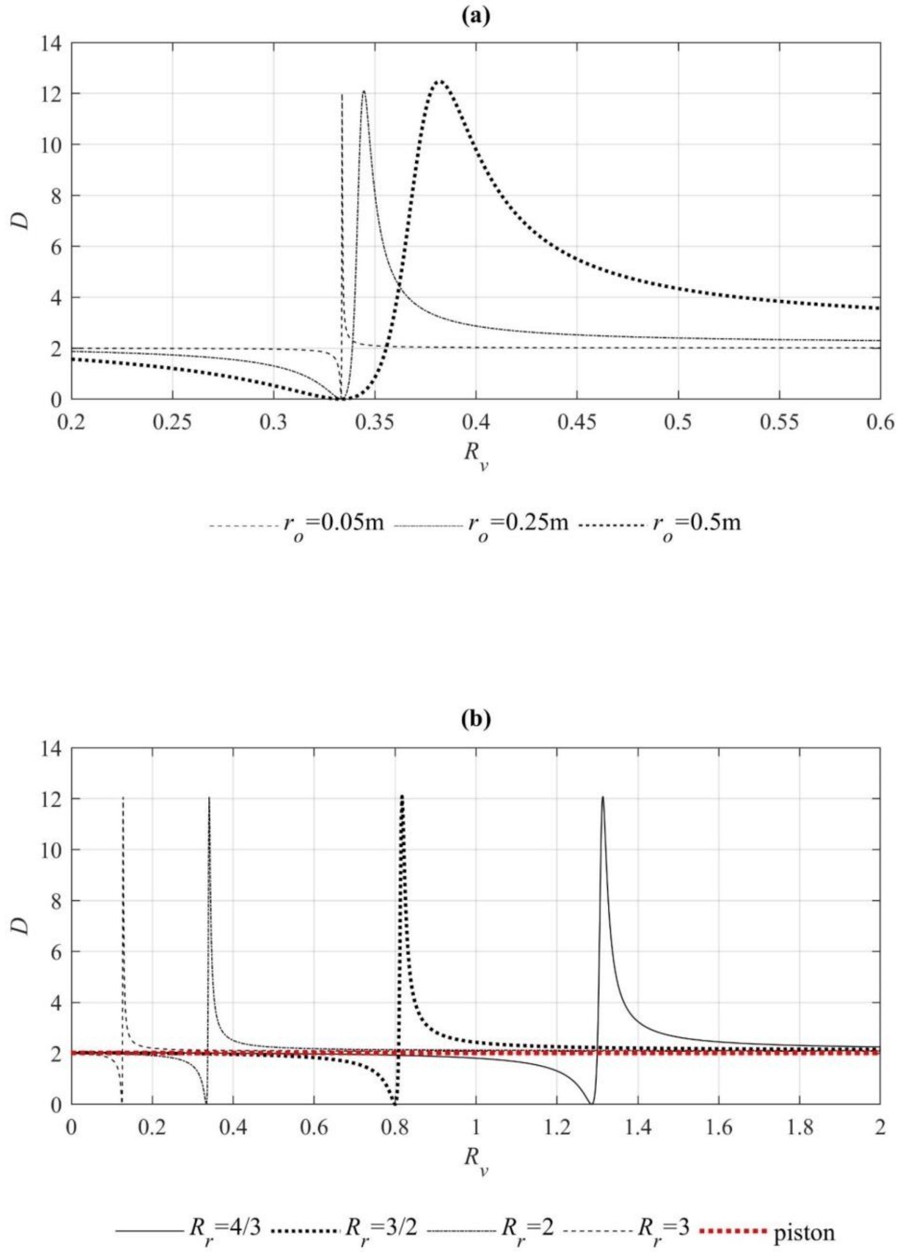

Figure 4. 2 (a) Effects of R_v and r_o on D at 125Hz with $R_r = 2$; (b) Effects of R_v and R_r on D at the frequency of 500Hz with $r_o = 0.05m$.

To study the effects of R_r and R_v on the directivity of the new source and the influence of its physical size on the radiation pattern, the directivity is plotted against R_v of assigned values of r_o with fixed R_r and of specified values of R_r with constant r_o respectively, which are indicated in figure 4.2. It reveals that the velocity ratio, R_v, is sensitive to achieve the maximal directivity, unless the size of the new sound source becomes unrealistic large or the frequencies of the two vibrating surfaces increases. As shown in figure 4.2(a), the physical size of the new piston-like source hardly affects the maximal directivity could be, and the proposed secondary source attains very high directivity, more than 10, with $r_o = 0.1m$. It suggests that the new secondary source can provide intense directional sound radiation field within very small size and even at very low frequencies.

Figure 4.2(b) illustrates the effects of R_v and R_r on D at the frequency of 500Hz for $r_o = 0.05m$. It can be observed that the new source can produce a very directional sound field with $D > 10$ under suitable combinations of R_v and R_r. There are cases where $D = 0$, which represent the situation at which no resultant sound is radiated out along the axis $\varphi = 0$. The R_v resulted in the largest D increases with decreasing R_r. In addition, R_v becomes less sensitive with smaller R_r, i.e. the outer annulus gets thinner. The directivity of a simple circular piston is also presented in figure 4.2(b) for the sake of easy comparison. One can observe that the newly proposed secondary source can produce much more directional sound field than a single circular piston even when the size of the new source is much smaller than that of the piston. Similar phenomenon is also observed at higher frequencies. The R_v resulted in the maximal directivity depends on and increases with frequency with fixed

R_r and r_o as shown in Figure 4.3. The rate of increase is very slow at frequency below 1000 Hz, but it becomes relatively rapid afterward.

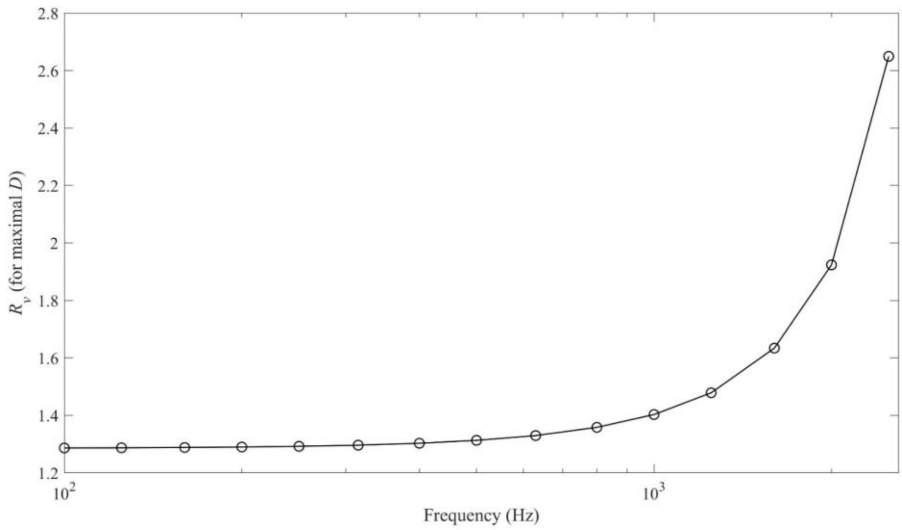

Figure 4. 3 Variation of R_v for maximal D with frequency for $R_r = 4/3$ and $r_o = 0.05m$.

Figure 4.4 illustrates the effect of R_v on the variation of sound radiation pattern H^* generated by the newly proposed source with $R_r = 4/3$ and $r_o = 0.05$ m at 500Hz. H^* is the sound magnitude $p(|\mathbf{x} - \mathbf{x}_s|, \varphi)$ normalized by the corresponding strongest sound radiation magnitude. At $R_v = 1$ and 2, the radiation is monopole-like and the direction of stronger sound radiation is at $\varphi = \pm 90°$ and $\varphi = 0°$ respectively. At minimum D ($D \sim 0$), the lateral sound radiation is very strong, leaving the frontal radiation insignificant (or even no frontal radiation). As R_v increases, a gradual increase in the frontal sound radiation strength is observed. However, the lateral and frontal sound radiation is 180°out-of-phase (not shown here). At $R_v = 1.3132$ where maximum D is recorded, the radiation is extremely frontal. Comparing to the results of piston source, shown in Figure 3.3(b), and that of the compound source of Chen et al. [Chen et al., 2010], the newly proposed source can produce more directional sound radiation even its diameter is small. The newly proposed source also gives a directivity much stronger that those of the multipoles of Beauvilain et al. [Beauvilain et al., 2000] at 250 Hz. Basically, similar pattern of D variation with R_v can be observed at other frequencies.

The control results by using the new piston-like secondary sources are compared with the case of using baffled piston sources of identical size ($r_o = 0.05m$) with the same geometric setting ($N = 5$, $d_s = d_e = 3$m), displayed in figure 4.5 at the frequency of 125 Hz (a) and 500 Hz (b). There is a remarkable improvement in the off-axis area, while the noise reduction in the middle is similar to that of piston sources. The direction of $\varphi = 0°$ has a deep trough of nearly 30 dB at 125 Hz and 20dB at 200Hz after active control, and the resultant acoustic far-field controlled by the new secondary sources benefits significantly due to the non-existing strong spillover effects.

In consideration of less sensitivity of the actuation parameter of velocity ratio R_v and the smaller the size of secondary source for practical implementation, the radius of the new source in the following discussion is kept at $0.05m$, and the value of R_r is set as $4/3$ without loss of generality. Besides, R_v is frequency-dependent, varying with respect to the frequency of interest as illustrated in figure 4.3.

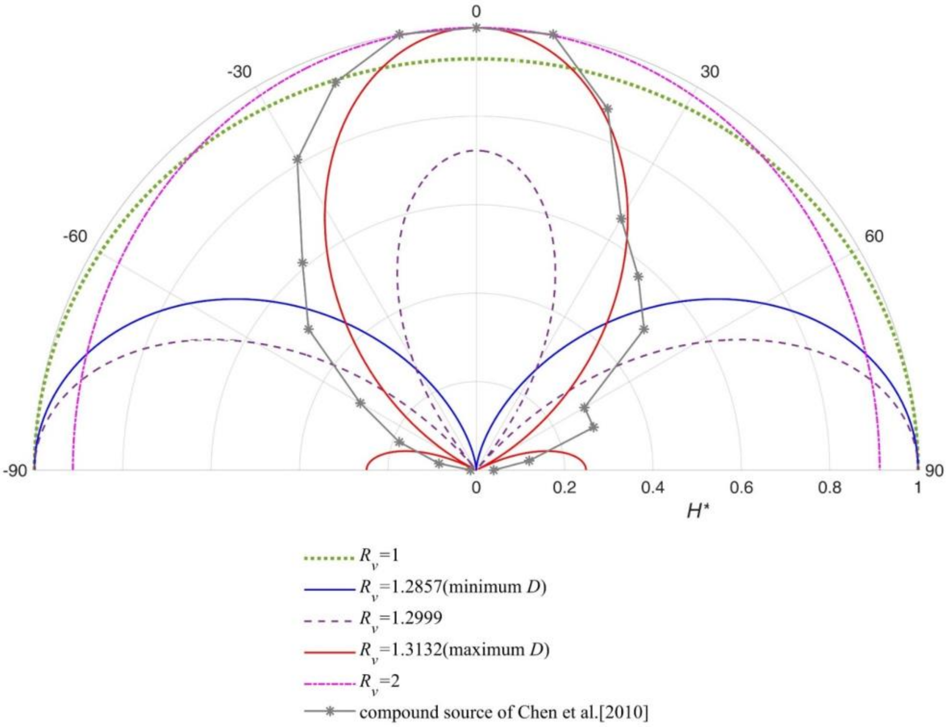

Figure 4. 4 Variation of directional sound radiation patterns of the newly proposed source with different R_v at the frequency of 500 Hz, $r_o = 0.05m$.

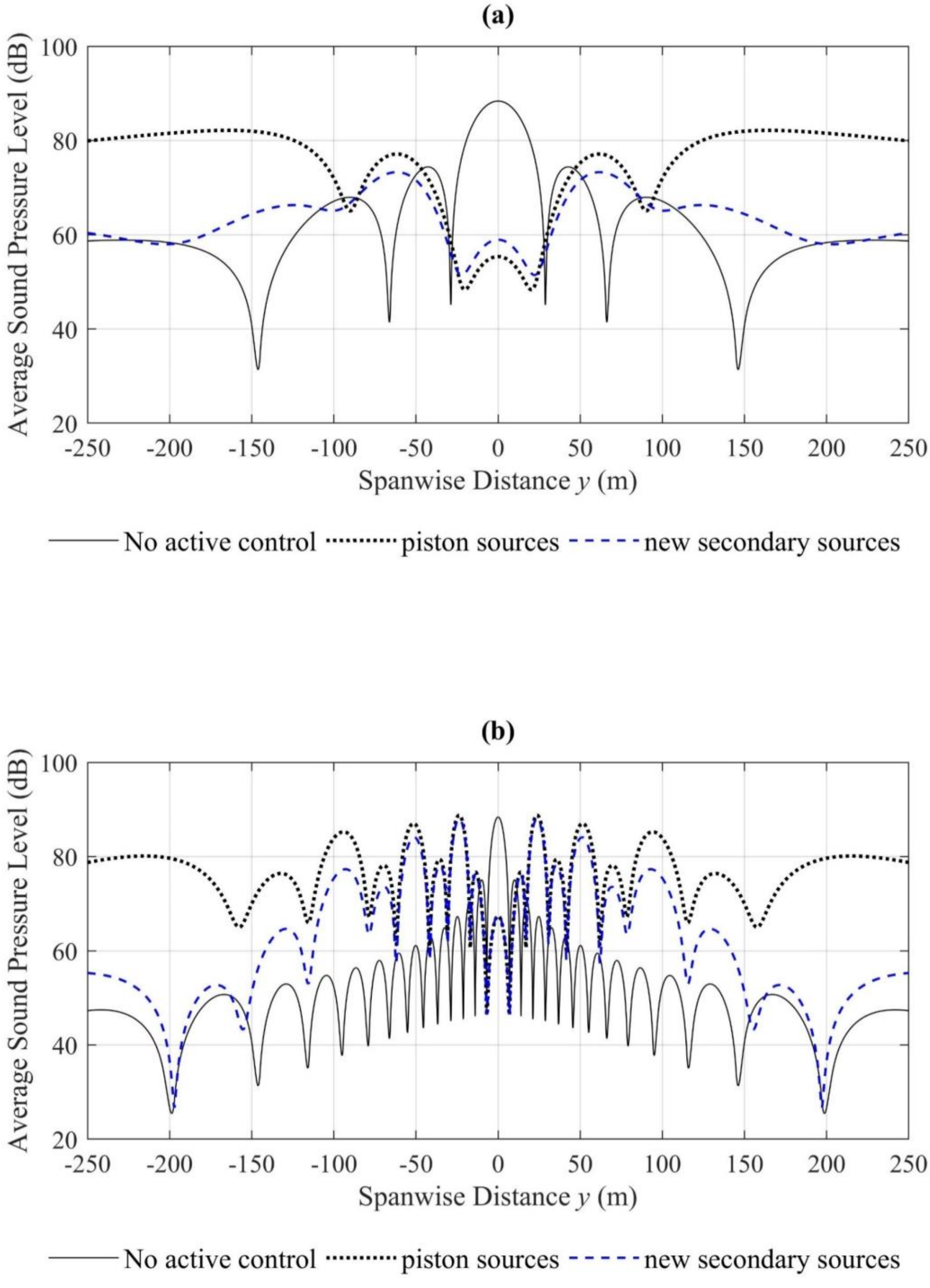

Figure 4. 5 Comparison of spanwise variations of averaged sound pressure level on the monitoring plane with piston sources of $r_o = 0.05m$ and newly proposed secondary sources of $r_o = 0.05m$ respectively, $N = 5$, $d_s = d_e = 3m$: (a) at frequency of 125 Hz; (b) at frequency of 500 Hz.

Another control performance result by the new secondary sources with respect to the spanwise distribution of the far-field sound pressure level on the monitoring plane is shown in figure 4.6. The active sound cancellation performance resulted from using the new source with $R_r = 4/3$, at the frequency of 500 Hz is represented by blue dot curve and red dash curve with N kept at 5 and other system configurations ($d_s = d_e = 3m$) the same as those in figure 3.3(a) for $r_o = 0.25m$ and $r_o = 0.05m$ respectively. R_v gives the most directional sound radiation at the tested frequency and for the given radius of new sources, which $R_v = 2.6492$ for $r_o = 0.25m$ and $R_v = 1.3132$ for $r_o = 0.05m$.

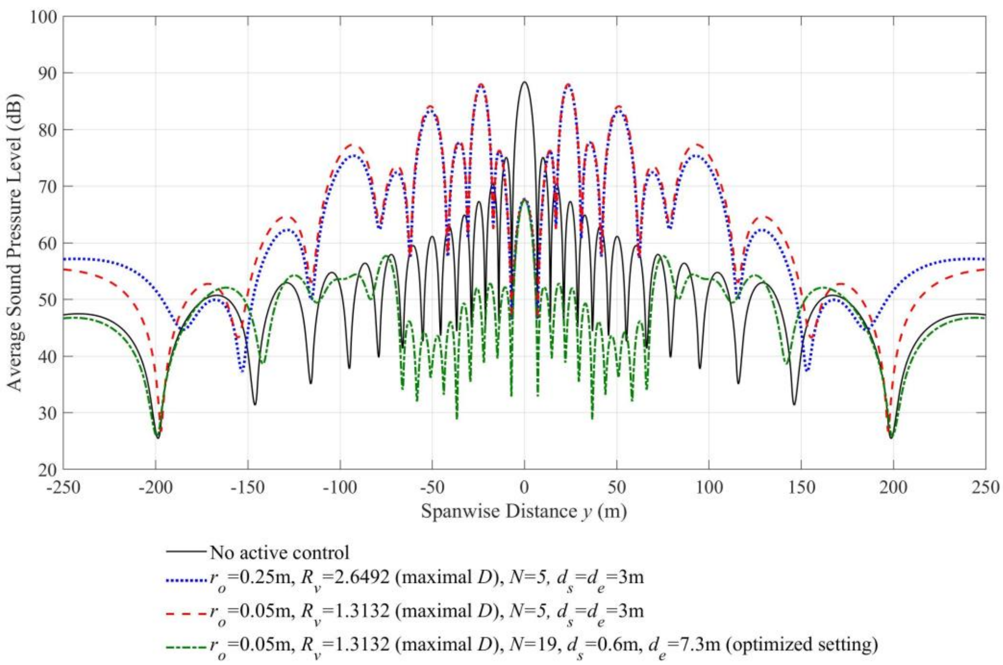

Figure 4. 6 Spanwise variation of average sound pressure level on the monitoring plane obtained using the new secondary sources ($R_r = 4/3$) at the frequency of 500Hz.

It is noticed by comparing the results shown in figure 3.3(a) and 10 that the spatial span of effective active attenuation is very much enlarged by using the newly proposed secondary source. The magnitude of the resultant sound field is also significantly lower than that resulted from the single piston secondary source cases. In addition, reflected by the discussion in the previous section that the size of the new source causes little change to its radiation pattern, it is suggested that using larger radii of the newly proposed secondary sources will not improve the overall active noise reduction very much. It should be also noted that smaller overall size of the new source enables the adoption of more secondary sources in the active control system, though the system will become more complicated afterward. The foregoing discussions will be focused on the effects of d_s and d_e on the global performance of the active control implemented using the new secondary source for different N.

4.2 Optimization of the positions of secondary sources and error microphones

4.2.1 The establishment of the optimization criterion

Following the preliminary study on the use of newly introduced secondary sources, a further optimization on the positions and numbers of the secondary sources and error microphones will be considered in this section. With the secondary sources dictated by the least square algorithm, the choice of the optimal spacing distance and ideal number of secondary sources and error microphones is examined by a performance index that could reflect the overall noise reduction capability of the active control system. The total potential energy reduction on the monitoring plane S_{mp}, Δ, is used as the descriptor of global control effectiveness:

$$\Delta = -10\log_{10}\left(\iint_{S_{mp}} \left| p + \sum_{n=1}^{N} p_{sn} \right|^2 dydz \Big/ \iint_{S_{mp}} |p|^2 dydz \right) \qquad (4.5)$$

In the surface integration, S_{mp} is discretized into regular grids with dimensions dy and dz set according to the frequency of interest and for simplicity, $dy = dz$. It should be noted that while d_s is restricted by the length of the linear source and the size of the secondary source, d_e can vary over a larger range for global control effectiveness. Thus Δ is an averaged measure covering the extent of the monitoring plane as a “global” criterion of a certain region.

4.2.2 The use of the new secondary sources comparing with the piston sources

The contour plots of the noise reduction index Δ with respect to the variations of the separating distance of control sources, d_s, and the spacing interval of error microphones, d_e, by using two secondary control sources at the frequency of 125 Hz are shown in figure 4.7. The figure 4.7(a) is the case of using two baffled circular piston sources, and the figure 4.7(b) of using two new secondary sources. In both cases d_s is ranging from $1m$ to $20m$ and d_e from $1m$ to $250m$. Besides, all the secondary sources are positioned symmetrically about y-axis. The noise reduction index results of using successively increasing numbers of three to six secondary sources at the frequency of 125 Hz are displayed in figure 4.7 to figure 4.11 respectively with the same range of the corresponding separating distances of controllers and microphones.

From figure 4.7 to figure 4.11, it is suggested that the best performance happens when the spacing of secondary sources are not identical to that of error microphones. Whatever number of secondary sources chosen to use in the control system, the optimal separating distance will not exceed $5m$. In terms of the separating distance of error microphones, the effective separation distances between the adjacent sensors for a validly performance cover a larger range than the ones of control sources. However, the best settings for the optimum intervals of the error sensors are almost less than $100m$.

Comparing the performance descriptor Δ of the newly proposed secondary sources to the traditional directional control sources of baffled circular pistons, we will find out that the new source performs generally better, especially when the numbers of controllers are reasonably small. More information will be drawn from the detailed inspection of the acoustic far field in subsequent analysis.

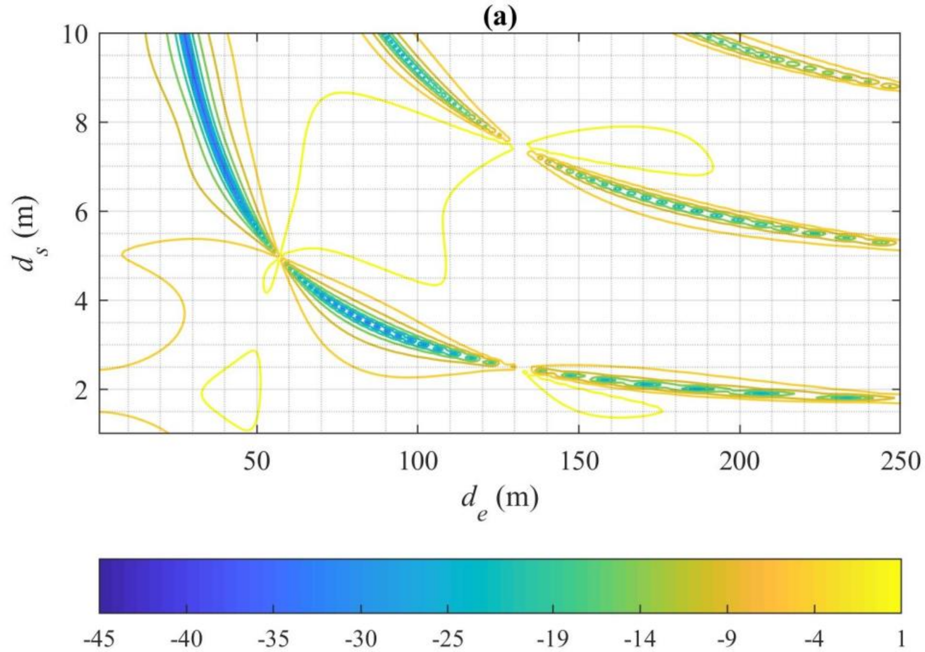

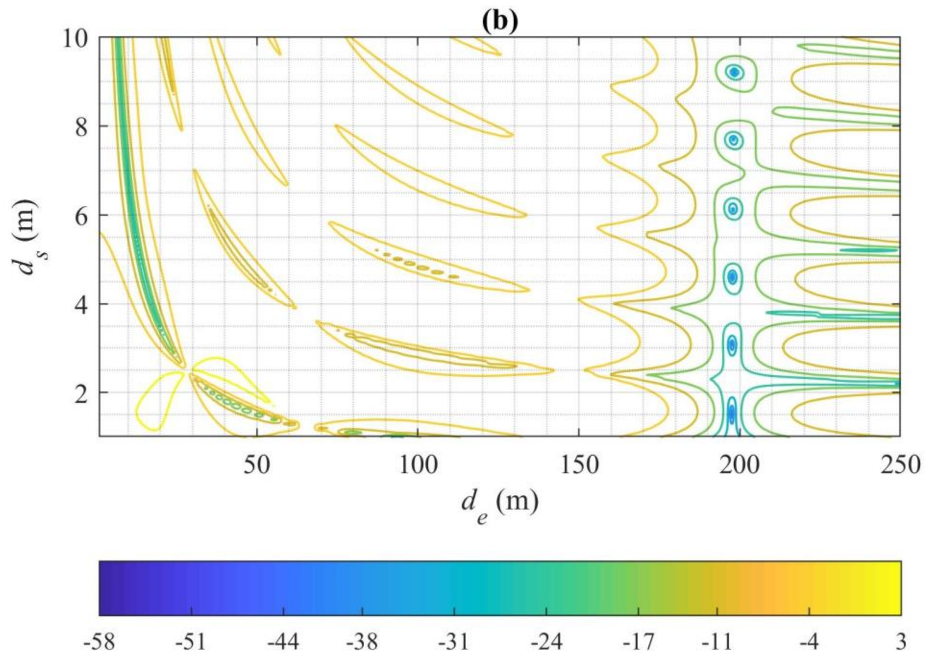

Figure 4. 7 Contour plots of Δ in dB with respect to d_s and d_e (at 125 Hz) (a) two baffled circular piston sources used; (b) two new secondary sources used.

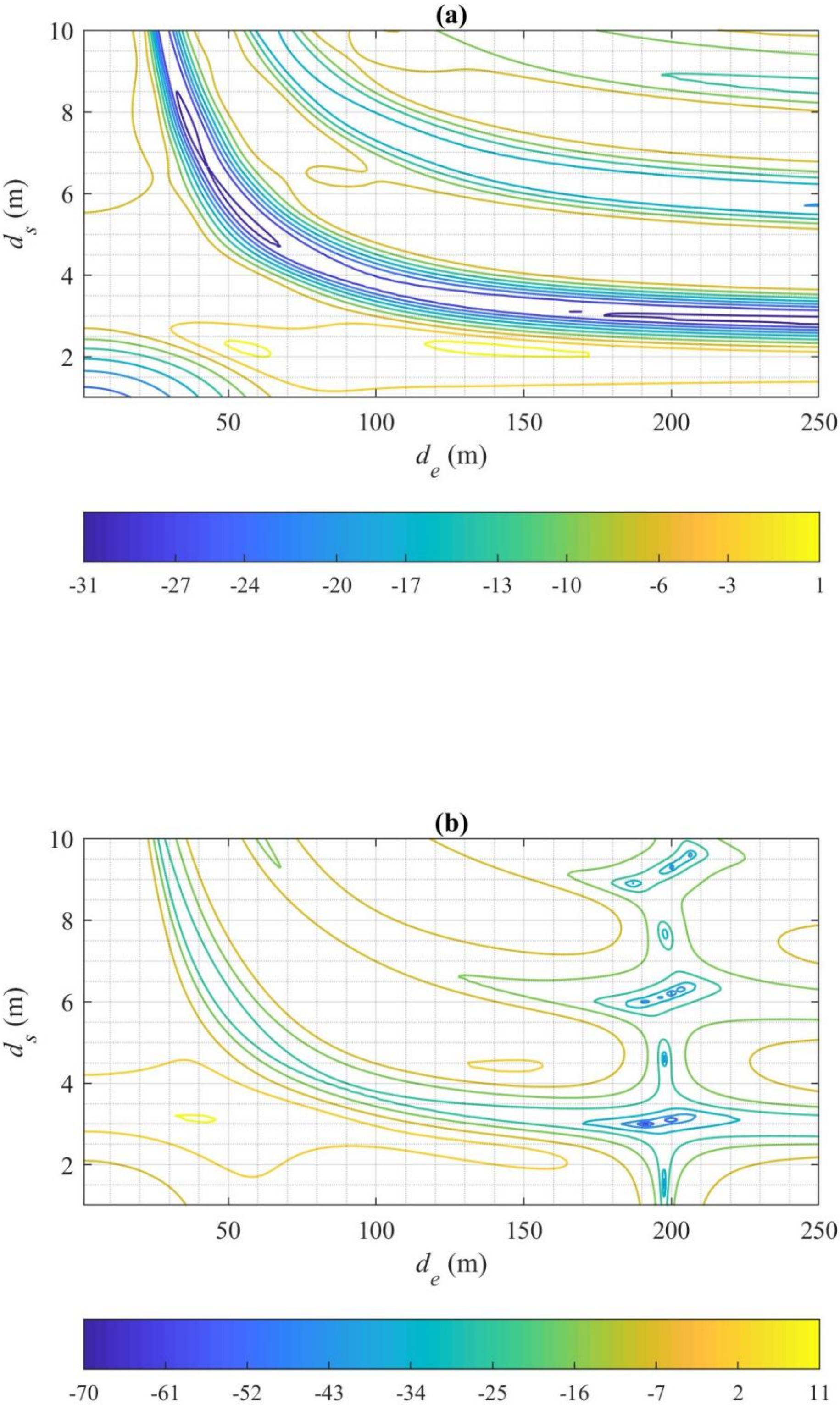

Figure 4. 8 Contour plots of Δ in dB with respect to d_s and d_e (at 125 Hz) (a) three baffled circular piston sources used; (b) three new secondary sources used.

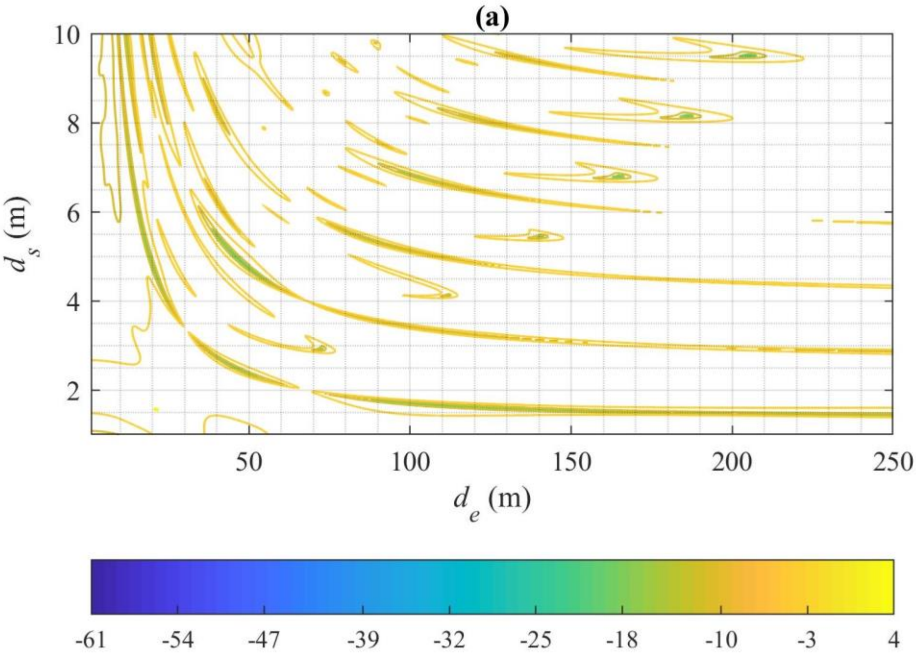

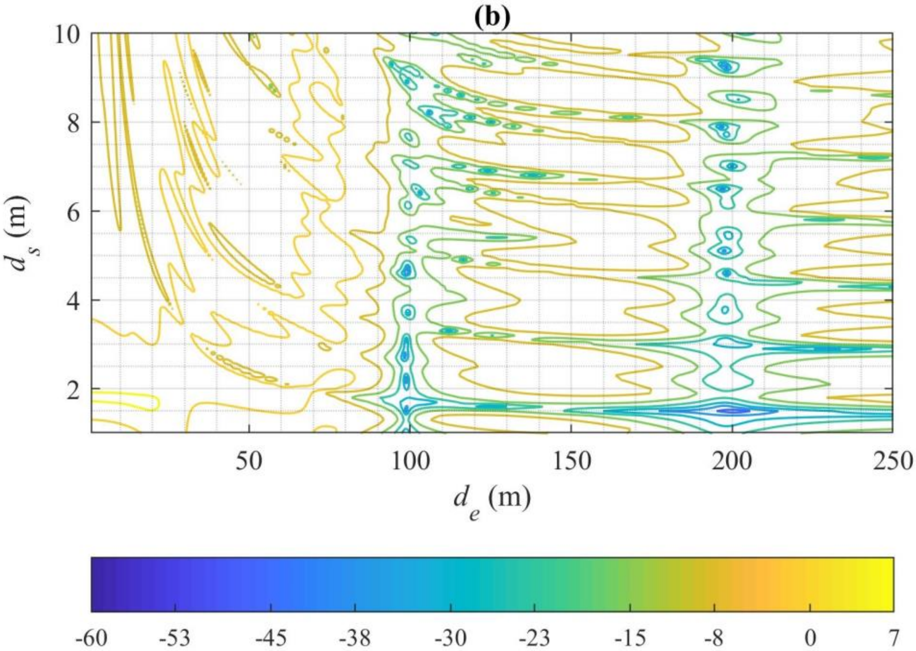

Figure 4. 9 Contour plots of Δ in dB with respect to d_s and d_e (at 125 Hz) (a) four baffled circular piston sources used; (b) four new secondary sources used.

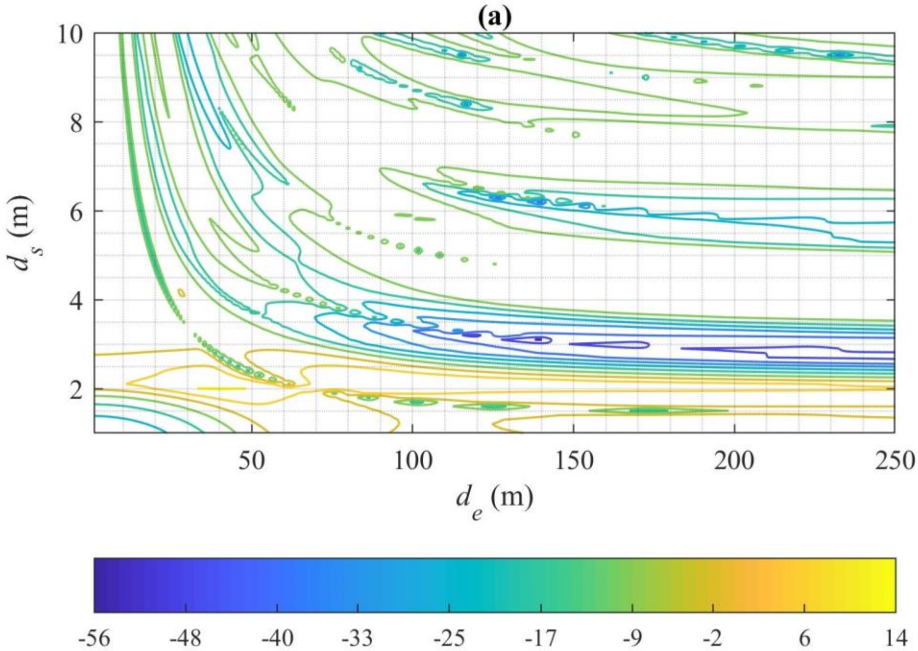

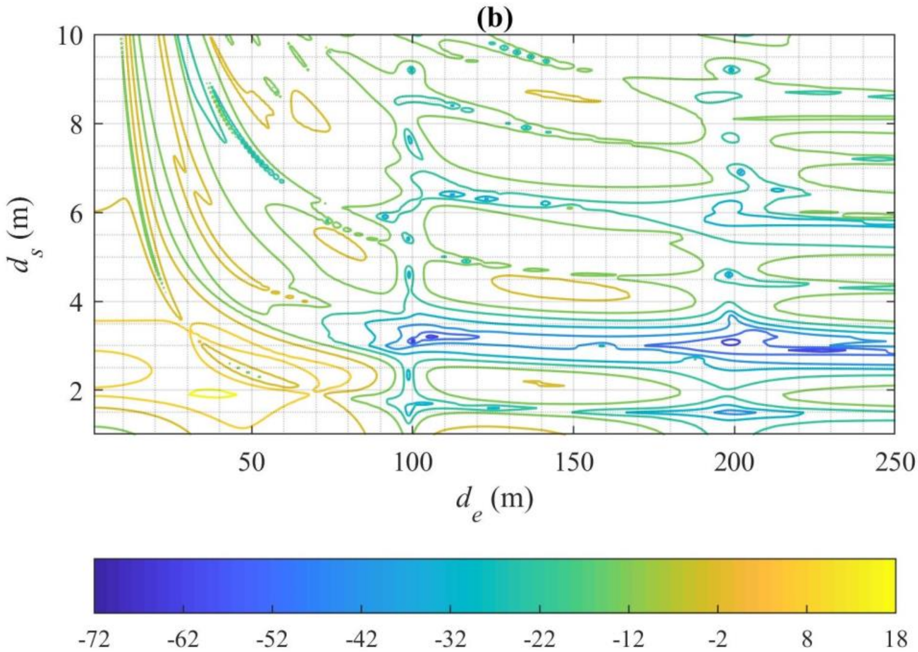

Figure 4. 10 Contour plots of Δ in dB with respect to d_s and d_e (at 125 Hz) (a) five baffled circular piston sources used; (b) five new secondary sources used.

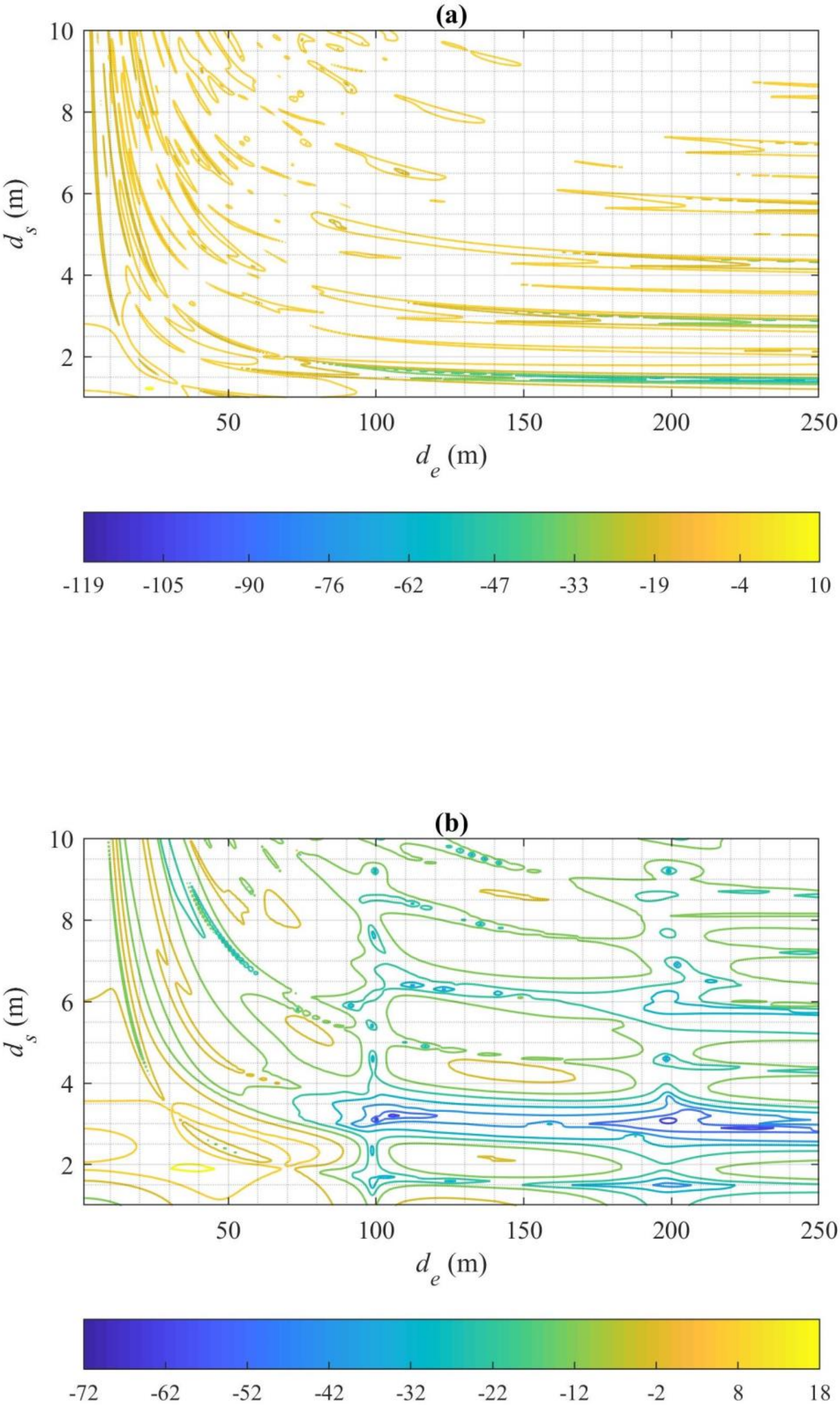

Figure 4. 11 Contour plots of Δ in dB with respect to d_s and d_e (at 125 Hz) (a) six baffled circular piston sources used; (b) six new secondary sources used.

Table 4. 1 The optimal spacing distances of d_s and d_e by maximizing Δ in the cases of using successively increasing numbers of secondary sources (at 125 Hz)

N	Piston sources ($a = 0.5m$)	Novel sources ($r_1 = 0.05m$)
2	$\Delta = 1.9dB$; $d_e = 20.7m$; $d_s = 1.0m$	$\Delta = 3.7dB$; $d_e = 18.1m$; $d_s = 1.7m$
3	$\Delta = 2.0dB$; $d_e = 136.8m$; $d_s = 2.2m$	$\Delta = 11.2dB$; $d_e = 39.7m$; $d_s = 3.1m$
4	$\Delta = 4.0dB$; $d_e = 21.2m$; $d_s = 1.6m$	$\Delta = 7.7dB$; $d_e = 17.5m$; $d_s = 1.7m$
5	$\Delta = 14.2dB$; $d_e = 36.3m$; $d_s = 2.0m$	$\Delta = 18.3dB$; $d_e = 36.9m$; $d_s = 1.9m$
6	$\Delta = 10.3dB$; $d_e = 23.3m$; $d_s = 1.2m$	$\Delta = 18.4dB$; $d_e = 21.1m$; $d_s = 1.2m$

To quantitatively reveal the properties of the optimum separating distances between the control sources and error microphones, the detailed contours of the control performance descriptor Δ with respect to d_s and d_e are plotted from figure 4.12 to figure 4.16, where the attention is paid on the active control results as the separation distance of control sources varying from $1m$ to $5m$ and the spacing interval of error microphones range from $1m$ to $100m$. Besides the detailed contours are focused on the positive Δ values. The global optimums of d_s, d_e and the related Δ are listed in table 4.1, for different numbers of secondary sources from two to six. It is indicated that with the same number of secondary sources used, the active control result by using the new introduced secondary sources are better than using the circular piston secondary sources at the low frequency of 125 Hz. In some situations, the new secondary sources can achieve a greater Δ value even with smaller number of control sources used than the baffled circular piston sources. The conventional piston sources will not efficiently reduce the acoustic radiation from a finite line source of $10m$ in such a large area framed by the observation plane, until progressively adding the number of secondary sources used up to 5. Concerning the novel directional secondary sources, the use of odd numbers, say 3 or 5, of secondary sources is prominently better performance than the even numbers cases, say 2 or 4; the similar phenomenon can be observed for piston sources. Even though using five or six piston sources can also provide a comparable control result with that of the new sources, the total noise attenuation on the monitoring plane by new sources still performs ahead of several more dBs of noise reduction. It is suggested that the location of the secondary source at the acoustic axis of primary line source is essentially to create relatively greater overall noise reduction. However, if even numbers of secondary sources are configured in the proposed active control system, the two sources in the middle will be much closer to the normal of primary line source for optimum performance.

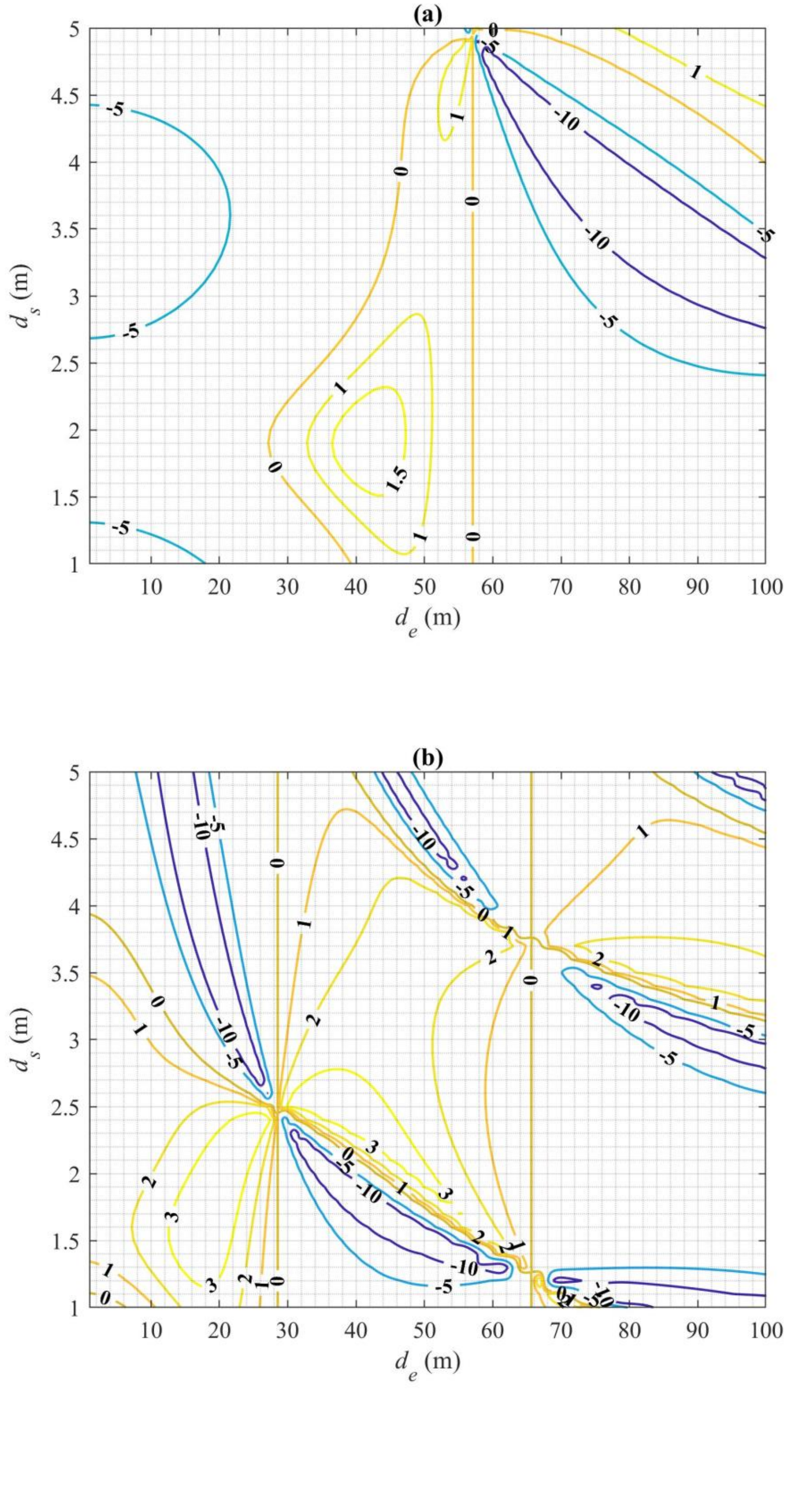

Figure 4. 12 Detailed contour plots of Δ in dB with respect to d_s and d_e (at 125 Hz) (a) two baffled circular piston sources used; (b) two new secondary sources used.

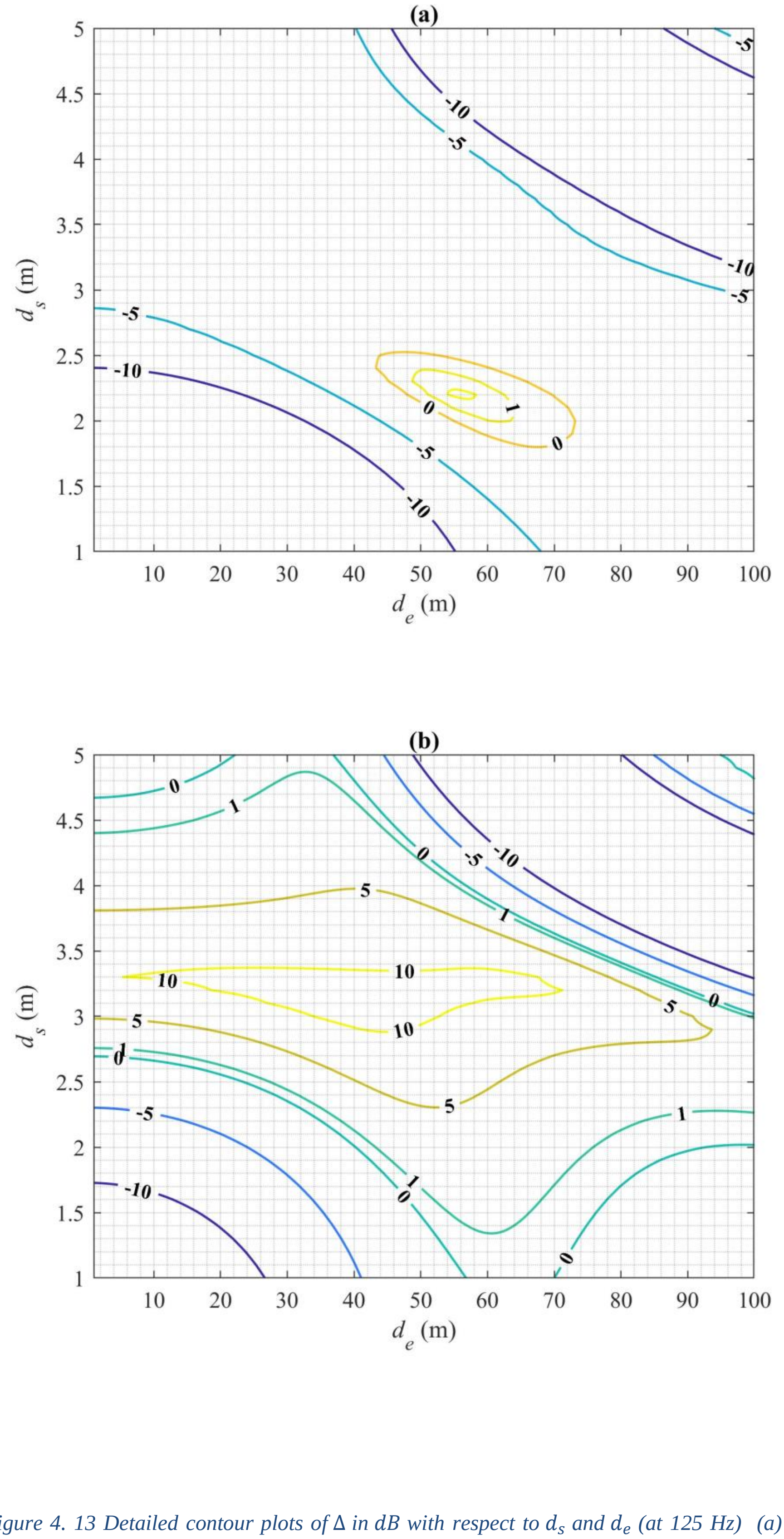

Figure 4. 13 Detailed contour plots of Δ in dB with respect to d_s and d_e (at 125 Hz) (a) three baffled circular piston sources used; (b) three new secondary sources used.

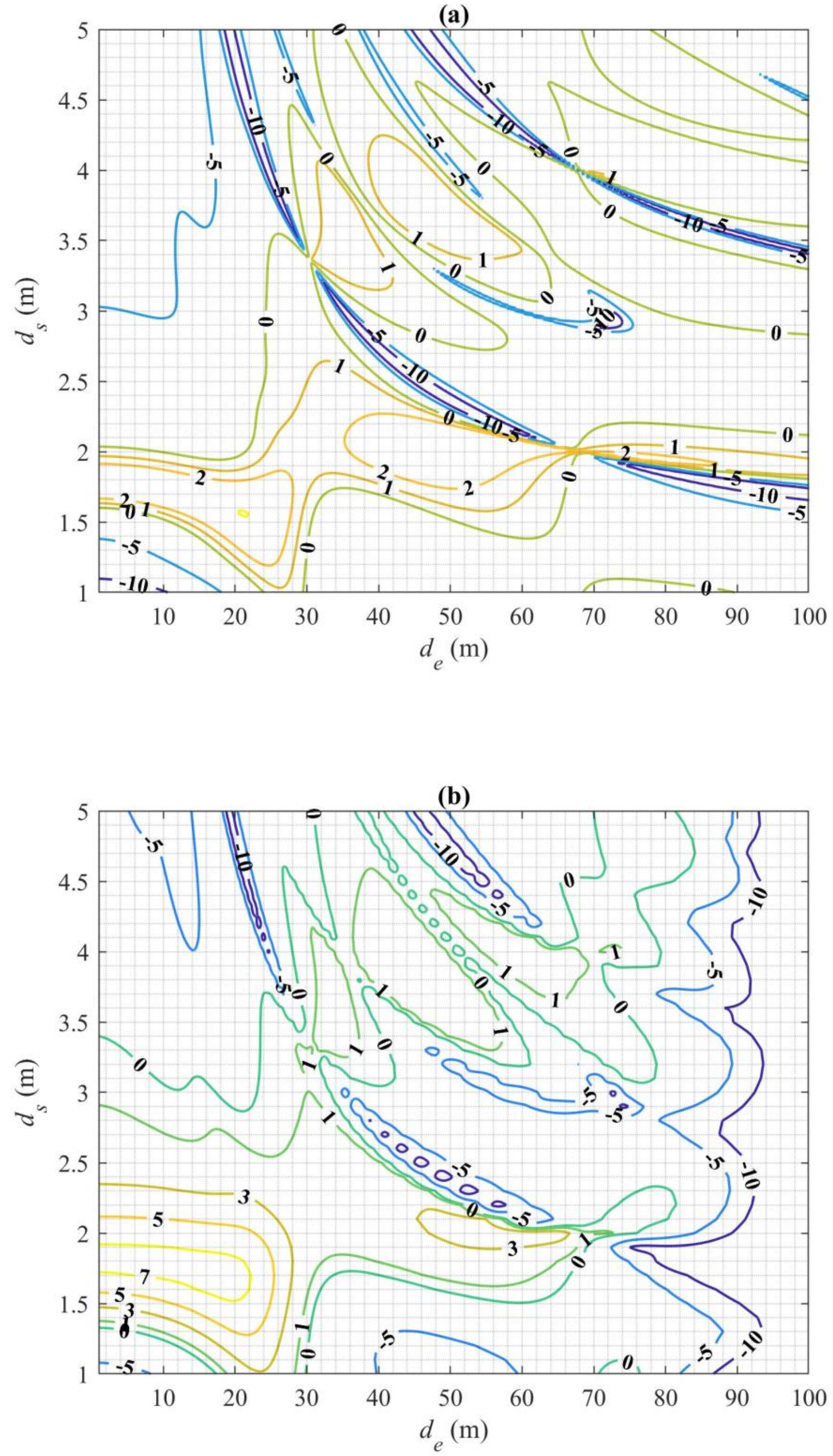

Figure 4. 14 Detailed contour plots of Δ in dB with respect to d_s and d_e (at 125 Hz) (a) four baffled circular piston sources used; (b) four new secondary sources used.

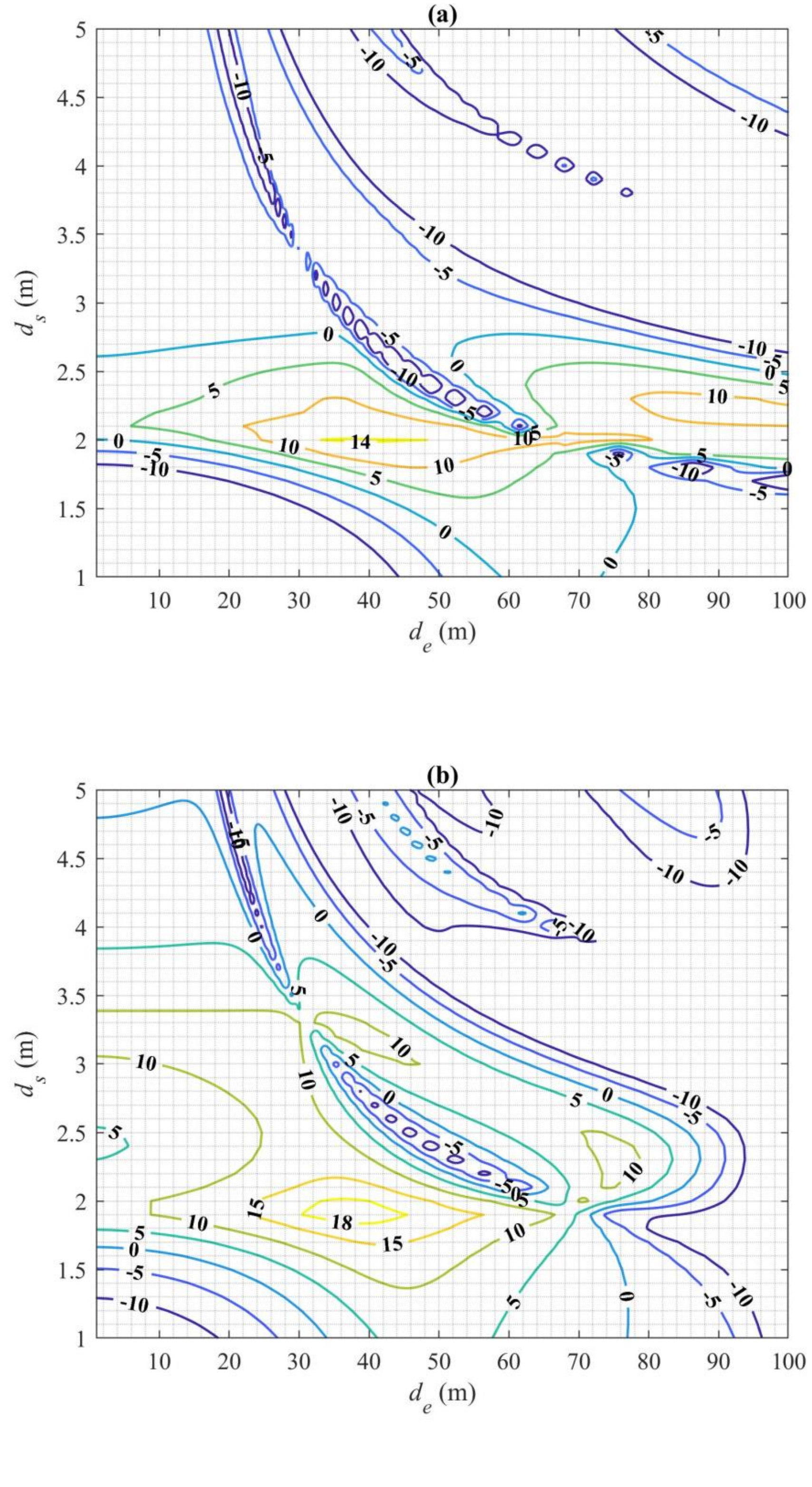

Figure 4. 15 Detailed contour plots of Δ in dB with respect to d_s and d_e (at 125 Hz) (a) five baffled circular piston sources used; (b) five new secondary sources used.

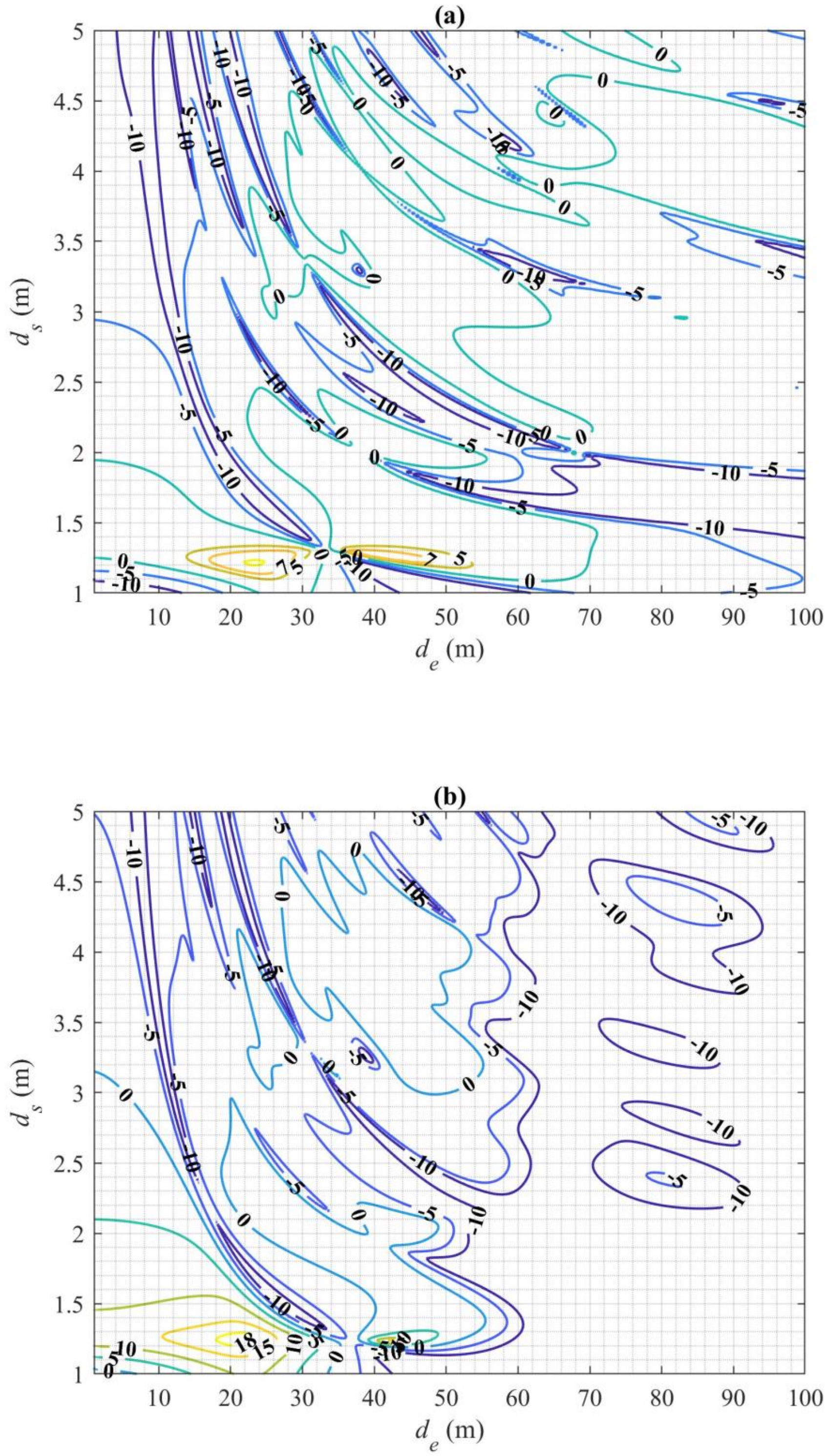

Figure 4. 16 Detailed contour plots of Δ in dB with respect to d_s and d_e (at 125 Hz) (a) six baffled circular piston sources used; (b) six new secondary sources used.

From examining the detailed contours that illustrate the effects of d_s and d_e to the performance descriptor Δ, it is shown that the maximum Δ becomes greater as the number of secondary sources used increases, while the range of d_s and d_e for good active control performance shrinks. But d_s is more "sensitive" than d_e for certain good performance. Generally, odd numbers of control sources perform better than even numbers; the new sources provide more excellent results comparing with the traditional baffled piston sources, both in regard of the global optimal Δ and the corresponding acceptable d_s and d_e range.

In addition, the far-field sound pressure level distributions of the above mentioned cases with optimized positions concerning all the controllers and acoustical sensors are plotted in figure 4.17, in which y-axis represents the value of the sound pressure level at the observation plane averaged along z-coordinate as shown in figure 3.1. These figures display a detailed noise control result of the proposed active system in the far field.

From figure 4.17, it is illustrated that as two control sources are used the control results for both piston sources and novel sources are inferior to an acceptable level, although the novel secondary sources provide fair better performance. As shown in figure 4.17(a), both types of control sources reduce the sound pressure in the middle area of the observation plane, while the novel sources provide more reduction of several dBs. But in both cases, the sound pressure in two side positions increases with a significant margin.

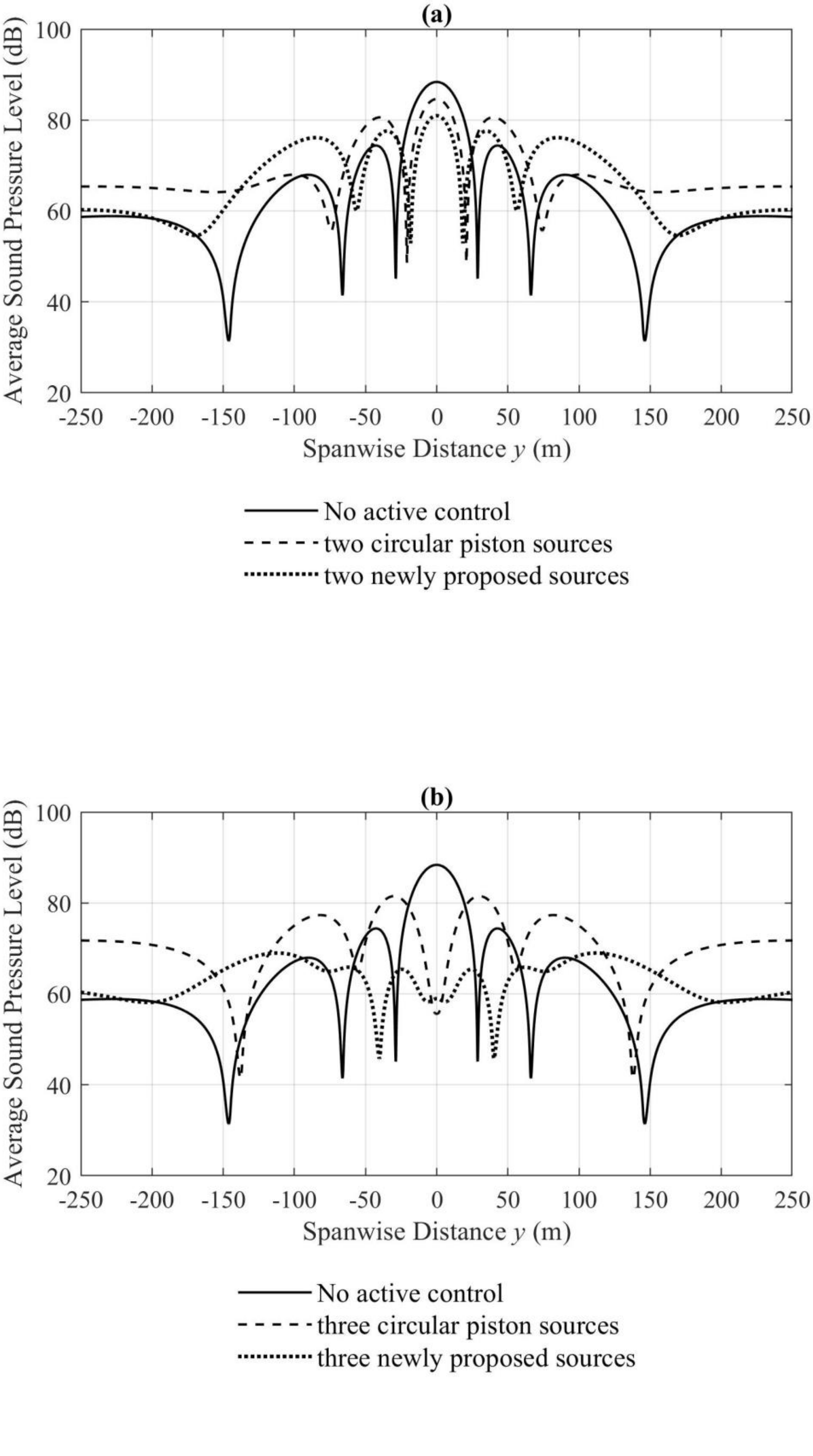

Figure 4. 17 Spanwise variation of averaged sound pressure level on the monitoring plane at the frequency of 125 Hz with different numbers of piston sources and newly proposed sources respectively

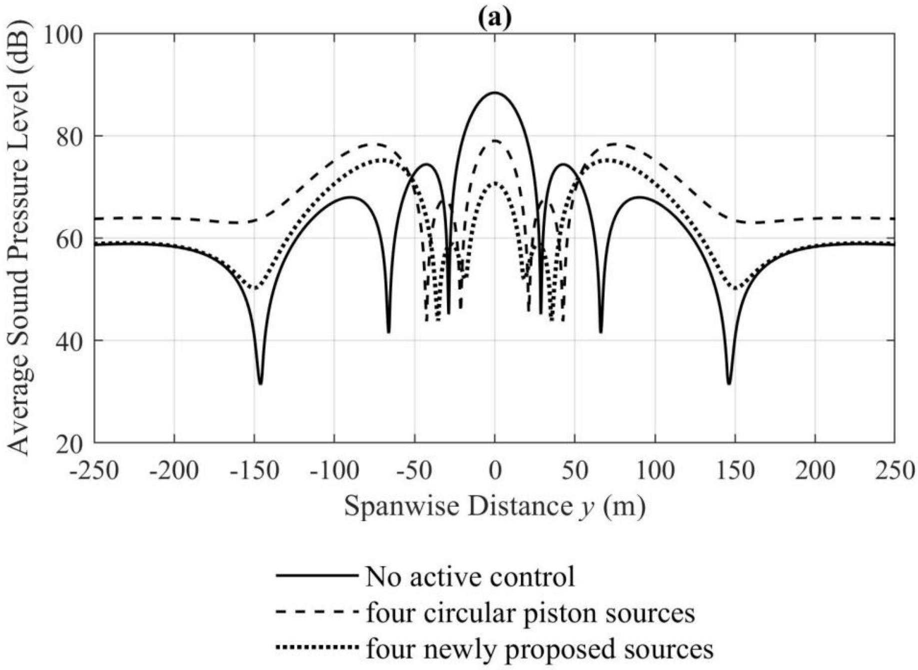

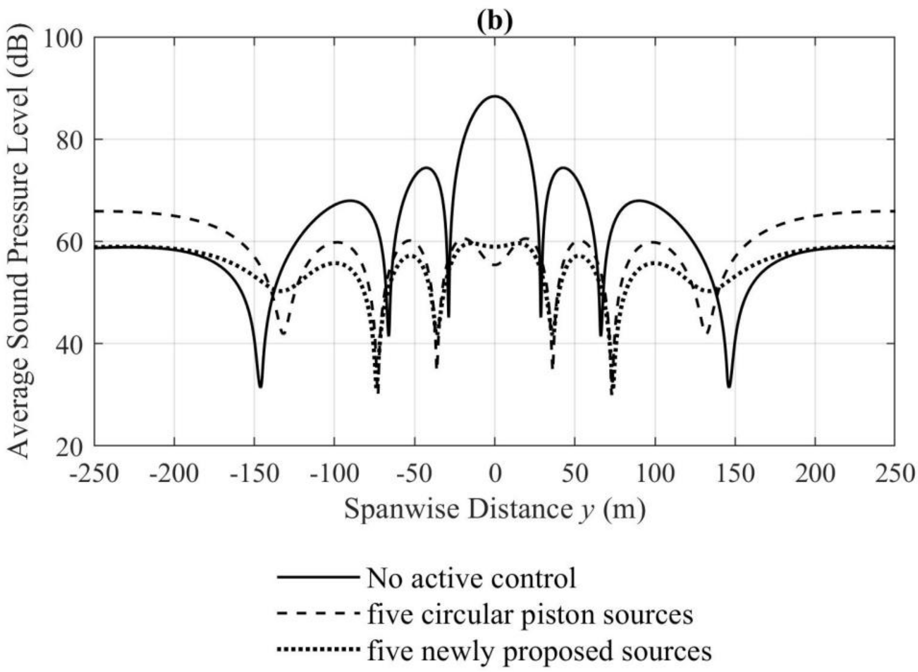

Figure 4. 18 Spanwise variation of averaged sound pressure level on the monitoring plane at the frequency of 125 Hz with different numbers of piston sources and newly proposed sources respectively

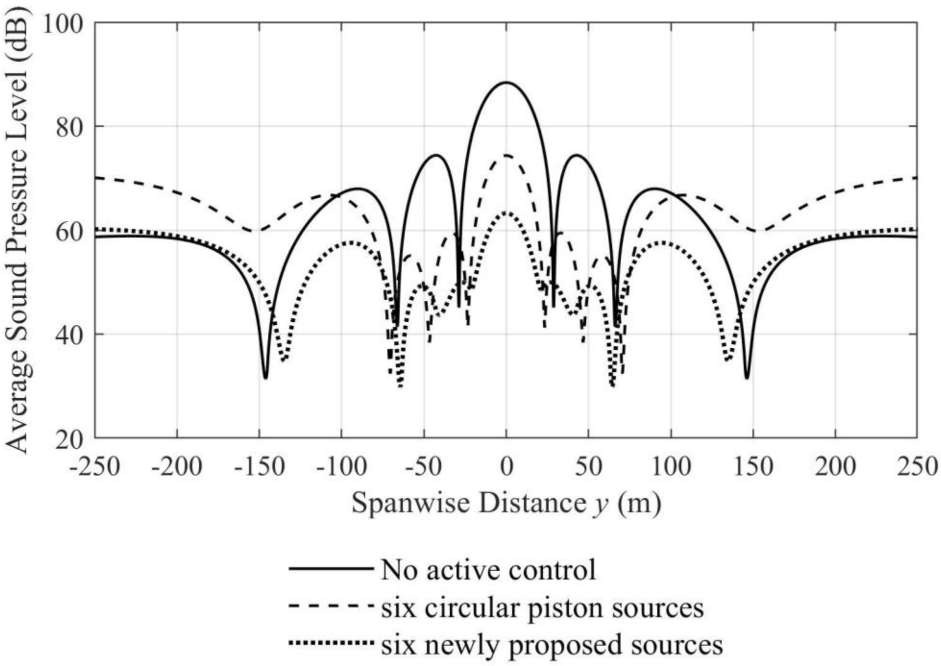

Figure 4. 19 Spanwise variation of averaged sound pressure level on the monitoring plane at the frequency of 125 Hz with different numbers of piston sources and newly proposed sources respectively

As three secondary sources are actuated in the active control system, the situation of the newly introduced novel directive secondary sources improves a lot, whereas the use of baffled circular piston sources remains ineffective with prominent sound increase at some positions away from the acoustic axis. Figure 4.13(b) suggests the optimal separating distances for error microphones are much more tolerant than the optimal spacing of control sources, for example, a noise reduction of $10dB$ considered. If four novel secondary sources are used, even with one additional secondary source, the control result is worse than the use of three new controllers. Meanwhile the optimal locations for the secondary sources and error sensors becomes less tolerant, displayed in figure 4.14. As the number of secondary sources used increased up to five, there is a sudden change in the overall noise reduction results. Both the new piston-like sources and conventional piston sources works pretty well as Δ is significantly greater than $10dB$, although the optimal spacing for the baffled piston sources is much more sensitive than the novel secondary sources. The sensitivity of d_s is also much higher than d_e. Comparing to the effective case of three novel sources used, the separating interval of five novel control sources for a significant overall noise attenuation is around $2m$, which is closer than the optimal secondary source spacing of approximately $3.3m$ when three new secondary sources are used. As can be inspected in figure 4.18(b), there is an overall noise reduction in the far field covering the range from $-250m$ to $+250m$ along the y-axis direction. The baffled piston sources are a bit less effective in the extreme off-axis area, while provide a deeper trough of the sound pressure in the middle. As the numbers of secondary sources used further increase, novel directive secondary sources can further improve the overall control performance within the range of monitoring plane, with more noise reduction everywhere except for the extreme off-axis positions. For the baffled circular piston sources, six piston sources cannot generate a large quiet zone as the case of five piston sources used, which shows that the middle secondary source is necessary for an improved active control result. Besides, when the configuration works quite well to provide a remarkable overall noise reduction, the optimal d_s and d_e for new sources and pistons are basically the same. This phenomenon is especially evident as shown in figure 4.15 and figure 4.16.

As illustrated by these profile plots from figure 4.17 to figure 4.19, the new directional sources generally provide better overall active control performance than the baffled circular pistons, which produced a smoother resultant sound field after control. As the numbers of the secondary sources engaged are small, say two or three controllers, the presence of the middle secondary source on the acoustic axis of the primary line source is critical for a significantly excellent performance. Even though six of these new piston-like sources can provide an acceptable control results, the use of odd numbers of secondary sources is more stable for a great overall noise attenuation from the case of even three novel directional controllers used. As for the optimal geometric configuration regarding the secondary sources and error microphones, it is suggested that the optimum locations are very similar whether piston sources are used or new sources where there is a great noise reduction occurring, that the performance descriptor Δ is greater than $10dB$. As shown in the previous discussion, the noise reduction index is a feasible indicator for the sound field after active control. If Δ is greater than $10dB$ there existing an acceptable overall active attenuation of primary source radiation within the range of the monitoring plane. Furthermore, as the active control performance descriptor, Δ, further increases, the extent of the sound pressure reduction in the far-field becomes more prominent. Finally, increasing the number of secondary sources used always improves the active control results, meanwhile the optimal spacing between secondary sources and error microphones will decrease accordingly.

An apparent merit of using the newly proposed secondary sources developed in this thesis is verified by comparing the use of three secondary sources, as indicated in figure 4.17(b). With only three controllers, the novel directional secondary sources achieve an extraordinary control result that attains a large quiet zone of significant attenuation in the middle and nearly causes no noise increase elsewhere. Even though, in figure 4.18(b), it suggests that using five baffled piston sources also can result in a very good overall performance. By using the same number of novel directional sources, it is still at great advantages in the extreme off-axis areas and on the implemented size of the controllers.

5 Effectiveness for broadband noise control

The previous analysis focuses on properties of the established active control system and the application of the newly proposed secondary sources mostly at the particularly low frequency of 125 Hz. The main advantage of the new source is to radiate a directional sound field starting from very low frequency, so that it is more effective to actively control an extended primary source than the conventional compact secondary sources. It also indicated that the size of the newly introduced secondary source is well-controlled, which make the proposed active control system can include substantial acoustic controllers within constraint linear space, which is an advantageous property for its application for the active broadband noise control.

In this chapter, we explore the possibility and effectiveness of the active control system illustrated in figure 2.1 with the use of the new secondary sources for a broadband primary noise radiation. The separating distances of the secondary sources d_s and of the error microphones d_e, i.e. the geometric configuration of the active control system, are determined by maximizing the performance descriptor Δ for the following discussion, which suggest the best active noise reduction can be for a given number of control sources at the frequency of calculation.

5.1 Using the odd numbers of secondary sources

To study the possibility of the newly proposed new sources for higher frequencies, the geometric configuration, i.e. d_s and d_e, need to be first optimized by maximizing Δ. As the extensive discussion in the last section, the combination of d_s and d_e affects significantly the global control effectiveness Δ at a certain frequency and a settled N value. It is also revealed that the secondary source array with odd number of sources performs better than its even counterpart at the frequency of 125 Hz, as also illustrated in figure 5.1 and figure 5.2. The cases of odd numbers of secondary sources used provides a greater optimal Δ, and the range of $\mathrm{d_s}$ and $\mathrm{d_e}$ for acceptable overall active noise reduction is relatively large than the situations when even numbers of controllers are engaged in this established control system. As shown in figure 5.1 (a), if three secondary sources are separated with a distance of $3.3m$, the error microphones spacing interval can be varying from $10m$ to $70m$ apart, in which the active control performance evaluated by Δ is always greater than 10dB at the frequency of 125 Hz. By adding the number of new secondary sources to seven, the optimal Δ further increases, and the choice of the separation distances of the secondary sources and error microphones for a decent active noise attenuation, say greater than 10dB, is still very large. Although these results are calculated at the frequency of 125Hz, it appears that a larger N will result in larger optimal Δ, which will be discussed in detail later at other frequencies. Moreover, the separating distance of the secondary sources d_s for achieving optimal Δ values becomes smaller. It is illustrated that if more secondary sources are used in the proposed active control system, the spacing between them shrinks accordingly, but the maximal Δ will increase. Comparing with the case of using four new secondary sources, as displayed in figure 5.1(b), the optimal Δ value and the range of d_s and d_e both deteriorate, where the two control sources in the middle will becomes more closely positioned to offset the missing of the secondary source at the acoustic axis of the primary line source.

In order to reveal a more general trend that the odd number of control sources will be a better choice, figure 5.3 to figure 5.8 shows the contours that indicate relationships of d_s and d_e to system performance Δ by using two to seven secondary sources respectively at discrete frequencies from 125 Hz to 250 Hz. By the information drawn from each subplot, several trends become evident. The active control performance for a given number of secondary sources deteriorates as the frequency of primary source increases. For example, in figure 5.4 (a), as three new secondary sources are activated at the frequency of 125 Hz, the optimal Δ is above 10dB and there is a large range of d_s and d_e that the performance descriptor is greater than 10dB; when the frequency increases to 175 Hz, as shown in figure 5.4 (c), the optimal Δ decrease to about 3dB and the corresponding system configuration for this performance shrinks remarkably; the active control system will not give any positive Δ value at frequency of 250 Hz if only three secondary sources are used, displayed in figure 5.4 (f). Similar phenomena will be discovered when different numbers of new secondary sources are used. It is also obvious as shown in figure 5.9, in which the optimal Δ at each frequency from 125Hz to 250Hz with 25Hz increment step by using two to seven newly proposed secondary sources separately. The control results using odd numbers of control sources are represented in red curves, and even ones in blue.

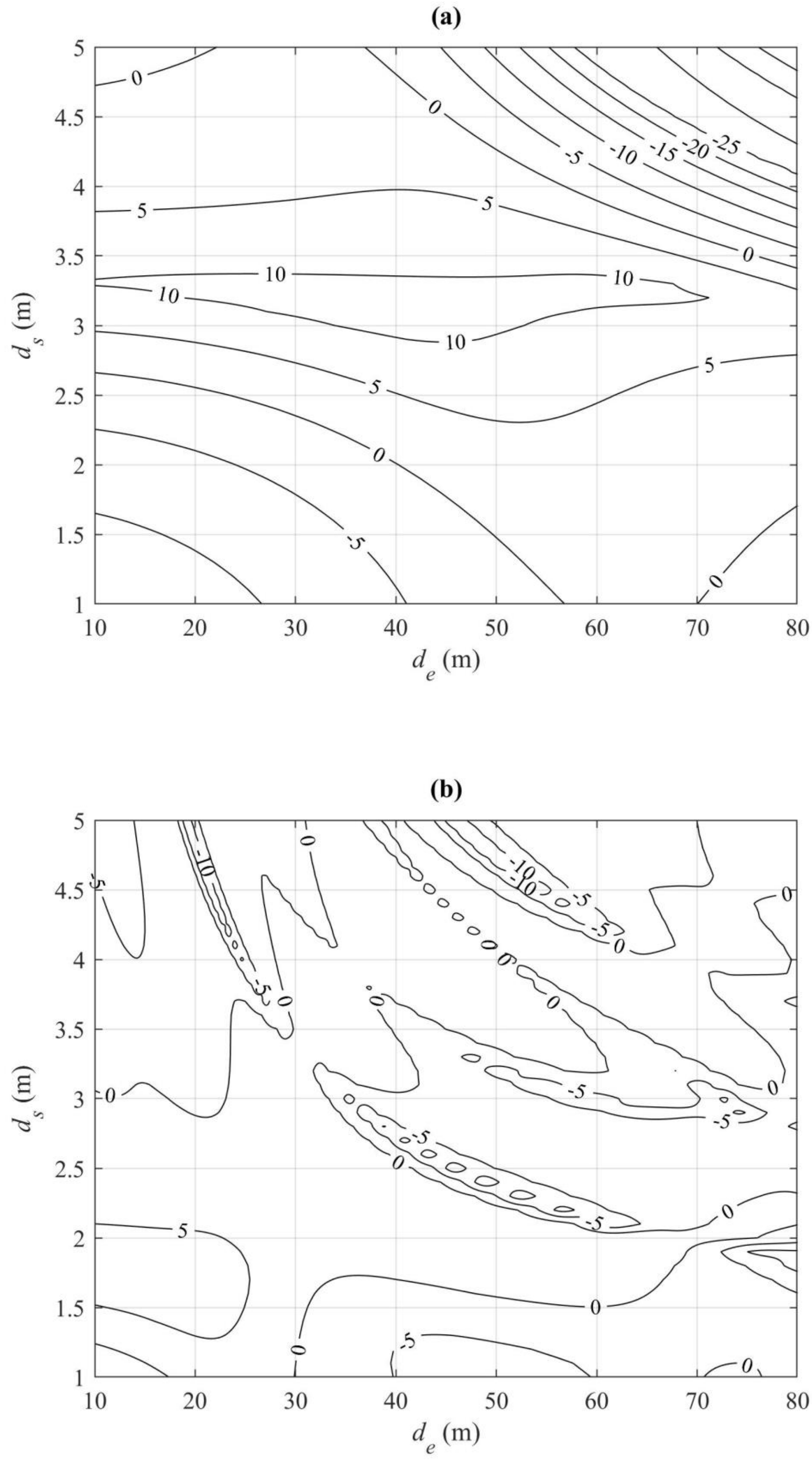

Figure 5. 1 Variations of Δ *with* N, d_s *and* d_e *at the frequency of 125 Hz.* $r_o = 0.05m$, $R_r = 4/3$, $R_v = 1.2874$. *(a)* $N = 3$*; (b)* $N = 4$.

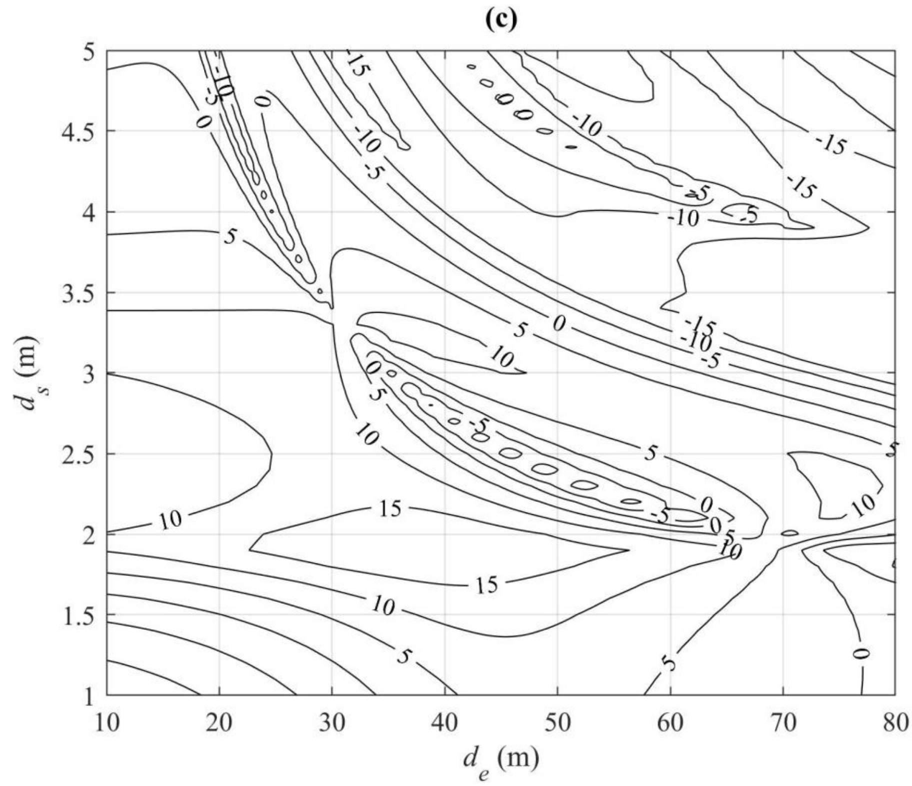

Figure 5. 2 Variations of Δ *with* N, d_s *and* d_e *at the frequency of 125 Hz.* $r_o = 0.05m$, $R_r = 4/3$, $R_v = 1.2874$, $N = 5$.

As illustrated in figure 5.9, by increasing the number of secondary sources, the active control result of optimal Δ will be improved dramatically, and the relevant varying range of d_s and d_e for the same active control results will be expanded consequently. According to figure 5.9, three secondary sources obtains about 12dB of Δ at frequency of 125 Hz, while five new sources can achieve approximately 18dB and seven new sources even up to 20dB, the same as to other frequencies; similarly, six secondary sources outperforms four secondary sources, which is better than only two new sources incorporated in the control system. Comparing the concerned varying range of d_s and d_e with three new sources activated that has the active control performance of Δ greater than 10dB in figure 5.4 (a) to the related d_s and d_e range with five secondary sources in figure 5.6 (a), or comparing the range of Δ above 15dB with five secondary sources in figure 5.6 (a) to that with seven secondary sources in figure 5.8 (a), it can be observed that the corresponding range of d_s and d_e of the latter case is comparatively bigger. Similar trend is found for the even numbers of new sources engaged.

Another conclusion can be drawn here, as same as discussed in the previous chapter, is that the use of odd numbers of control sources is better than the situations of even control sources. Although the active performance at the frequency of 200Hz, 225Hz or 250Hz by three new sources is worse than the cases by two. Mostly the overall active noise reduction evaluated by Δ is greater when odd numbers of controller are engaged in the active control system than even number. As the number of new sources is up to seven, the Δ does not decrease very much as frequency increases, while six new sources can provide an excellent control result at 125 Hz and then deteriorates significantly for higher frequencies. Besides, the tolerant separation range regarding secondary sources and error microphones of odd numbers of secondary sources is reasonably large than that of even numbers of sources for comparable noise reduction. For instance, the varying range of d_s and d_e for Δ greater than 7dB with three secondary sources at 125 Hz in figure 5.4 (a) is bigger than that with four secondary sources in figure 5.5 (a); or the d_s and d_e range for Δ above 10dB with five secondary sources at 175 Hz in figure 5.6 (b) is bigger than that with six sources in figure 5.7 (b).

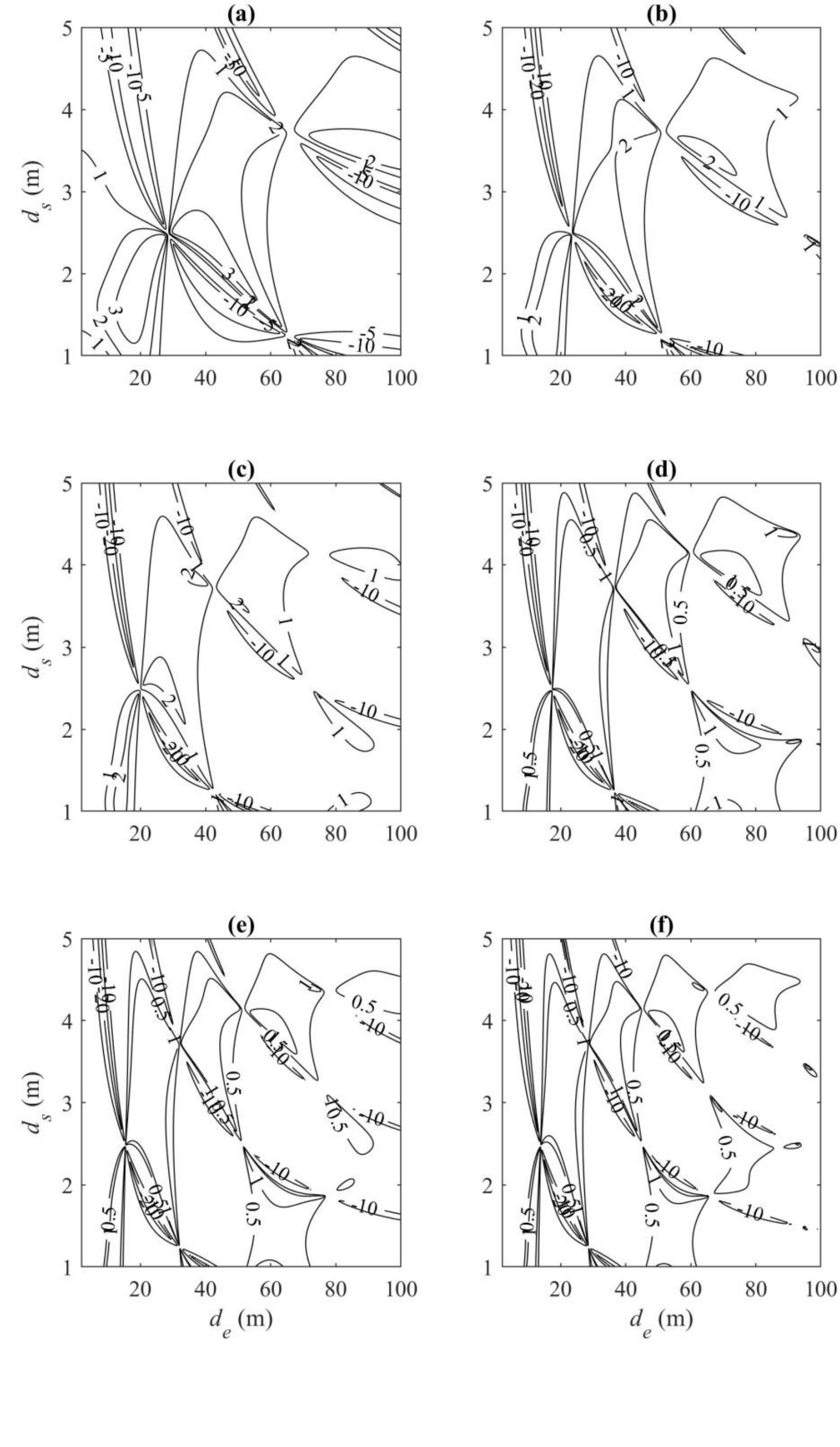

Figure 5. 3 Variations of Δ *with* d_s *and* d_e *with two new sources at the frequency of (a)*125 Hz*; (b)*150 Hz*; (c)*175 Hz*; (d)*200 Hz*; (e)*225 Hz*; (f)*250 Hz*;*

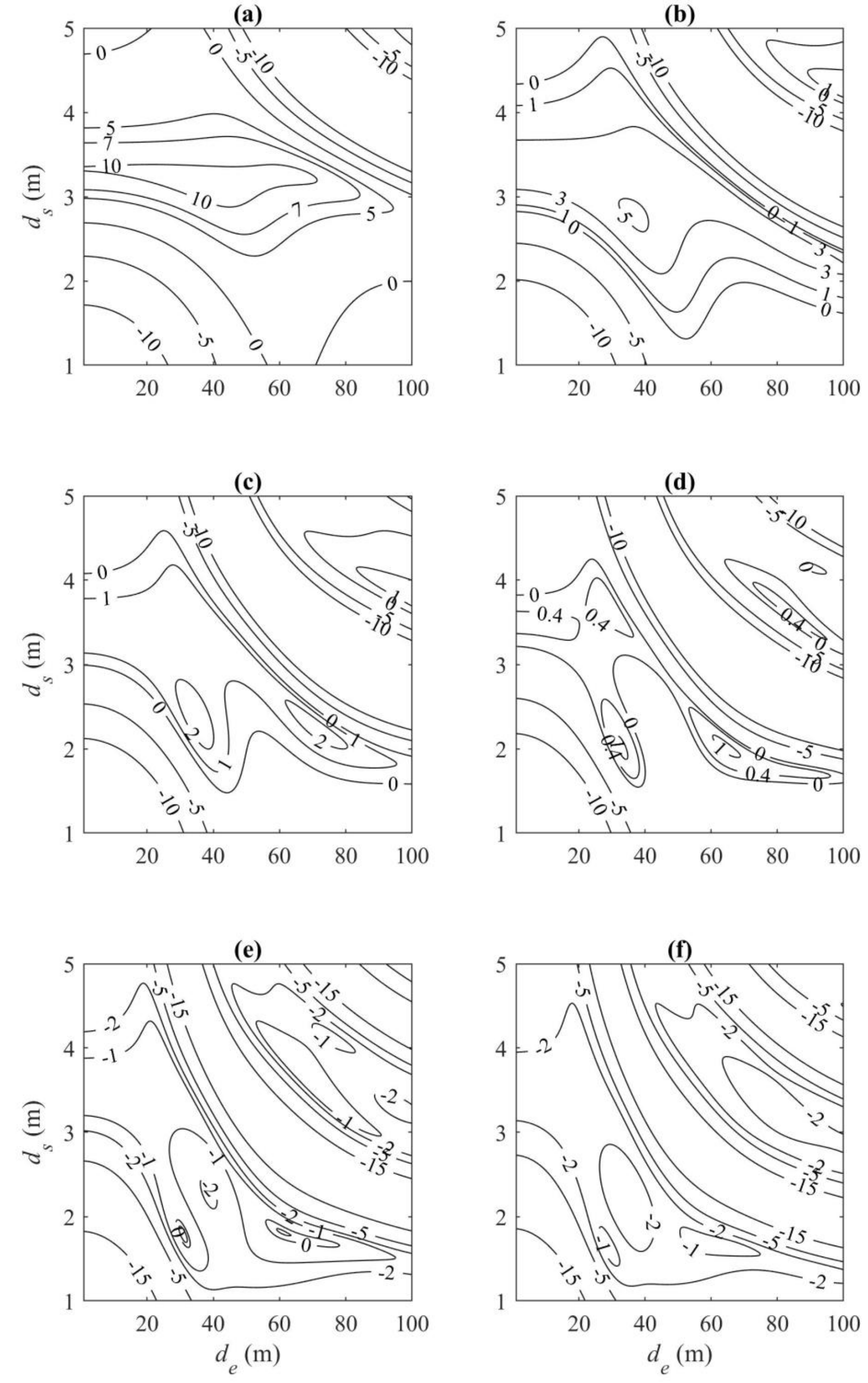

*Figure 5. 4 Variations of Δ with d_s and d_e with three new sources at the frequency of (a)*125 Hz*; (b)*150 Hz*; (c)*175 Hz*; (d)*200 Hz*; (e)*225 Hz*; (f)*250 Hz*;*

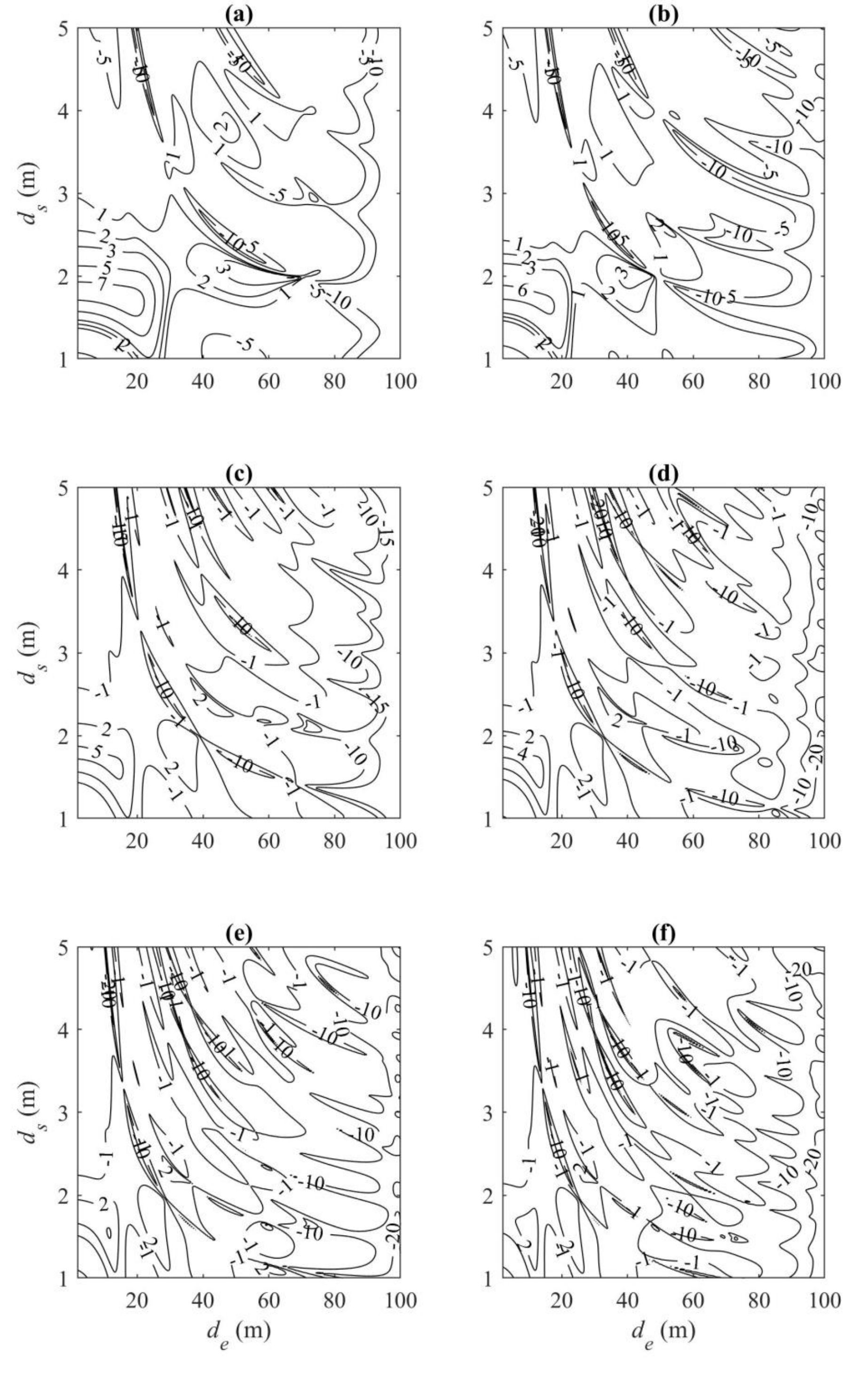

*Figure 5. 5 Variations of Δ with d_s and d_e with four new sources at the frequency of (a)*125 Hz*; (b)*150 Hz*; (c)*175 Hz*; (d)*200 Hz*; (e)*225 Hz*; (f)*250 Hz*;*

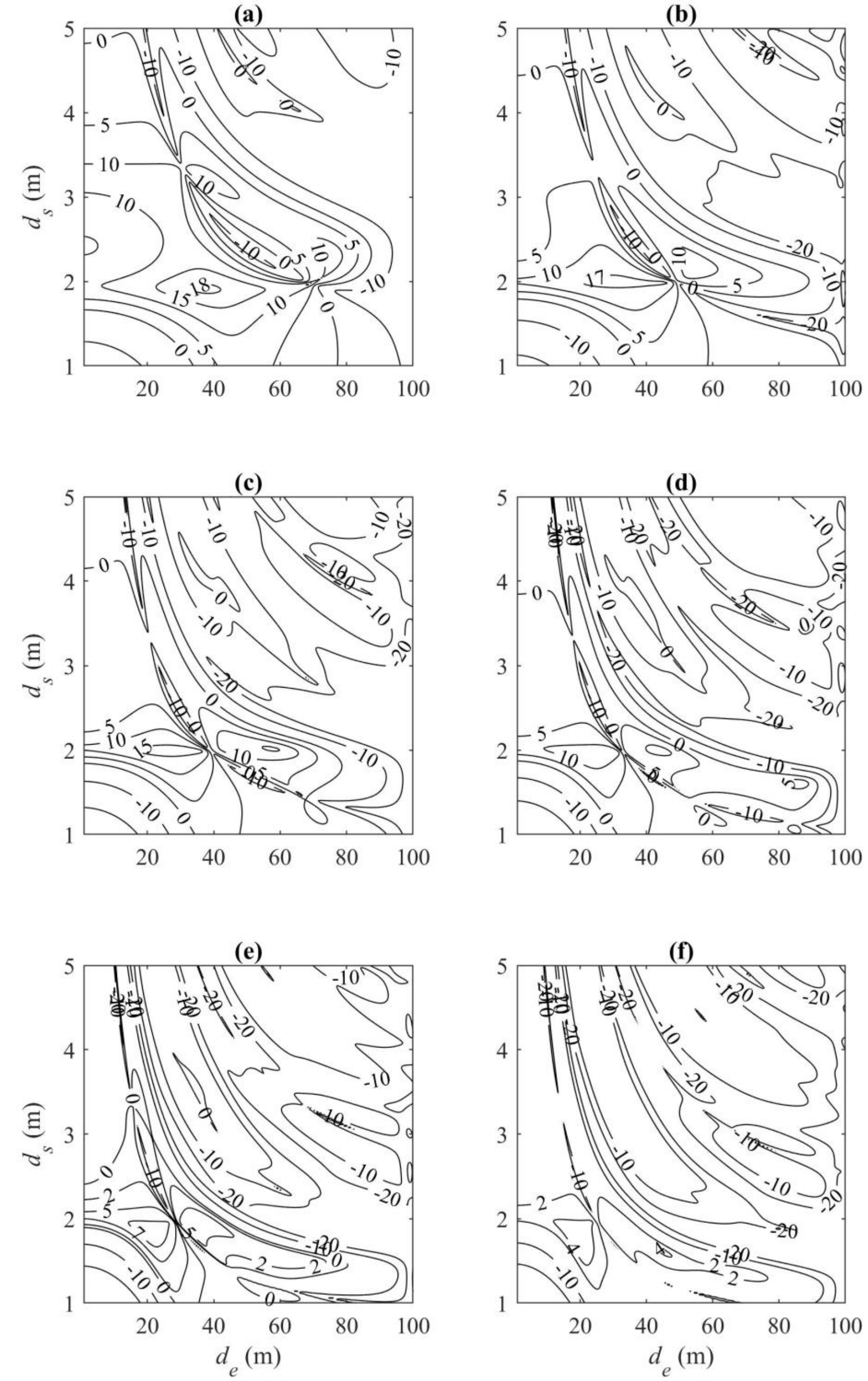

Figure 5. 6 Variations of Δ *with* d_s *and* d_e *with five new sources at the frequency of (a)*125 Hz*; (b)*150 Hz*; (c)*175 Hz*; (d)*200 Hz*; (e)*225 Hz*; (f)*250 Hz*;*

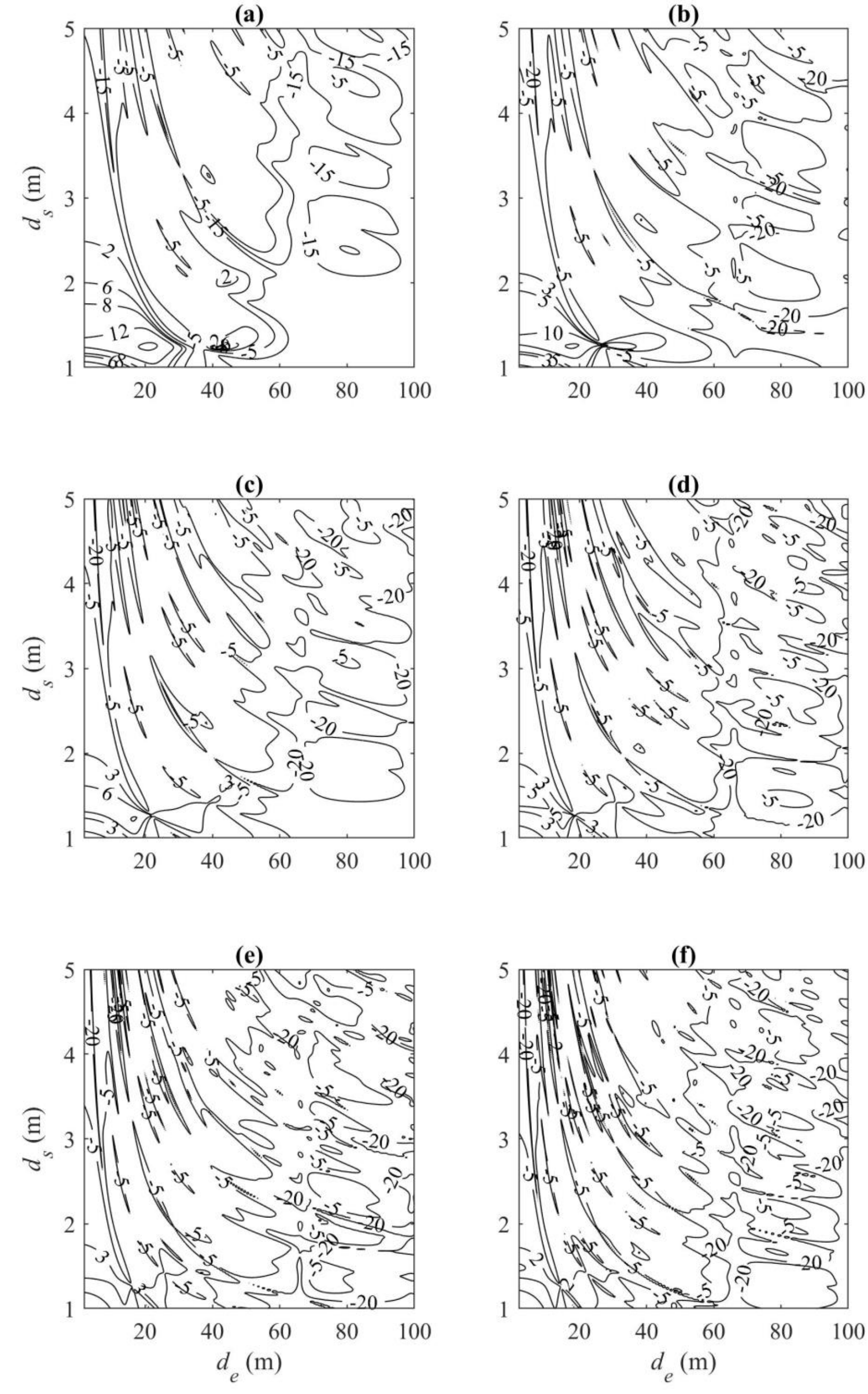

Figure 5. 7 Variations of Δ *with* d_s *and* d_e *with six new sources at the frequency of (a)*125 Hz*; (b)*150 Hz*; (c)*175 Hz*; (d)*200 Hz*; (e)*225 Hz*; (f)*250 Hz*;*

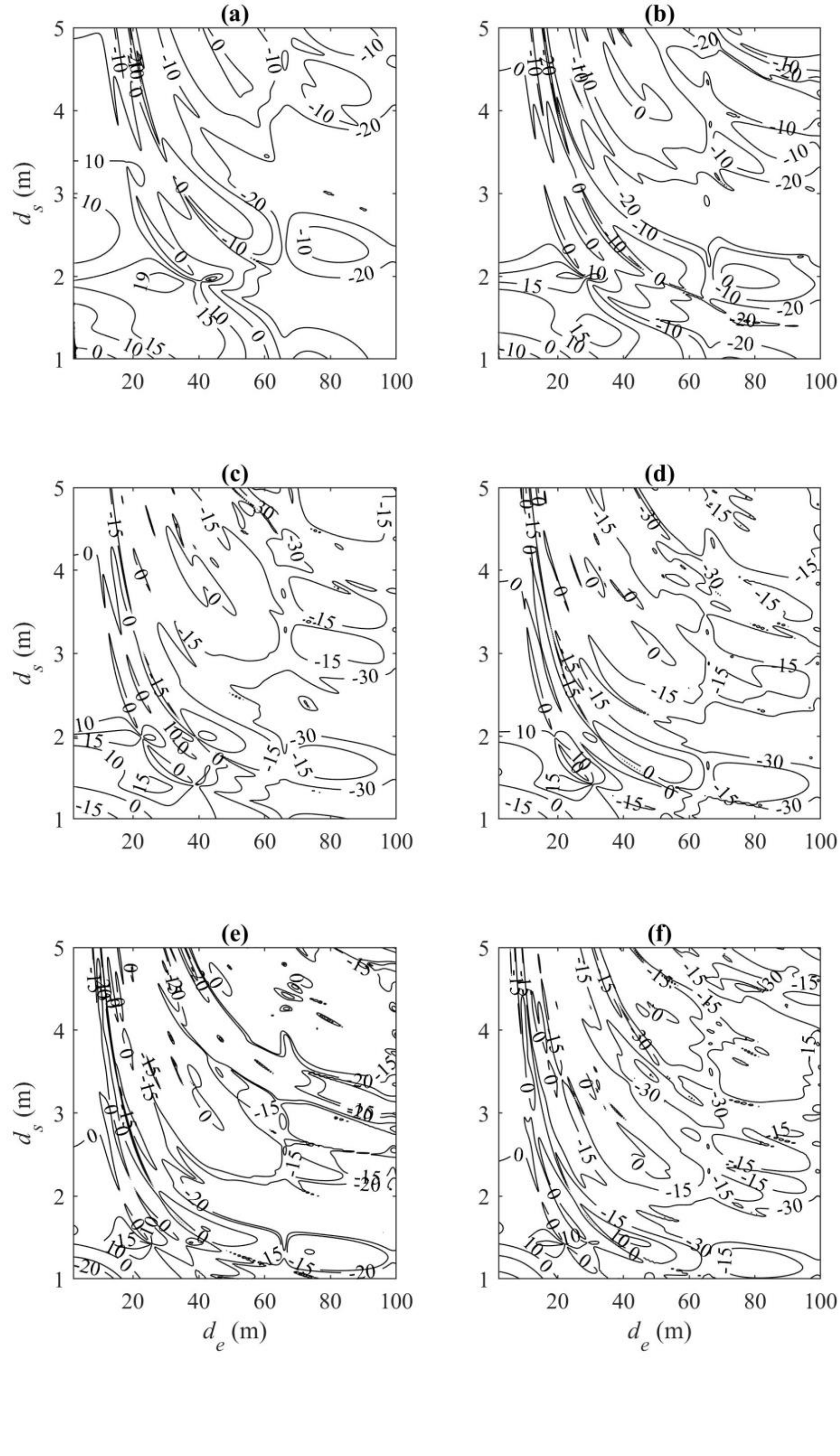

Figure 5. 8 Variations of Δ *with* d_s *and* d_e *with seven new sources at the frequency of (a)*125 Hz*; (b)*150 Hz*; (c)*175 Hz*; (d)*200 Hz*; (e)*225 Hz*; (f)*250 Hz*;*

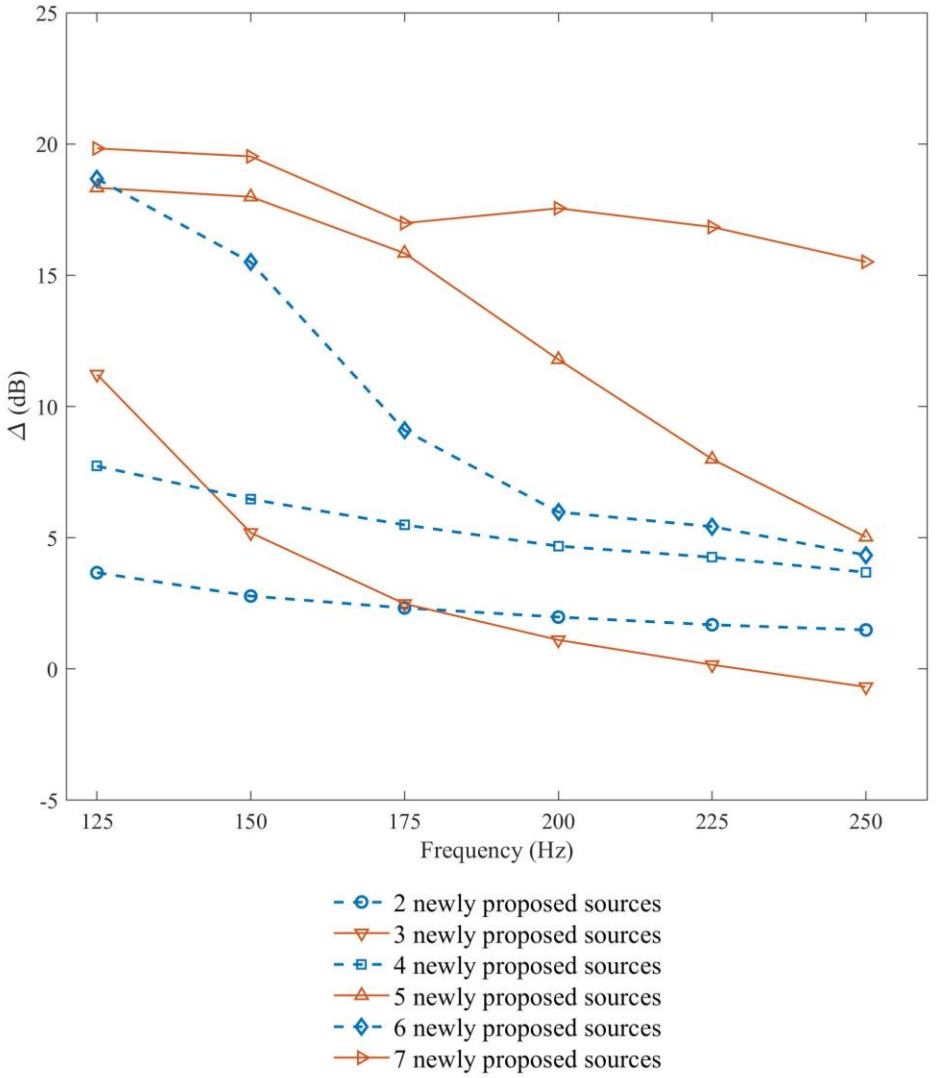

Figure 5. 9 Optimal Δ by using different number of newly proposed secondary sources at frequencies from 125Hz to 250Hz

Since the rest of this chapter is focused on the study of the newly developed secondary sources for broadband noise control towards higher frequencies, it will be exclusively considering the use of odd numbers of controllers and error microphones symmetrically located about the y-axis. In addition, it is very crucial to incorporating massive number of new secondary sources for high frequency noise control.

5.2 Active control performance at higher frequencies by the new secondary sources

In this section, it is checked first whether the established active control system can produce a phenomenal noise reduction in the far field at discrete of higher frequencies among a large area of the monitoring plane as does at the low frequencies. Figure 5.10 (a) shows the variations of d_s, d_e and Δ with N at the frequency of 1000 Hz. It is observed that Δ does not vary much or the rate of increase of Δ is very slow when N exceeds a certain level. It also suggests that d_s and d_e decreases as the number of secondary sources engaged increases, but variation of d_s is relatively small comparing to the degree of change of d_e. The same phenomenon is also observed at other frequencies from low frequency of 125 Hz to relatively high frequency of 2500Hz (shown in figure 5.11 and figure 5.12). Figure 5.11 and 5.12 plot the variations of optimal Δ with respect to N, where the increasement interval of N is two and the maximal N is less than 100 in order to seek the optimal N value. It requires much more secondary sources especially when the radiation of the primary source is greater than 1000 Hz. Additionally, the maximal Δ will declines when the frequency of interest goes up. It suggests that the active control system can provide an excellent overall noise reduction, that Δ is greater than 10dB, evaluated on the monitoring plane, even at 1000 Hz. However, the number of secondary sources used dramatically increases as the primary source radiation is beyond 1000 Hz. It can be observed that more secondary sources are required for higher frequencies control, while the optimal Δ gradually falls off. At the frequency of 2000Hz there is only merely above 5dB total noise reduction; at the frequency of 2500Hz it is about 2dB. Though significantly reduced, this kind of performance has a relatively large frequency range for promising engineering applications.

Figure 5.10 (b) shows the amplitudes of secondary source strengths at the frequency of 1000 Hz with the optimized d_s and d_e by 21 new sources, 31 new sources and 51 new sources respectively. It is revealed that the amplitudes decrease as the number of sources increases. As N exceeds the threshold of the stable phase that the further increasement get tiny, the further addition of the secondary sources on two side become very trivial with extremely small amplitudes comparing with the middle ones. The total spanwise of the secondary sources is comparable to the length of primary finite line source as to an optimal setting of d_s and N. Since the spanwise of the monitoring plane is fairly large, the primary sound field at the positions of extremely off-axis region is properly weak, so that it requires several sources on the very side with minute strength catering for this part, especially a perfectly optimized overall control result is sought. Based on this observation, the criterion of the choice of optimal N can be established accordingly as will discussed in detail later.

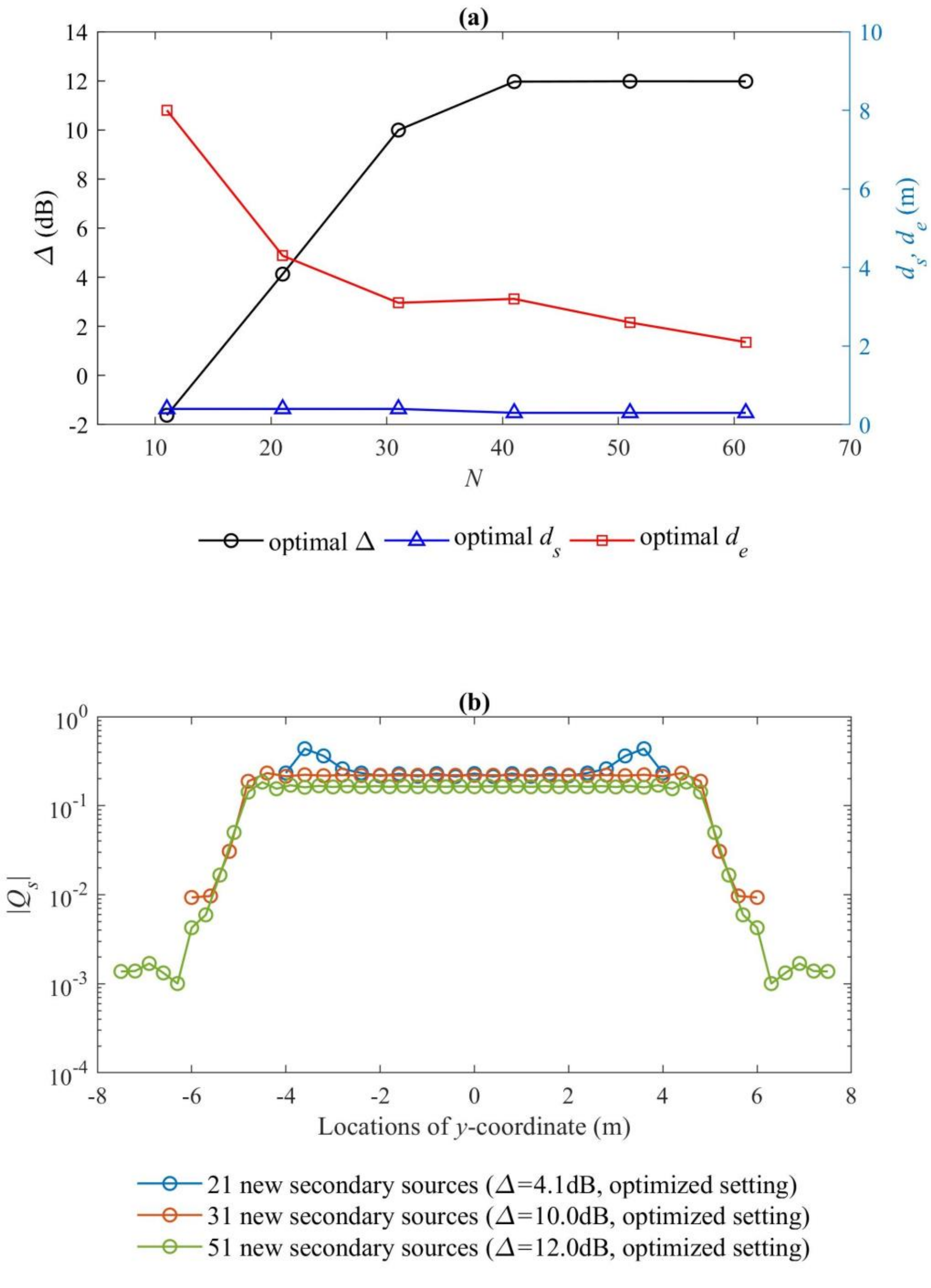

Figure 5. 10 (a) Variations of d_s, d_e and Δ with N at the frequency of 1000 Hz, $R_v = 1.4031$, $r_o = 0.05m$, $R_r = 4/3$; (b) Amplitudes of the new secondary sources plotted against their locations along y-axis for 21 new secondary sources ($\Delta = 4.1dB$), 31 secondary sources ($\Delta = 10.0dB$) and 51 secondary sources ($\Delta = 12.0dB$) respectively, with their optimized settings at the frequency of 1000Hz.

From the dependence of the optimal d_e and d_s with N, albeit the number of secondary sources needed for acceptable performance at higher frequencies remarkably increases, the separation distance is also reduced accordingly, which make the whole system setting still compact enough for a realistic implementation. An optimized geometric configuration, including multiple arrays of newly devised secondary sources combined, of the proposed active control system for broadband noise control will be proposed in the coming section.

Some examples of the variations of d_s, d_e as well as N with frequency for optimal control are summarized in Table 5.1. The optimal N is chosen to be the number of secondary sources above which further improvement of Δ is less than 1 dB for $N < 100$ in this study. It is observed that the optimal N increases while d_s decreases with increasing frequency. Therefore, the smaller the size of the secondary source, the better will be the broadband control performance, which is the focus of following discussion. It is obvious that the optimized Δ decreases with increasing frequency, that is quite typical for active control. However, as will be checked later, from the spanwise variation of the averaged sound pressure on the monitoring plane, the noise reduction within the region of -50 m $< y <$ 50 m is still strong at about 7 to 8dB even at 2500 Hz (figure 5.17 (b)), while the corresponding global control effectiveness is not satisfactory. In addition, it is noticed that the product $(N-1)d_s$ does not vary much with frequency and is roughly equal to the length of the finite line source.

There is a cut-off frequency above which this kind of control system cannot perform well though the noise cancellation on the central region (–50 m < y < 50 m) remains significant. Under the current setup, this cut-off frequency is around 2700 Hz where Δ falls close to 0dB. It should be noted that d_s cannot be less than 0.1 m for a secondary source radius $r_o = 0.05\,m$. However, one can expect the high frequency control performance of the present system will be improved if the size of the secondary source can be reduced further.

Figure 5.13 and 5.14 is the selected plots of the variation of Δ with respect to d_s and d_e with optimal N at frequency of 125 Hz, 250 Hz, 500 Hz and 1000 Hz respectively. It is evident that variation rate of Δ with respect to d_s and d_e at the optimal point becomes higher as frequency increases, and the situation that more secondary sources are used to tackle higher frequencies of the primary noise source exaggerates this phenomenon. In addition to the fact that the optimal Δ deteriorates with the frequencies of interest increasing, the choices of the settings of the proposed active control system for a decent control result get greatly restricted. As shown in figure 5.13, when the d_s is settled at about 2m at the frequency of 125 Hz with 7 new sources, the varying range of the d_m is more than 10m for the performance descriptor Δ greater than 20dB; while as the frequency increased to 250 Hz, the varying range of the d_m is reduced to less than 2m for Δ greater than 19dB with $d_s \approx 0.9m$ and $N = 13$; when the frequency of primary source raises up to 500 Hz, the relevant separating distances of control sources and error sensors for good active control performance will be further restrained as illustrated in figure 5.14 (a). At the frequency of 1000Hz (figure 5.14(b)), as $N = 35$ for the optimal active control performance, the chosen settings regarding d_s and d_e values are confined at certain combinations for a performance of Δ above 10dB.

The averaged sound pressure level spanwise along y-coordinates after active control under optimized setting listed in table 5.1 was plotted from figure 5.15 to figure 5.17. As the frequency of concern increases, the finite primary line source gets much more directional very quickly, in which the multi-lobe primary sound field is more and more concentrating in the middle of acoustic axis. This phenomenon makes the pill over effect becomes more vulnerable for active control, where our new secondary source shows its advantageous benefits.

As illustrated in figure 5.15(a), 5.15(b) and 5.16(a), it displays that there is nearly no sound amplification in the controlled sound field, which has a wide span of $500m$ long in the y-direction, by using the newly proposed secondary sources with the optimized setting up to the frequency of 500 Hz. Even though at the frequency of 1000Hz (figure 5.16(b)), there is slight noise increase of several dBs at the position about 70m away from the normal axis, the whole controlled sound field still possess a significant noise reduction, only expect for the extreme off-axis positions. The effective noise reduction range is approximately from -150m to 150m along y-direction at the frequency of 125Hz and 250Hz, and from about -70m to 70m at the frequency of 500Hz and 1000Hz, where the primary noise magnitude can be attenuate more than 10dB, for lower frequencies there is more reduction.

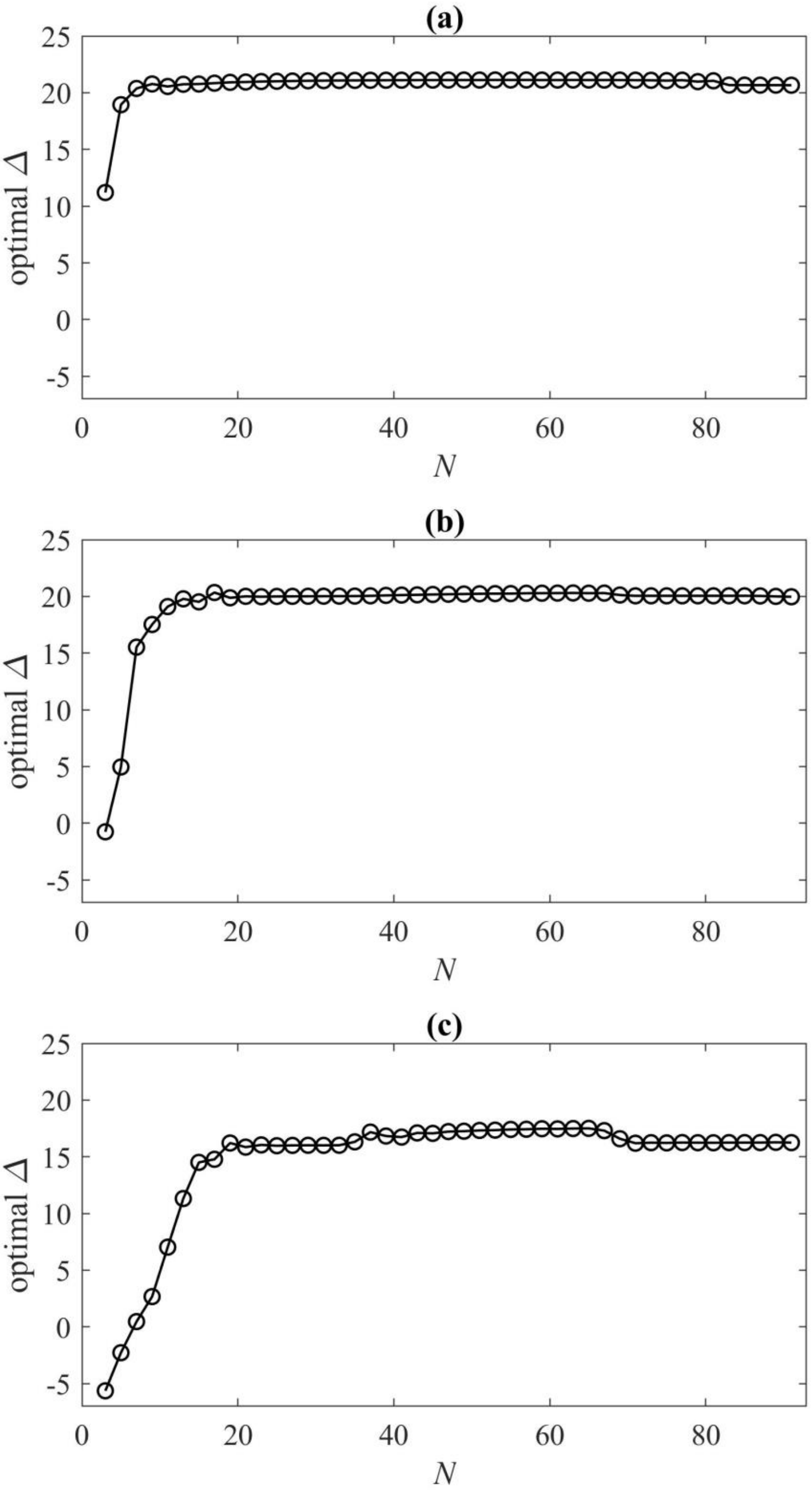

Figure 5. 11 Variations of optimal Δ with N and at the frequency of (a) 125 Hz, $R_v = 1.2874$; (b) 250 Hz, $R_v = 1.2925$; (c) 500 Hz, $R_v = 1.3132$. ($r_o = 0.05m$, $R_r = 4/3$)

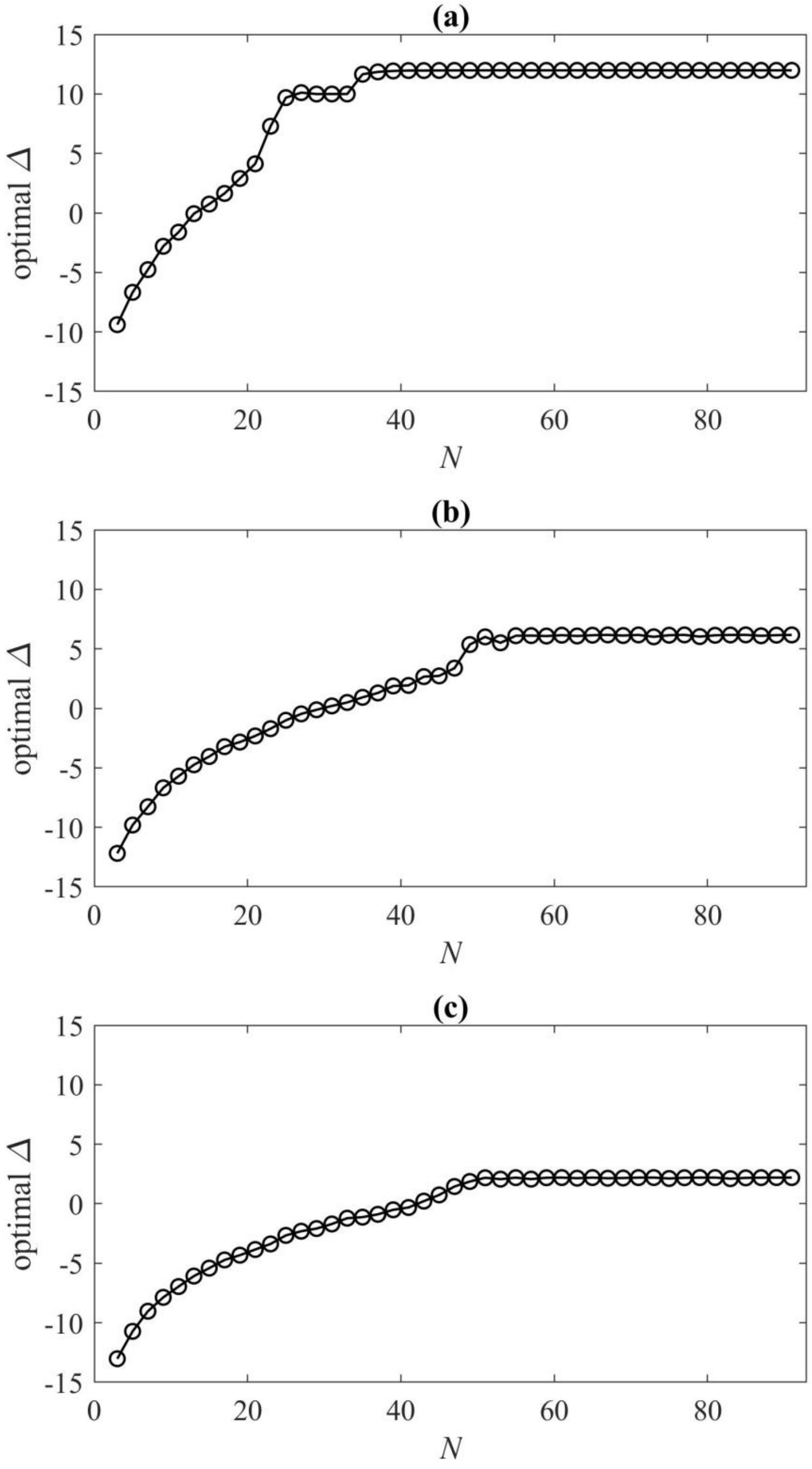

Figure 5. 12 Variations of optimal Δ with N and at the frequency of (a) 1000 Hz, $R_v = 1.4031$; (b) 2000 Hz, $R_v = 1.9240$; (c) 2500 Hz, $R_v = 2.6492$. ($r_o = 0.05m$, $R_r = 4/3$)

Table 5. 1 Examples of optimal settings for control systems with the new secondary sources

Centre Frequency (Hz)	Optimal Control Setting			Δ (dB)
	N	d_s (m)	d_e (m)	
125	7	1.9	29.8	20.4
250	13	0.9	15.7	19.8
500	19	0.6	7.3	16.2
1000	35	0.3	3.7	11.7
2000	51	0.2	1.8	6.0
2500	51	0.2	1.4	2.2

Thanks to the very small physical size of the new secondary sources, we can use substantial controllers in the active control system, in which 35 secondary sources are used at the frequency of 1000Hz, and even 51 used at 2000Hz and 2500Hz. The active control result at 2000Hz, when $\Delta = 6dB$ for the optimal setting, does not possess such an extraordinary noise reduction within the area of the monitoring plane as the cases at 1000Hz alike. There is evident noise amplification at the two sides of the monitoring plane. But it is not serious as the case when conventional secondary sources are used shown in figure 3.1 and figure 3.2. The control result at 2500Hz displays similar character, while the resultant sound field increase gets even worse. However, if one takes the whole noise concern area of the monitoring plane into consideration, there is still noise reduction happened, mostly in the middle where the noise reduction in the region of $-50m < y < 50m$ spanwise remains greater than 7dB (figure 5.17).

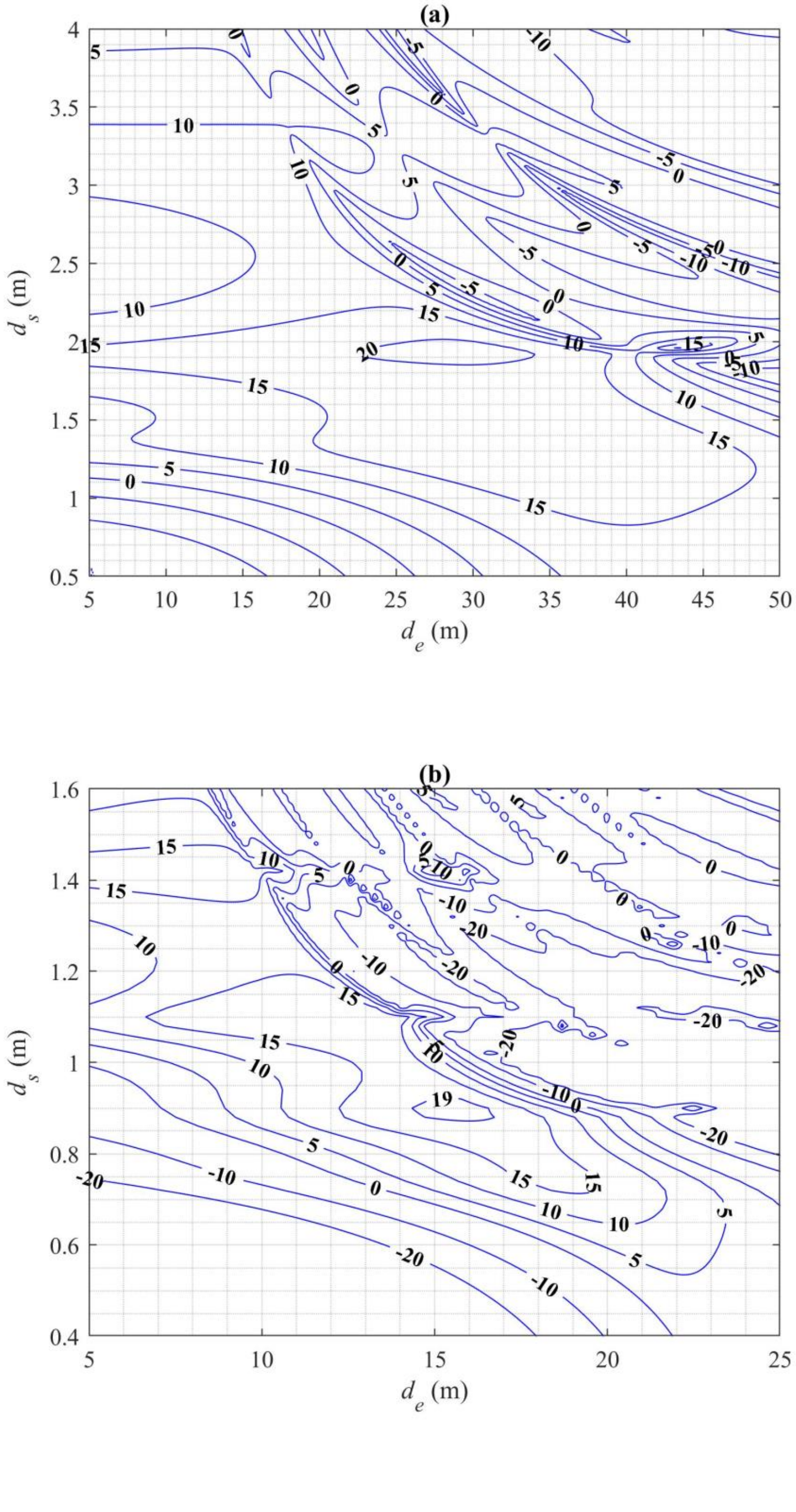

Figure 5. 13 Variations of Δ *with* N, d_s *and* d_e *at the frequency of (a) 125 Hz (*$N = 7$, $r_o = 0.05m$, $R_r = 4/3$, $R_v = 1.2874$*); (b) 250 Hz (*$N = 13$, $r_o = 0.05m$, $R_r = 4/3$, $R_v = 1.2925$*).*

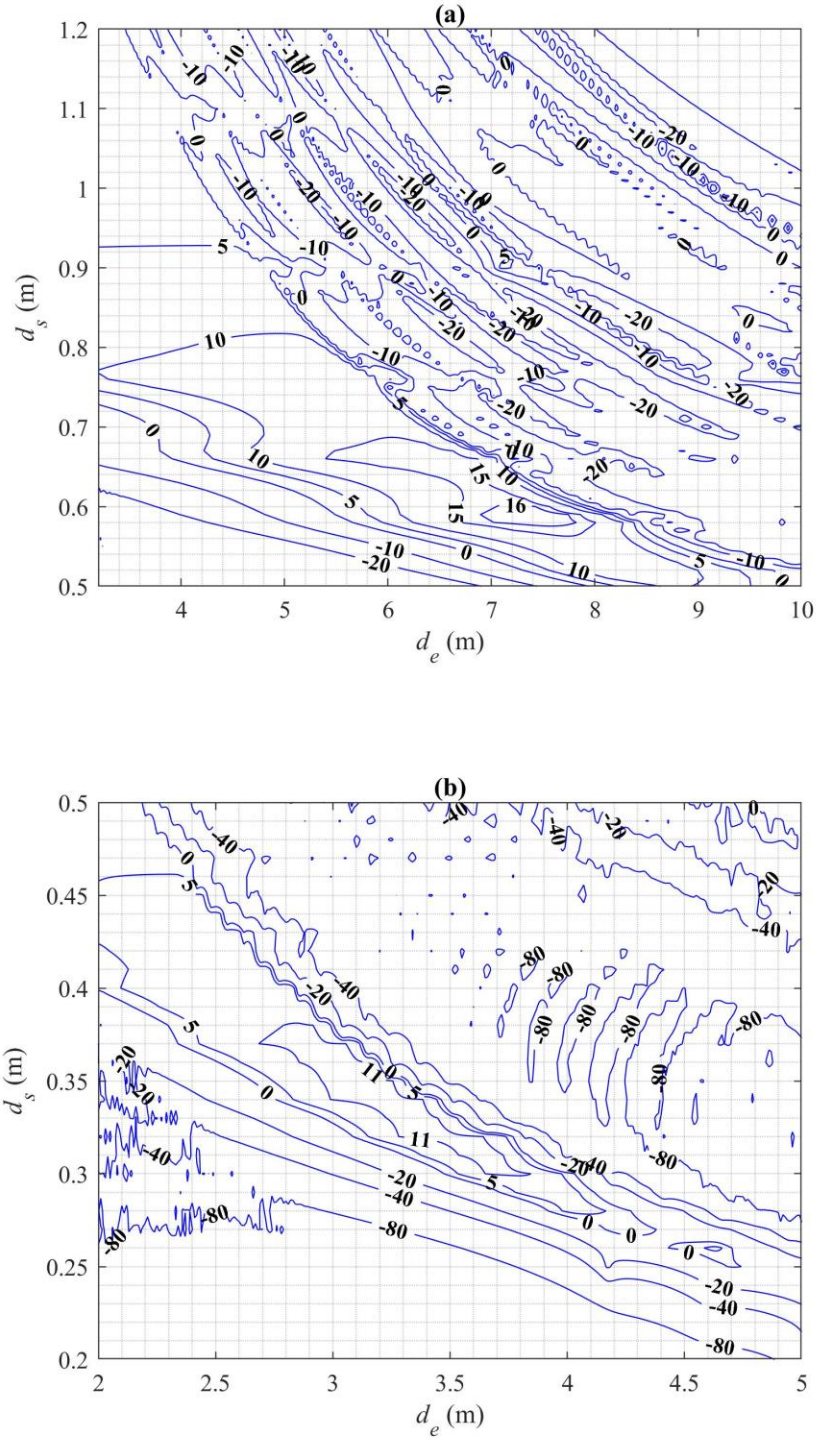

Figure 5. 14 Variations of Δ with N, d_s and d_e at the frequency of (a) 500 Hz ($N = 19$, $r_o = 0.05m$, $R_r = 4/3$, $R_v = 1.3132$); (b) 1000 Hz ($N = 35$, $r_o = 0.05m$, $R_r = 4/3$, $R_v = 1.4031$).

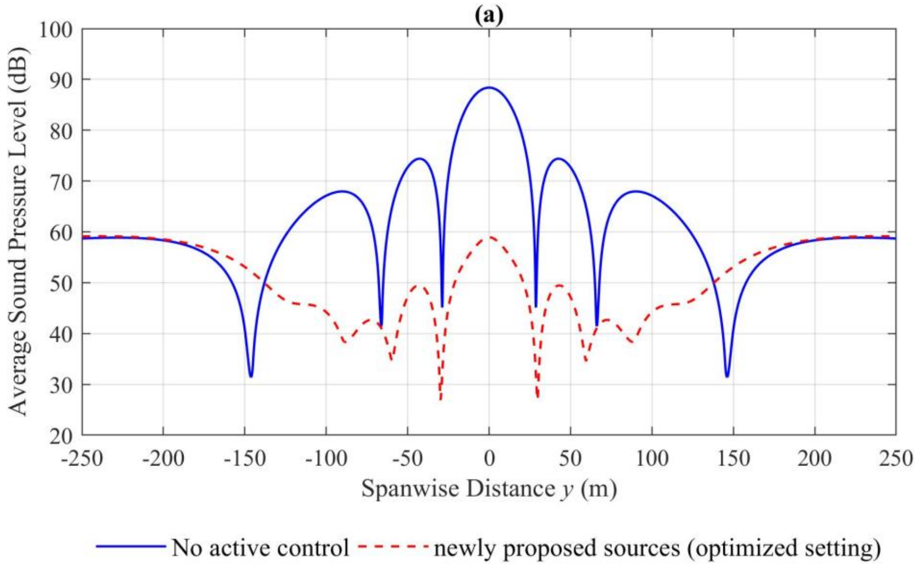

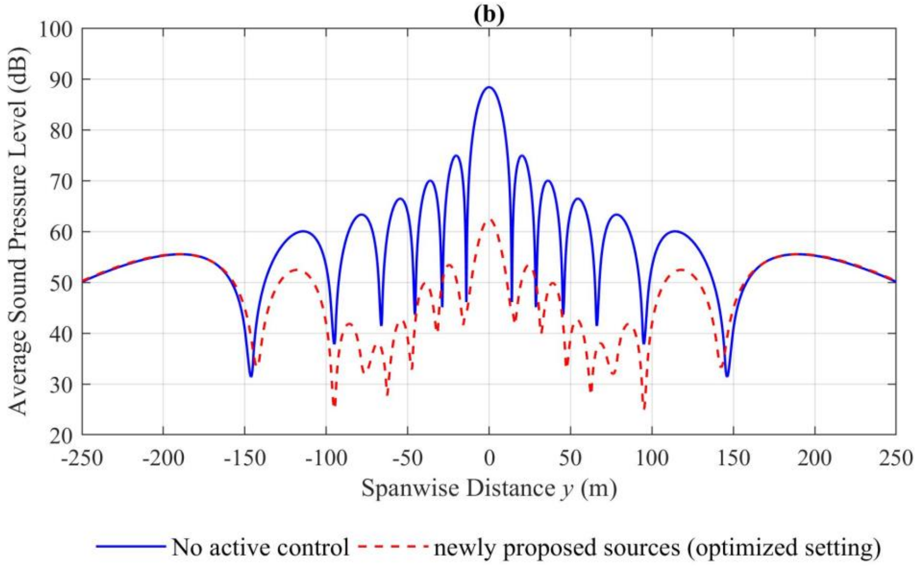

Figure 5. 15 Spanwise variation of averaged sound pressure level on the monitoring plane by the newly proposed sources at the frequency of (a) 125 Hz; *(b)* 250 Hz. *with optimized setting and maximized directivity*

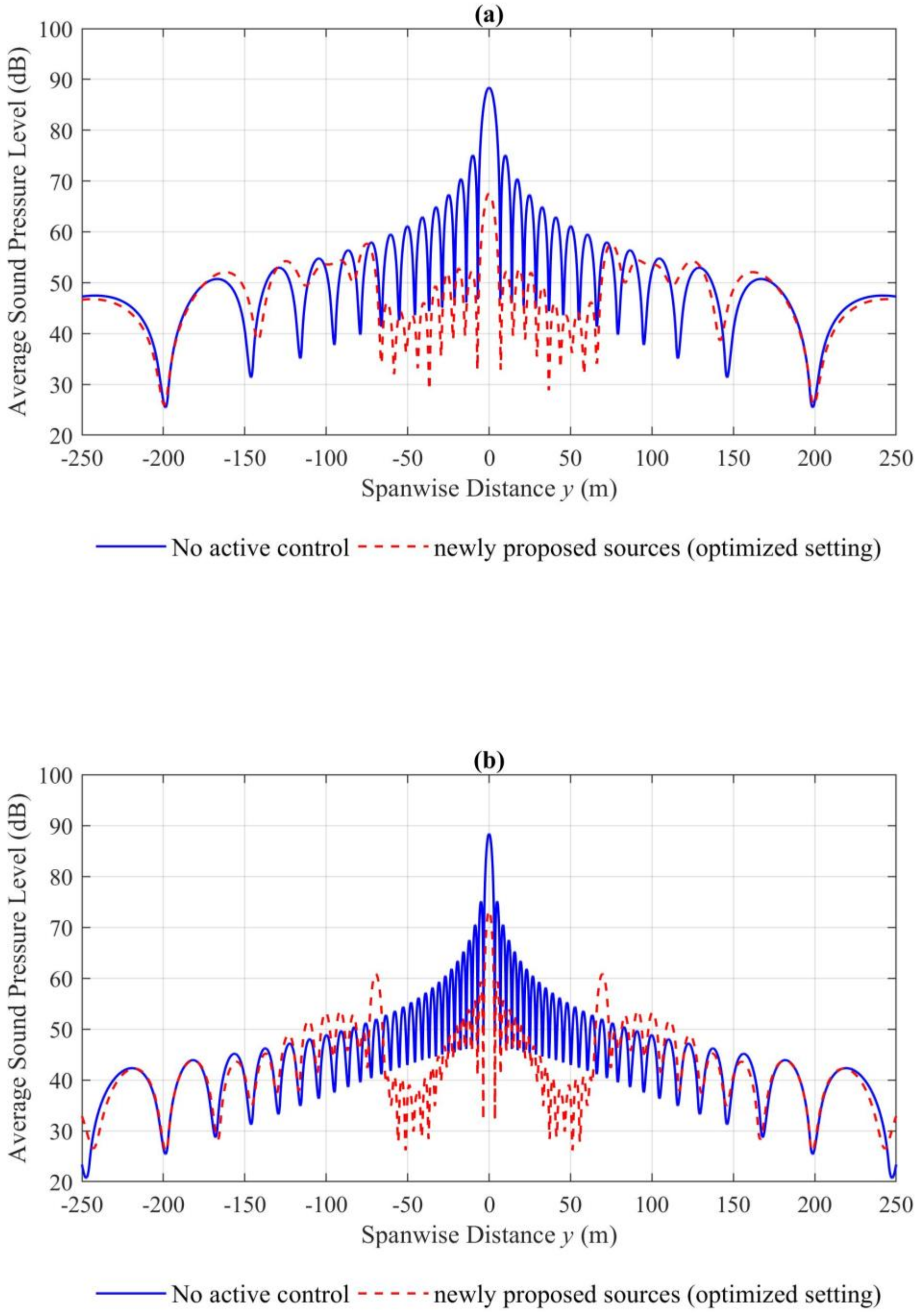

Figure 5. 16 Spanwise variation of averaged sound pressure level on the monitoring plane by the newly proposed sources at the frequency of (a) 500 Hz; *(b)* 1000 Hz. *with optimized setting and maximized directivity*

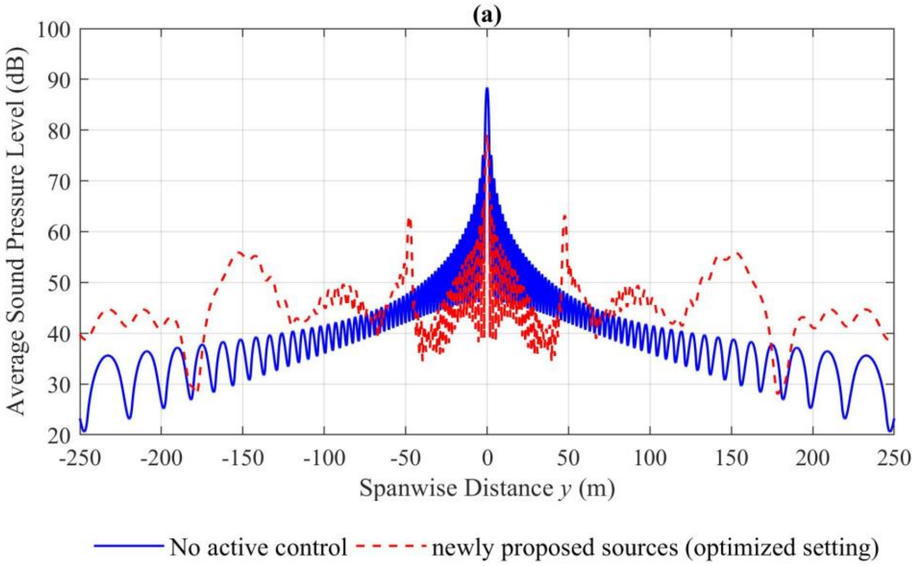

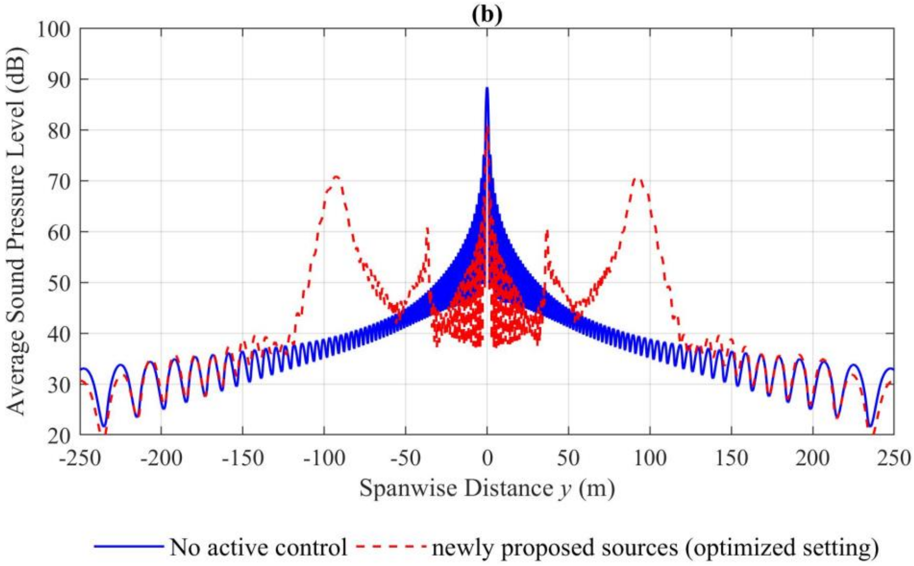

Figure 5. 17 Spanwise variation of averaged sound pressure level on the monitoring plane by the newly proposed sources at the frequency of (a) 2000 Hz; *(b)* 2500 Hz. *with optimized setting and maximized directivity*

Since the size of new sources is small and so is the separation distance of the optimized setting, the active control system proposed here will not become enormously large. It remains its possibility for a realistic application, especially for the ability of such a wide frequency range of effective noise control.

5.3 The configuration of active control system for broadband noise

Based on the previous analysis of the active control system, this section is focused on the capability on the broadband noise control, which the Δ spectra of different sets of optimized configurations are under the loupe.

The bandwidth of effective global control varies with secondary source array setting and is relatively narrow except at low frequencies as shown in figure 5.18 and figure 5.19 with the settings optimized at discrete frequencies from 125Hz to 2500Hz respectively (listed in table 5.1). Strong sound amplification is found outside the effective bandwidths. However, it is still possible to setup an assembly of secondary source arrays to provide significant broadband global sound reduction, at least below the cut-off frequency. Each array will cater for the active control within a separate frequency band. One can actually start seeking the optimal settings with the 250 Hz source array, which is already able to cover the active control at the frequencies between 65 Hz to 280 Hz. Table 5.2 summarizes such an assembly and figure 5.20 illustrates the corresponding Δ spectrum.

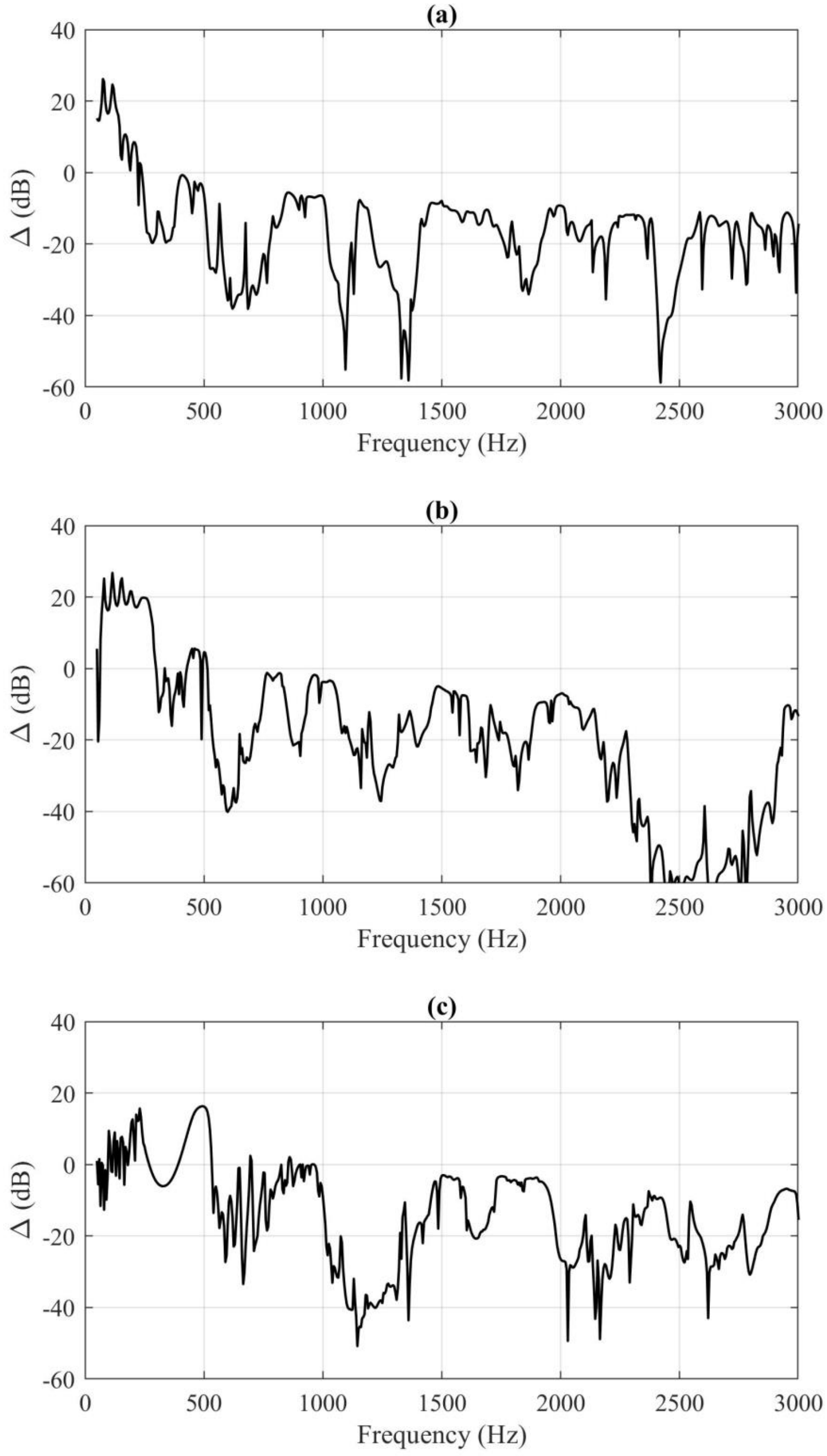

Figure 5. 18 Examples of the spectral variations of Δ *under optimal secondary sources settings in Table 2 (a) optimized at* 125Hz*; (b) optimized at* 250Hz*; (c) optimized at* 500Hz*.*

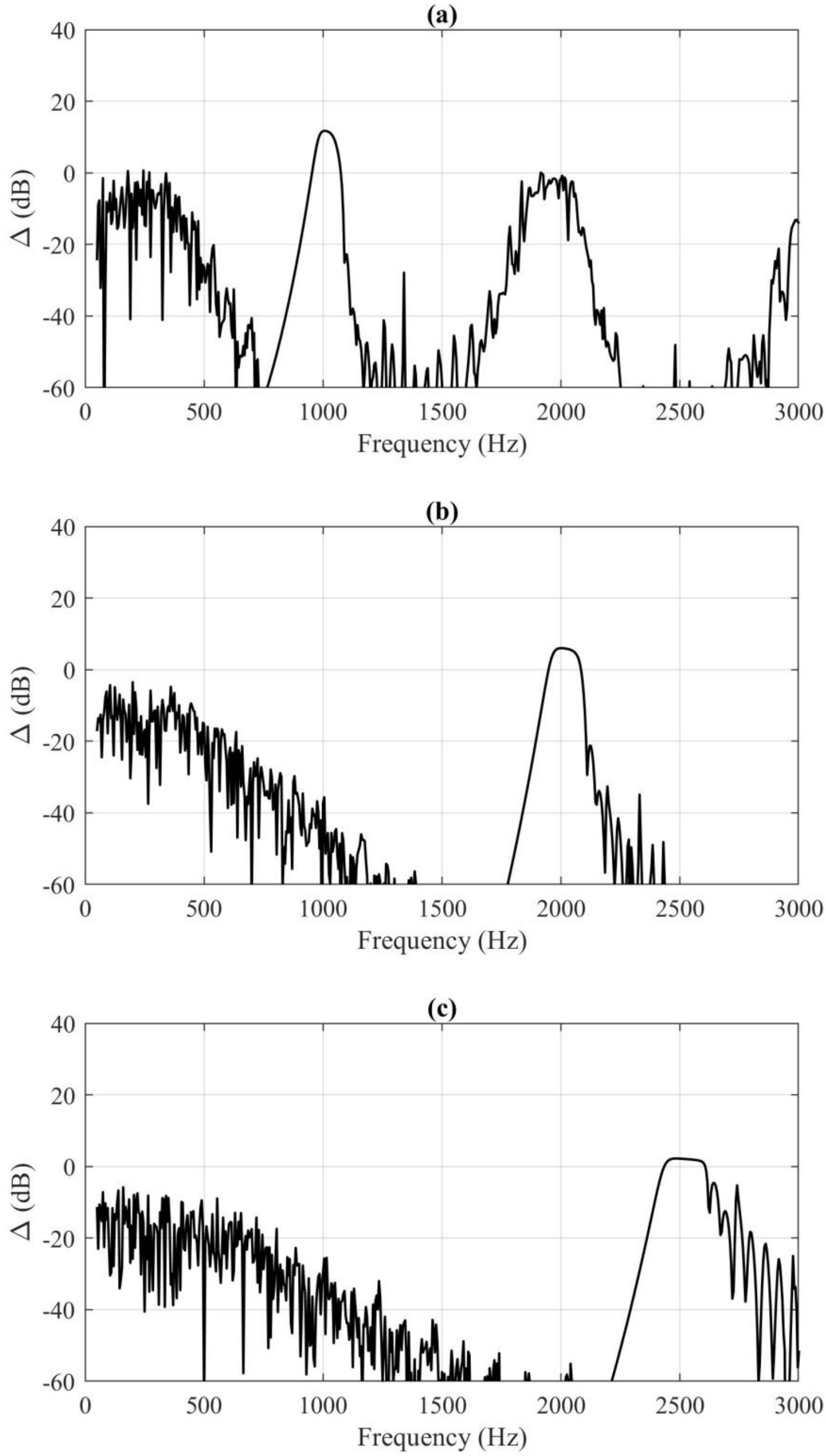

Figure 5. 19 Examples of the spectral variations of Δ *under optimal secondary sources settings in Table 2 (a) optimized at* 1000Hz*; (b) optimized at* 2000Hz*; (c) optimized at* 2500Hz*.*

Table 5. 2 Secondary source array assembly for broadband active control

Array	Control Band Frequency (Hz)			Array Setting		
	Centre	Lower Cut-off	Upper Cut-off	N	d_s (m)	d_e (m)
A	250	65	280	13	0.9	15.7
B	350	280	370	13	0.9	10.8
C	400	370	430	19	0.6	9.6
D	500	430	525	19	0.6	7.3
E	600	525	635	19	0.6	5.8
F	680	635	730	29	0.4	5.1
G	800	730	845	29	0.4	4.2
H	900	845	970	29	0.4	3.6
I	1000	970	1060	35	0.3	3.7
J	1100	1060	1175	35	0.3	3.3
K	1250	1175	1300	35	0.3	2.9
L	1380	1300	1420	35	0.3	2.6
M	1450	1420	1475	57	0.2	2.4
N	1500	1475	1525	57	0.2	2.3
O	1550	1525	1585	57	0.2	2.2
P	1630	1585	1645	57	0.2	2.1
Q	1700	1645	1715	57	0.2	2.0
R	1750	1715	1790	57	0.2	1.9
S	1800	1790	1885	57	0.2	1.8
T	1900	1885	1970	51	0.2	1.9
U	2000	1970	2070	51	0.2	1.8
V	2100	2070	2180	51	0.2	1.7
W	2200	2180	2305	51	0.2	1.6
X	2400	2305	2445	51	0.2	1.5
Y	2500	2445	2605	51	0.2	1.4

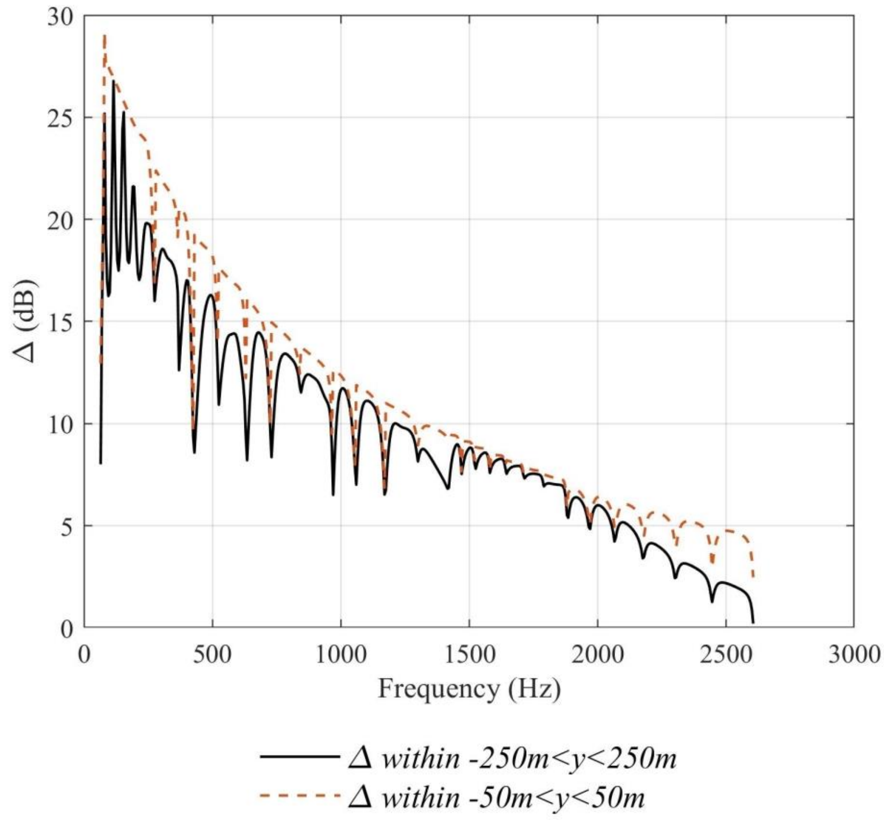

Figure 5. 20 Δ spectrum obtained using the broadband active control assembly shown in Table 3

The spectral variation of Δ evaluated within the central region –50 m < y < 50 m of the monitoring plane using the secondary control source arrays given in table 5.2 is also presented by the red dashed curve in figure 5.20. Stronger noise reduction is observed within the central region, which is consistent with the previous analysis that the active noise reduction always very significant near the acoustic axis of primary line source.

It should be noted that the 25 arrays can be aligned into a single linear array which is symmetrical about y = 0 as shown in figure 5.21 because of the small radii of the secondary sources. The actual number of secondary sources

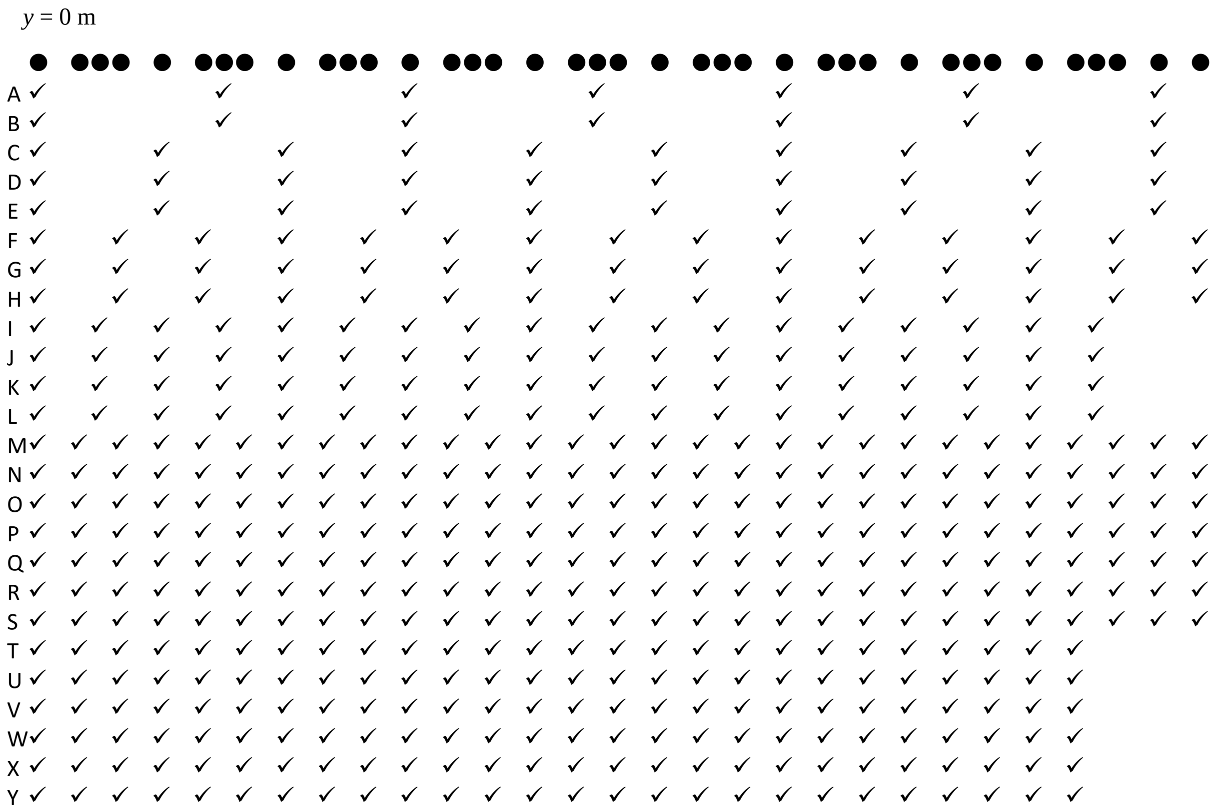

Figure 5. 21 Control source array arrangement for the assembly shown in Table 3 (● : Secondary control source).

required is just 75. Large number of microphones is needed for global control as expected [Nelson et al., 1987b]. One should also note that the number of secondary sources and error microphones can be reduced if one does not require optimal performance and/or high frequency noise attenuation. The latter is true for general traffic noise [Berglund et al., 1996] and human noise control [Mehta et al., 1999].

5.4 The active control system scalability with respect to the length of primary line source

The length of primary line source, l, affects the active control performance. As a graduated guess, the number of secondary sources as well as that of error microphones required for optimal control performance will increase with the source length. Table 5.3 lists some suggested optimal settings at discrete frequencies from 125 Hz to 2500 as to the length of 20m and 30m finite line source respectively.

Table 5. 3 Optimal control systems with new secondary sources for scaled up line sources

l (m)	Centre Frequency (Hz)	Optimal Control Setting			Δ (dB)
		N	d_s (m)	d_e (m)	
20	125	19 (15)	0.8 (1.9)	15.9 (12.8)	23.1 (18.3)
	250	35 (35)	0.6 (0.9)	8.8 (5.7)	23.7 (18.7)
	500	37	0.6	3.6	18.2
	1000	77	0.3	1.7	12.3
	2000	103	0.2	0.9	6.3
	2500	103	0.2	0.7	2.6
30	125	27 (21)	1.1 (1.9)	11.3 (9.0)	25.2 (18.5)
	250	47 (49)	0.8 (0.9)	5.0 (4.0)	22.8 (22.1)
	500	63	0.6	2.1	17.8
	1000	145	0.3	0.9	13.9
	2000	185	0.2	0.5	7.4
	2500	179	0.2	0.4	3.2

The criterion of choosing the optimal N and the corresponding optimized d_s and d_e is that mentioned in section 5.2. It is noted that the values of d_s at frequencies at and above 500 Hz are the same as those for the case of l = 10 m (Table 5.2). The numbers in parenthesis show the situation when the values of d_s are kept the same as those for the case of l = 10 m at the frequencies of 125 Hz and 250 Hz. In fact, the corresponding control performances are still comparable to that of the l = 10 m case. The error microphone separation d_e decreases with increasing l because of the increasing number of nodal planes on the monitoring plane resulted from the longer linear primary source. One can also observe that d_e is approximately inversely proportional to l for the cases of optimal control performance. This matches with the sound field pattern of the finite length linear source given in equation (2.1) when kl is large. Besides, it is noticed that the total length of the error microphone array, which is equal to $(N-1)d_e$, at a fixed frequency is nearly independent of l when d_s is kept unchanged, especially for $l \geq 20$ m. For all the above cases, the noise reduction within the central region of the monitoring plane remains significant even though the global control effectiveness at higher frequencies appears not satisfactory. This phenomenon in the foregoing analysis are basically in-line with those of Guo et al. [Guo et al., 1997]. In their study, the primary source for active control in free space is a simple monopole source.

6 Conclusions and future works

6.1 Conclusions

The active attenuation of noise radiated from a coherent line source of finite length in an unrestricted space is numerically investigated in this thesis. A new type of the piston-like secondary source is proposed for this purpose. The active noise control performance over the frequency range from 100Hz to 2500Hz is examined. This frequency range spans over the major frequency range of traffic noise and human speech.

The active control system with multiple secondary sources and the equivalent number of error microphones is illustrated in Chapter 2, which is configurated with a typical arrangement of positioning the acoustic controllers and sensors in two parallel rows. Then the theoretical model for the subsequent analysis is established, including the determination of optimal secondary source strengths by least square method. In the present study, the global effectiveness of active noise reduction is described by the reduction of the average sound pressure level on a 500 m long monitoring plane at a distance 100 m from the primary source.

In chapter 3, the active control results by using the simple sound sources, say the monopoles and baffled circular pistons, are demonstrated first. It unveils that conventional control sources are hardly effective for this extensive primary linear source, where significant sound amplification occurs especially in the off-axis region. As compact simple secondary sources radiate the acoustic energy omnidirectionally, while the primary coherent line source radiate directionally with a multi-lobe sound pattern in the far-field. The sound fields from the primary source and the secondary sources need to be in a good match for an effective active noise control. The piston sources of large radii produce an improved noise reduction. However, such a size is impossible for practical implementation.

A new secondary source is proposed in chapter 4, and for optimizing the geometric configuration of the established active control system, a performance descriptor Δ evaluated on the monitoring plane is introduced as well. This newly proposed secondary source consists of a central circular core and an outer annulus, and both parts can axially oscillate independently. By actuating the central core and outer annulus out of phase, it is demonstrated that this source type can produce a much more directional secondary sound field than a single circular piston even its size is much smaller than the latter. Though the overall source directivity is very sensitive to the vibration ratio of the two parts, making the outer annulus thinner can mitigate this issue.

By optimizing the separation distances between secondary sources and that between error microphones, the best control performance achieved by the new sources is remarkably better than that by piston sources, which gives rise to more effective global sound reduction with wider noise reduction region and less sound increases in the off-axial areas.

After illustrating that the active control system by using multiple newly proposed secondary sources can give prominently excellent performance at low frequencies, the possibilities and effectiveness of the new sources for attenuating broadband noise is studied in chapter 5. It is observed that the secondary source array with odd number of sources outperforms its even number counterpart, and it is critical to incorporate substantial secondary sources for effective active control at high frequencies. The small physical size of new sources enables the use of more secondary sources within a relatively compact region, significantly improving the active control performance. It is found that the active control system with the new sources can result in 11.7dB global noise reduction measured at the frequency of 1000 Hz. Although the performance deteriorates with increasing frequency, a cut-off frequency above which this kind of active control system will not produce a decent overall noise reduction is around 2700 Hz. Nevertheless, the noise reduction within the central region of the receiver plane remains significant in all the cases.

An example of a secondary source array for broadband noise control up to about 2600 Hz is provided. It is an assembly of 25 arrays that can be aligned into a single linear array within relatively compact span. The total number of secondary sources required is just 75.

Finally, the scalability of the active control system with respect to the length of primary line source is checked. It is revealed that the active control results are comparable to that of $l = 10m$ by including more secondary sources. The spacing between adjacent error microphones d_e decreases with the increasing l where the total span of the error microphones, $(N-1)d_e$, is virtually independent of l.

In general, the introduced active noise control system with the newly proposed control sources creates an excellent noise reduction around a relatively large extent in an extraordinarily wide frequency range. This is due to the advantage of the new sources being of high directivity and tiny physical size.

6.2 Future works

The most natural and reasonable next step of this study is an analytical investigation into a more complex construction of the newly proposed secondary source with multi-annuli. It will be motivated by the possibilities of higher directivities, even smaller size, or less sources required with which the active control system can provide remarkable global noise attenuation.

Another consequential exploration is about diving into the active control result along z-coordinates. A long strip, along y-axis, of monitoring plane is utilized in this study because of the primary sound field radiated from a coherent line source and the linear arrangement of secondary sources. Since the new source is axisymmetric about the normal of the vibrating surfaces through the center, the variation along the span of z-direction is still important in some scenarios. In order to achieve noise active control results along both y and z axes, the secondary sources may be positioned as a rectangular array or an array of other two-dimensional patterns rather than aligned into a linear row.

Since traffic noise sources like a highway or a fast-moving train, are theoretically suitable to be modeled as an incoherent line source, the study of the active control on an incoherent line source, both with finite or infinite length, using the proposed active noise control system and the new piston-like secondary sources will be studied. These active control results can be valuable for real scenario applications.

Finally, from a pragmatic point of view, the development and implementation of this newly proposed secondary source is of practical value. As the radiation pattern of the new source is vulnerable to inaccurate vibrating velocities, the actuation mechanism of the new source is considerably crucial to the success of this new design. Experimental study is recommended.

Appendix: Matrix Manipulation on the Optimization of Secondary Source Strengths

To achieve the optimized sound field within the range of monitoring plane, the least square method is applied over all the error microphones by defining a cost function U as the sum of the squared magnitudes of resultant sound pressures at the position of N microphones, so that

$$U = \mathbf{p}_e^{\boldsymbol{H}}\mathbf{p}_e = \left(\boldsymbol{Z}_{pe}Q_l + \boldsymbol{Z}_{se}\mathbf{Q}_s\right)^{\boldsymbol{H}}\left(\boldsymbol{Z}_{pe}Q_l + \boldsymbol{Z}_{se}\mathbf{Q}_s\right) \tag{A.1}$$

where H denotes the Hermitian transpose of matrix, $\boldsymbol{Z}_{pe}Q_l$ represents the sound pressures from the primary line source only at the positions of error microphones and it will be denoted by $\mathbf{P}_{pe}$ in the subsequent derivation for conciseness. The expression of the column vector representing all the sound pressures at the error microphone positions can be referred to Chapter 2. Then the quadratic cost function becomes

$$
\begin{aligned}
U = \mathbf{p}_e^{\boldsymbol{H}}\mathbf{p}_e = \left(\mathbf{P}_{pe} + \boldsymbol{Z}_{se}\mathbf{Q}_s\right)^{\boldsymbol{H}}\left(\mathbf{P}_{pe} + \boldsymbol{Z}_{se}\mathbf{Q}_s\right) \\
&= \left({\mathbf{P}_{pe}}^H + (\boldsymbol{Z}_{se}\mathbf{Q}_s)^H\right)\left(\mathbf{P}_{pe} + \boldsymbol{Z}_{se}\mathbf{Q}_s\right) \\
&= \left({\mathbf{P}_{pe}}^H + {\mathbf{Q}_s}^H{\boldsymbol{Z}_{se}}^H\right)\left(\mathbf{P}_{pe} + \boldsymbol{Z}_{se}\mathbf{Q}_s\right) \\
&= {\mathbf{Q}_s}^H{\boldsymbol{Z}_{se}}^H\boldsymbol{Z}_{se}\mathbf{Q}_s + {\mathbf{Q}_s}^H{\boldsymbol{Z}_{se}}^H\mathbf{P}_{pe} \\
&+ {\mathbf{P}_{pe}}^H\boldsymbol{Z}_{se}\mathbf{Q}_s + {\mathbf{P}_{pe}}^H\mathbf{P}_{pe}
\end{aligned}
\tag{A.2}
$$

where ${\boldsymbol{Z}_{se}}^H\boldsymbol{Z}_{se}$ is a $N \times N$ matrix, ${\boldsymbol{Z}_{se}}^H\mathbf{P}_{pe}$ is a $N \times 1$ column vector, ${\mathbf{P}_{pe}}^H\boldsymbol{Z}_{se}$ is a $1 \times N$ row vector and ${\mathbf{P}_{pe}}^H\mathbf{P}_{pe}$ is a scalar. By making the substitutions that

$$
{\boldsymbol{Z}_{se}}^H\boldsymbol{Z}_{se} = \boldsymbol{\alpha} = \alpha_R + j\alpha_I \tag{A.3}
$$

$$
{\boldsymbol{Z}_{se}}^H\mathbf{P}_{pe} = \boldsymbol{\beta} = \beta_R + j\beta_I \tag{A.4}
$$

$$
{\mathbf{P}_{pe}}^H\mathbf{P}_{pe} = c \tag{A.5}
$$

and $\mathbf{Q}_s = \mathrm{Q}_{sR} + j\mathrm{Q}_{sI}$, equation A.2 now becomes

$$
\begin{aligned}
U = {\mathbf{Q}_s}^H\boldsymbol{\alpha}\mathbf{Q}_s + {\mathbf{Q}_s}^H\boldsymbol{\beta} + \boldsymbol{\beta}^{\boldsymbol{H}}\mathbf{Q}_s + c \\
&= (\mathrm{Q}_{sR} + j\mathrm{Q}_{sI})^{\boldsymbol{H}}(\alpha_R + j\alpha_I)(\mathrm{Q}_{sR} + j\mathrm{Q}_{sI}) \\
&+ (\mathrm{Q}_{sR} + j\mathrm{Q}_{sI})^{\boldsymbol{H}}(\beta_R + j\beta_I) \\
&+ (\beta_R + j\beta_I)^{\boldsymbol{H}}(\mathrm{Q}_{sR} + j\mathrm{Q}_{sI}) + c
\end{aligned}
\tag{A.6}
$$

After calculating the matrix Hermitian, the cost function then can be expressed by

$$U = \mathrm{Q}_{sR}{}^{T}\alpha_R\mathrm{Q}_{sR} + \mathrm{Q}_{sI}{}^{T}\alpha_R\mathrm{Q}_{sI} - 2\mathrm{Q}_{sR}{}^{T}\alpha_I\mathrm{Q}_{sI} + 2\beta_R{}^{T}\mathrm{Q}_{sR} + 2\beta_I{}^{T}\mathrm{Q}_{sI} + c \tag{A.7}$$

where T represents the matrix transpose.

If all the locations of the secondary sources and error microphones are determined, then the only unknowns remain Q_{sR} and Q_{sI}. Now differentiating the cost function with respect to $\mathbf{Q}_s$ by differentiating U with respect to the real and imaginary parts of the vector $\mathbf{Q}_s$ respectively, that

$$\mathrm{d}U/\mathrm{d}\mathbf{Q}_s = \partial U/\partial \mathrm{Q}_{sR} + j\,\partial U/\partial \mathrm{Q}_{sI} \tag{A.8}$$

where

$$\partial U/\partial \mathrm{Q}_{sR} = \partial\left(\mathrm{Q}_{sR}{}^{T}\alpha_R\mathrm{Q}_{sR}\right)/\partial \mathrm{Q}_{sR} - 2\,\partial\left(\mathrm{Q}_{sR}{}^{T}\alpha_I\mathrm{Q}_{sI}\right)/\partial \mathrm{Q}_{sR} + 2\,\partial\left(\beta_R{}^{T}\mathrm{Q}_{sR}\right)/\partial \mathrm{Q}_{sR} \tag{A.9}$$

$$\partial U/\partial \mathrm{Q}_{sI} = \partial\left(\mathrm{Q}_{sI}{}^{T}\alpha_R\mathrm{Q}_{sI}\right)/\partial \mathrm{Q}_{sI} - 2\,\partial\left(\mathrm{Q}_{sR}{}^{T}\alpha_I\mathrm{Q}_{sI}\right)/\partial \mathrm{Q}_{sI} + 2\,\partial\left(\beta_I{}^{T}\mathrm{Q}_{sI}\right)/\partial \mathrm{Q}_{sI} \tag{A.10}$$

Explicitly, if $Q_{sR} = \begin{bmatrix} q_{sR1} \\ q_{sR2} \\ \vdots \\ q_{sRN} \end{bmatrix}$, $Q_{sI} = \begin{bmatrix} q_{sI1} \\ q_{sI2} \\ \vdots \\ q_{sIN} \end{bmatrix}$, $\alpha_R = \begin{bmatrix} \alpha_{R11} & \alpha_{R12} & \cdots & \alpha_{R1N} \\ \alpha_{R21} & \alpha_{R22} & \cdots & \alpha_{R2N} \\ \vdots & \vdots & \ddots & \vdots \\ \alpha_{RN1} & \alpha_{RN2} & \cdots & \alpha_{RNN} \end{bmatrix}$, $\alpha_I = \begin{bmatrix} \alpha_{I11} & \alpha_{I12} & \cdots & \alpha_{I1N} \\ \alpha_{I21} & \alpha_{I22} & \cdots & \alpha_{I2N} \\ \vdots & \vdots & \ddots & \vdots \\ \alpha_{IN1} & \alpha_{IN2} & \cdots & \alpha_{INN} \end{bmatrix}$, $\beta_R = \begin{bmatrix} \beta_{R1} \\ \beta_{R2} \\ \vdots \\ \beta_{RN} \end{bmatrix}$ and $\beta_I = \begin{bmatrix} \beta_{I1} \\ \beta_{I2} \\ \vdots \\ \beta_{IN} \end{bmatrix}$, the above matrix terms in equation A.9 and A.10 can be expressed as

$$Q_{sR}{}^{T}\alpha_R Q_{sR} = \sum_{N}^{i=1}\sum_{n=N}^{n=1}\alpha_{Rin}q_{sRi}q_{sRn} \tag{A.11}$$

$$Q_{sR}{}^{T}\alpha_I Q_{sI} = \sum_{N}^{i=1}\sum_{n=N}^{n=1}\alpha_{Iin}q_{sRi}q_{sIn} \tag{A.12}$$

$$Q_{sI}{}^{T}\alpha_R Q_{sI} = \sum_{N}^{i=1}\sum_{n=N}^{n=1}\alpha_{Rin}q_{sIi}q_{sn} \tag{A.13}$$

$$\beta_R{}^{T}Q_{sR} = \sum_{N}^{i=1}\beta_{Ri}q_{sRi} \tag{A.14}$$

$$\beta_I{}^{T}Q_{sI} = \sum_{N}^{i=1}\beta_{Ii}q_{sIi} \tag{A.15}$$

By using equation A.11 to A.15, one obtains that

$$\partial U/\partial Q_{sR} = 2\alpha_R Q_{sR} - 2\alpha_I Q_{sI} + 2\beta_R \tag{A.16}$$

$$\partial U/\partial Q_{sI} = 2\alpha_R Q_{sI} + 2\alpha_I Q_{sR} + 2\beta_I \tag{A.17}$$

giving

$$\partial U/\partial \mathbf{Q}_s = 2(\alpha\mathbf{Q}_s + \beta) \tag{A.18}$$

In order to make the cost function U has its minimum, that the sum of squared sound pressure at all locations of error microphones are minimized, as α is positive definite, then $\partial U / \partial \mathbf{Q}_s = 0$, and thus the optimal secondary source strengths $\mathbf{Q}_{s,opt}$ is

$$\mathbf{Q}_{s,opt} = -\alpha^{-1}\beta = -\left(\boldsymbol{Z}_{se}{}^{H}\boldsymbol{Z}_{se} + \gamma\boldsymbol{I}\right)^{-1}\boldsymbol{Z}_{se}{}^{H}\mathbf{P}_{pe} \qquad \text{(A.19)}$$

where $\gamma\boldsymbol{I}$ is a regulation factor in case that $\boldsymbol{Z}_{se}{}^{H}\boldsymbol{Z}_{se}$ sometimes is not stable.

Since $\boldsymbol{Z}_{se}$ is a $N \times N$ square matrix, finally

$$\mathbf{Q}_{s,opt} = -\boldsymbol{Z}_{se}{}^{-1}\mathbf{P}_{pe} = -\boldsymbol{Z}_{se}{}^{-1}\boldsymbol{Z}_{pe}Q_l \qquad \text{(A.20)}$$

References

Ahuja, K., & Stevens, J. C. (1991). Recent advances in active noise control. *AIAA journal*, *29*(7), 1058-1067.

Alexander, T. S. (2012). *Adaptive signal processing: theory and applications*. Springer Science & Business Media.

Angevine, O. L. (1981). Active acoustic attenuation of electric transformer noise. *Proceedings of Inter-Noise, 81'*, 303-306.

Azarpeyvand, M. (2005). Active noise cancellation of a spherical multipole source using a radially vibrating spherical baffled piston. *Acoustical Physics*, *51*(6), 609-618.

Beauvilain, T. A., Bolton, J. S., & Gardner, B. K. (2000). Sound cancellation by the use of secondary multipoles: Experiments. *The Journal of the Acoustical Society of America*, *107*(3), 1189-1202.

Berglund, B., Hassmen, P., & Job, R. S. (1996). Sources and effects of low-frequency noise. *The Journal of the Acoustical Society of America*, *99*(5), 2985-3002.

Berge, T., Pettersen, O. K. O., & Sorsdal, S. (1987, September). Active noise cancellation of transformer noise. In *INTER-NOISE and NOISE-CON Congress and Conference Proceedings*, Vol. 1987, No. 5, 537-540.

Bolton, J. S., Gardner, B. K., & Beauvilain, T. A. (1995). Sound cancellation by the use of secondary multipoles. *The Journal of the Acoustical Society of America*, *98*(4), 2343-2362.

Boodoo, S., Paurobally, R., & Bissessur, Y. (2015). A review of the effect of reflective surfaces on power output of sound sources and on actively created quiet zones. *Acta Acustica united with Acustica*, *101*(5), 877-891.

Bu, B., Bao, C. C., & Jia, M. S. (2018). Design of a planar first-order loudspeaker array for global active noise control. *IEEE/ACM Transactions on Audio, Speech, and Language Processing*, *26*(11), 2240-2250.

Burgess, J. C. (1981). Active adaptive sound control in a duct: A computer simulation. *The Journal of the Acoustical Society of America*, *70*(3), 715-726.

Canevet, G. (1978). Active sound absorption in an air conditioning duct. *Journal of Sound Vibration*, *58*, 333-345.

Chen, K., & Koopmann, G. H. (2002). Active control of low-frequency sound radiation from vibrating panel using planar sound sources. *Journal of vibration and Acoustics*, *124*(1), 2-9.

Chen, W., Pu, H., & Qiu, X. (2010). A compound secondary source for active noise radiation control. *Applied Acoustics*, *71*(2), 101-106.

Clark, R. L., & Fuller, C. R. (1992). Experiments on active control of structurally radiated sound using multiple piezoceramic actuators. *The Journal of the Acoustical Society of America*, *91*(6), 3313-3320.

Clarkson, P. M. (1993). *Optimal and adaptive signal processing*. FL: CRC Press.

Conover, W. B. (1956). Fighting noise with noise. *Noise control*, *2*(2), 78-92.

Craig, S. E. (1993). Active control of hum from large power transformers-the real world. In *Second conference on active control of sound and vibration*, 279-290.

Dorling, C. M., Eatwell, G. P., Hutchins, S. M., Ross, C. F., & Sutcliffe, S. G. C. (1989). A demonstration of active noise reduction in an aircraft cabin. *Journal of Sound Vibration*, *128*, 358-360.

Cunefare, K. A., & Koopmann, G. H. (1991). Global optimum active noise control: Surface and far-field effects. *The Journal of the Acoustical Society of America*, *90*(1), 365-373.

Duhamel, D., & Sergent, P. (1998). Active noise control of an incoherent line source. *Journal of sound and vibration*, *212*(1), 141-164.

Duke, C. R., Sommerfeldt, S. D., Gee, K. L., & Duke, C. V. (2009). Optimization of control source locations in free-field active noise control using a genetic algorithm. *Noise Control Engineering Journal*, *57*(3), 221-231.

Elliott, S. J. (2008). A review of active noise and vibration control in road vehicles. *ISVR Technical Memorandum, No 981*

Elliott, S. J. (2009). Active Control in Vehicles and in the Inner Ear. *International Journal of Acoustics and Vibration*, *14*(4), 212-219.

Elliott, S. J., Joseph, P., Nelson, P. A., & Johnson, M. E. (1991). Power output minimization and power absorption in the active control of sound. *The Journal of the Acoustical Society of America*, *90*(5), 2501-2512.

Elliott, S. J., and Nelson, P. A. (1993). Active noise control. *IEEE signal processing magazine*, *10*(4), 12-35.

Elliot, S. J., Nelson, P. A., Stothers, I. M., & Boucher, C. C. (1990). In-flight experiments on the active control of propeller-induced cabin noise. *Journal of Sound and Vibration*, *140*(2), 219-238.

Elliott, S. J., Stothers, I. M., Nelson, P. A., McDonald, A. M., Quinn, D. C., & Saunders, T. (1988, August). The active control of engine noise inside cars. In *INTER-NOISE and NOISE-CON Congress and Conference Proceedings*. Vol. 1988, No. 3, 987-990.

Ffowcs Williams, J. E. (1984). Review Lecture-Anti-sound. *Proceedings of the Royal Society of London. A. Mathematical and Physical Sciences*, *395*(1808), 63-88.

Fry, A. (Ed.). (2013). *Noise Control in Building Services: Sound Research Laboratories Ltd*. Elsevier.

Fuller, C. R., & Von Flotow, A. H. (1995). Active control of sound and vibration. *IEEE Control Systems Magazine*, *15*(6), 9-19.

Gardonio, P. (2002). Review of active techniques for aerospace vibro-acoustic control. *Journal of aircraft*, *39*(2), 206-214.

Gee, K. L., & Sommerfeldt, S. D. (2004). Application of theoretical modeling to multichannel active control of cooling fan noise. *The Journal of the Acoustical Society of America*, *115*(1), 228-236.

George, N. V., & Panda, G. (2013). Advances in active noise control: A survey, with emphasis on recent nonlinear techniques. *Signal processing*, *93*(2), 363-377.

Giouvanakis, M., Sevastiadis, C., & Papanikolaou, G. (2019). Low-Frequency Noise Attenuation in a Closed Space Using Adaptive Directivity Control Sources of a Quadrupole Type. *Archives of Acoustics*, *44*(1), 71-78.

Guicking, D. (1992). Recent advances in active noise control. In *Recent Developments in Air-and Structure-Borne Sound and Vibration*. Vol. 1, 313-320.

Guicking, D. (2007). Active control of sound and vibration: History–fundamentals–state of the art. *Oscillations, Waves and Interactions–60 Years Drittes Physikalisches Institute*, 107-138.

Guo, J., & Pan, J. (1997). Further investigation on actively created quiet zones by multiple control sources in free space. *The Journal of the Acoustical Society of America*, *102*(5), 3050-3053.

Guo, J., & Pan, J. (1998). Effects of reflective ground on the actively created quiet zones. *The Journal of the Acoustical Society of America*, *103*(2), 944-952.

Guo, J., & Pan, J. (1999). Actively created quiet zones for broadband noise using multiple control sources and error microphones. *The Journal of the Acoustical Society of America*, *105*(4), 2294-2303.

Guo, J., Pan, J., & Bao, C. (1997). Actively created quiet zones by multiple control sources in free space. *The Journal of the Acoustical Society of America*, *101*(3), 1492-1501.

Guo, J., Pan, J., & Hodgson, M. (2007). A brief review of active control of environmental noise and its applications. *ICSV14. Cairns. Australia*.

Hansen, C. H. (1997, June). Active noise control-from laboratory to industrial implementation. In *NOISE CON 97*. 3-38.

Hansen, C. H. (2004). Current and future industrial applications of active noise control. *Noise Control Engineering Journal*, *53*(5), 181-196.

Hansen, C. H., Qiu, X., Barrault, G., Howard, C. Q., Petersen, C. D., & Singh, S. (2007, July). Optimisation of active and semi-active noise and vibration control systems. In *Proceedings of 14th International Congress on Sound and Vibration (ICSV14), Cairns, Australia*.

Hart, C. R., & Lau, S. K. (2012). Active noise control with linear control source and sensor arrays for a noise barrier. *Journal of Sound and Vibration*, *331*(1), 15-26.

Hesselmann, N. (1978). Investigation of noise reduction on a 100 kVA transformer tank by means of active methods. *Applied acoustics*, *11*(1), 27-34.

Jessel, M. J. (1988, August). 25 jears with active noise control-A survey and comments with reference to Guickling's bibliography. In *INTER-NOISE and NOISE-CON Congress and Conference Proceedings*. Vol. 1988, No. 3, 953-958.

Jessel, M. J. M., & Angevine, O. L. (1980). Active acoustic attenuation of a complex noise source. *Inter-noise 80 proceedings*, 689-694.

Jiang, J., & Li, Y. (2018). Review of active noise control techniques with emphasis on sound quality enhancement. *Applied Acoustics*, *136*, 139-148.

Joseph, P., Elliott, S. J., & Nelson, P. A. (1994). Near field zones of quiet. *Journal of sound and vibration*, *172*(5), 605-627.

Huang, H., Qiu, X., & Kang, J. (2011). Active noise attenuation in ventilation windows. *The Journal of the Acoustical Society of America*, *130*(1), 176-188.

Kajikawa, Y., Gan, W. S., & Kuo, S. M. (2012). Recent advances on active noise control: open issues and innovative applications. *APSIPA Transactions on Signal and Information Processing*, *1*.

Kajikawa, Y., Gan, W. S., & Kuo, S. M. (2013, September). Recent applications and challenges on active noise control. In *2013 8th International Symposium on Image and Signal Processing and Analysis (ISPA), IEEE*. 661-666.

Kang, J., Chourmouziadou, K., Sakantamis, K., Wang, B. and Hao, Y., (2013). Soundscape of European Cities and Landscapes, Soundscape-COST, Oxford.

Kido, K. (1975). Reduction on noise by use of additional sound sources. *Proc. Inter-Noise 75,* 64-65.

Kinsler, L. E., Frey, A. R., Coppens, A. B., & Sanders, J. V. (1999). Fundamentals of acoustics. Fundamentals of Acoustics, 4th Edition, by Lawrence E. Kinsler, Austin R. Frey, Alan B. Coppens, James V. Sanders

Kryter, K. D. (1985). The Effects of Noise on Man, Academic Press, New York.

Kuo, S. M., & Morgan, D. R. (1999). Active noise control: a tutorial review. *Proceedings of the IEEE*, *87*(6), 943-973.

Kuo, S. M., & Morgan, D. R. (2000, September). Review of DSP algorithms for active noise control. In *Proceedings of the 2000. IEEE International Conference on Control Applications. Conference Proceedings*. 243-248.

Kurata, Y. (1991). Adaptive active attenuation of interior car noise. In *Proc. Int. Symp. on Active Control of Sound and Vibration*. 297-302.

Kurze, U. J. (1974). Noise reduction by barriers. *The Journal of the Acoustical Society of America*, *55*(3), 504-518.

Kwon, B., & Park, Y. (2013). Interior noise control with an active window system. *Applied Acoustics*, *74*(5), 647-652.

Lau, S. K., & Tang, S. K. (2001). Sound fields in a rectangular enclosure under active sound transmission control. *The Journal of the Acoustical Society of America*, *110*(2), 925-938.

Leitch, R. R., & Tokhi, M. O. (1987). Active noise control systems. *IEE Proceedings A (Physical Science, Measurement and Instrumentation, Management and Education, Reviews)*, *134*(6), 525-546.

Lin, Z., Lu, J., Shen, C., Qiu, X., & Xu, B. (2004). Active control of radiation from a piston set in a rigid sphere. *The Journal of the Acoustical Society of America*, *115*(6), 2954-2963.

McManus, K. R., Poinsot, T., & Candel, S. M. (1993). A review of active control of combustion instabilities. *Progress in energy and combustion science*, *19*(1), 1-29.

McDonald, A. M. (1991). Active noise and vibration control within the automobile. In *Proc. 1991 Acoust. Soc. Jpn, Int. Symp. Active Control of Sound and Vibration*. 147-156.

Mehta, M., Johnson, J., & Rocafort, J. (1999). *Architectural acoustics: principles and design*.

Miller, P. L. (1977). Room Air Diffusion System-design Techniques-air Diffusion Performance Index. *ASHRAE Journal-American Society of Heating Refrigerating and Air-conditioning Engineers*, *19*(4), 37-40.

Moreau, D., Cazzolato, B., Zander, A., & Petersen, C. (2008). A review of virtual sensing algorithms for active noise control. *Algorithms*, *1*(2), 69-99.

Nelson, P. A., Curtis, A. R. D., Elliott, S. J., & Bullmore, A. J. (1987a). The minimum power output of free field point sources and the active control of sound. *Journal of Sound and Vibration*, *116*(3), 397-414.

Nelson, P. A., Curtis, A. R. D., Elliott, S. J., & Bullmore, A. J. (1987b). The active minimization of harmonic enclosed sound fields, Part I: Theory. *Journal of Sound and Vibration*, *117*(1), 1-13.

Nelson, P. A., & Elliott, S. J. (1991). *Active control of sound*. Academic press.

Olson, H. F., & May, E. G. (1953). Electronic sound absorber. *The Journal of the Acoustical Society of America*, *25*(6), 1130-1136.

Olson, H. F. (1956). Electronic control of noise, vibration, and reverberation. *The Journal of the Acoustical Society of America*, *28*(5), 966-972.

Omoto, A., & Fujiwara, K. (1993). A study of an actively controlled noise barrier. *The journal of the acoustical society of America*, *94*(4), 2173-2180.

Paul, Lueg. (1936). *U.S. Patent No. 2,043,416*. Washington, DC: U.S. Patent and Trademark Office.

PAWEŁCZYK, M. (2008). Active noise control-a review of control-related problems. *Archives of Acoustics*, *33*(4), 509-520.

Peake, N., & Crighton, D. G. (2000). Active control of sound. *Annual Review of Fluid Mechanics*, *32*(1), 137-164.

Qiu, X., & Hansen, C. H. (2000). Secondary acoustic source types for active noise control in free field: Monopoles or multipoles?. *Journal of sound and vibration*, *232*(5), 1005-1009.

Qiu, X., Lu, J., & Pan, J. (2014, October). A new era for applications of active noise control. In *INTER-NOISE and NOISE-CON Congress and Conference Proceedings*. Vol. 249, No. 7, 1254-1263.

Rafaely, B. (2009). Spherical loudspeaker array for local active control of sound. *The Journal of the Acoustical Society of America*, *125*(5), 3006-3017.

Ross, C. F. (1978). Experiments on the active control of transformer noise. *Journal of Sound and Vibration*, *61*(4), 473-480.

Ross, C. F. (1981). A demonstration of active control of broadband sound. *Journal of Sound and Vibration*, *74*(3), 411-417.

Ross, C. F. (1991, April). The control of noise inside passenger vehicles. In *Proc. Recent Advances in Active Control of Sound Vibration*. 671-681.

Santiago, T., & Bernhard, R. J. (1993, May). Active control of the directivity of a sound source. In *INTER-NOISE and NOISE-CON Congress and Conference Proceedings* (Vol. 1993, No. 1, pp. 601-606). Institute of Noise Control Engineering.

Simpson, M. A., Luong, T. M., Swinbanks, M. A., Russell, M. A., & Leventhall, H. G. (1989). Full scale demonstration tests of cabin noise reduction using active noise control. *Inter-noise 89- Engineering for environmental noise control*, 459-462.

Simshauser, E. D., & Hawley, M. E. (1955). The Noise‐Cancelling Headset—An Active Ear Defender. *The Journal of the Acoustical Society of America*, *27*(1), 207-207.

Snyder, S. D., Hill, S. G., Burgan, N. C., Tanaka, N., & Cazzolato, B. S. (2004). Acoustic-centric modal filter design for active noise control. *Control engineering practice*, *12*(8), 1055-1064.

Sun, Y., Yang, T., Zhu, M., & Pan, J. (2017). The use of an active controlled enclosure to attenuate sound radiation from a heavy radiator. *Journal of Sound and Vibration*, *392*, 1-17.

Svensson, P. U., & Kleiner, M. (1995). Review of active systems in room acoustics and electroacoustics. In *Proceeding of Active*. Vol. 95, 9.

Swanson, D. C. (1989). Active noise attenuation using a self-tuning regulator as the adaptive control algorithm. *Proc. Internoise'89*, 467-470.

Tanaka, N., & Tanaka, M. (2010). Active noise control using a steerable parametric array loudspeaker. *The Journal of the Acoustical Society of America*, *127*(6), 3526-3537.

Tao, J., Wang, S., Qiu, X., & Pan, J. (2016). Performance of an independent planar virtual sound barrier at the opening of a rectangular enclosure. *Applied Acoustics*, *105*, 215-223.

Tang, S. K., Tong, Y. G., & Tsui, K. L. (2016). Sound transmission across a plenum window with an active noise cancellation system. *Noise Control Engineering Journal*, *64*(4), 423-431.

Tichy, J. (1991). Current and future issues of active noise control. *Journal of the Acoustical Society of Japan (E)*, *12*(6), 255-262.

Tong, Y. G., Tang, S. K., Kang, J., Fung, A., & Yeung, M. K. L. (2015). Full scale field study of sound transmission across plenum windows. *Applied acoustics*, *89*, 244-253.

Warnaka, G. E., Tichy, J., & Poole, L. A. (1981, October). Improvements in adaptive active attenuators. In *INTER-NOISE and NOISE-CON Congress and Conference Proceedings*. Vol. 1981, No. 4, 307-310

Warnaka, G. E. (1982). Active attenuation of noise-the state of the art. *Noise Control Engineering Journal*, *18*, 100-110.

WHO, (2011). Burden and Disease from Environmental Noise. Quantification of Healthy Life Years Lost in Europe, World Health Organization, Bonn.

Wright, S. E., & Vuksanovic, B. (1996). Active control of environmental noise. *Journal of sound and vibration*, *190*(3), 565-585.

Wright, S. E., & Vuksanovic, B. (1997). Active control of environmental noise, II: Non-compact acoustic sources. *Journal of Sound and Vibration*, *202*(3), 313-359.

Wright, S. E., & Vuksanovic, B. (1999). Active control of environmental noise, IV: practical extensions to ECAS theory. *Journal of sound and vibration*, *222*(4), 635-668.